Engineering Overview of ACS SASSI NQA V4.3 Application to Seismic SSI Analysis of Safety-Related NPP Buildings

Ghiocel Predictive Technologies Inc.

Dr. Dan M. Ghiocel

Member of ASCE 4 & 43 Standards

Email: dan.ghiocel@ghiocel-tech.com

Ghiocel Predictive Technologies Inc.

http://www.ghiocel-tech.com

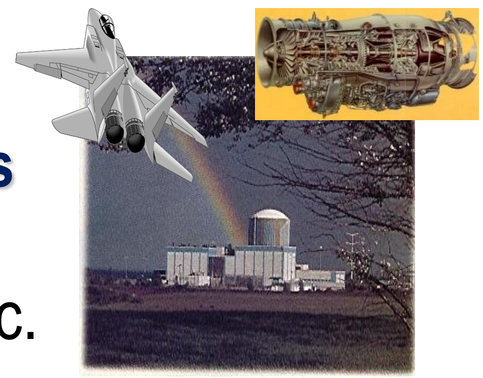

Part 2: ACS SASSI Methodology

GP Technologies, Inc., Rochester, New York

October 2021

Day 1B Presentation Content:

1. ACS SASSI Flexible Volume Substructuring SSI Methodology

2. ACS SASSI Motion Incoherency Modeling

1. ACS SASSI Flexible Volume Substructuring SSI Methodology

Theoretical and Implementation Aspects

Flexible Volume Substructuring (FVS) in Complex Frequency

SSI Analysis Methods and Models

Real

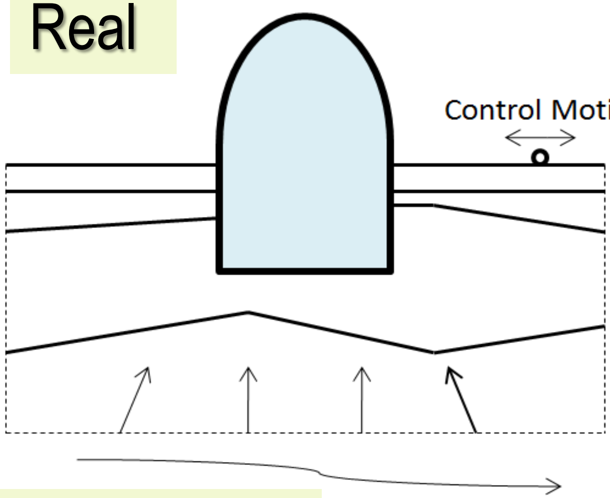

Idealized

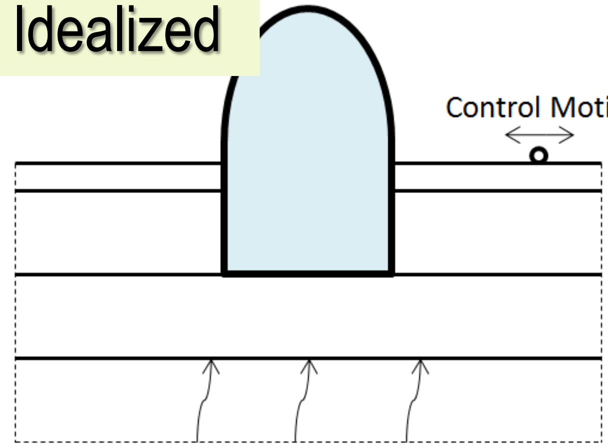

Vertical wave propagation is used to replace actual complex ground motion pattern, but still produce specified motion at control point.

Direct Approach
(Single Step Analysis)
(Single FE Model)

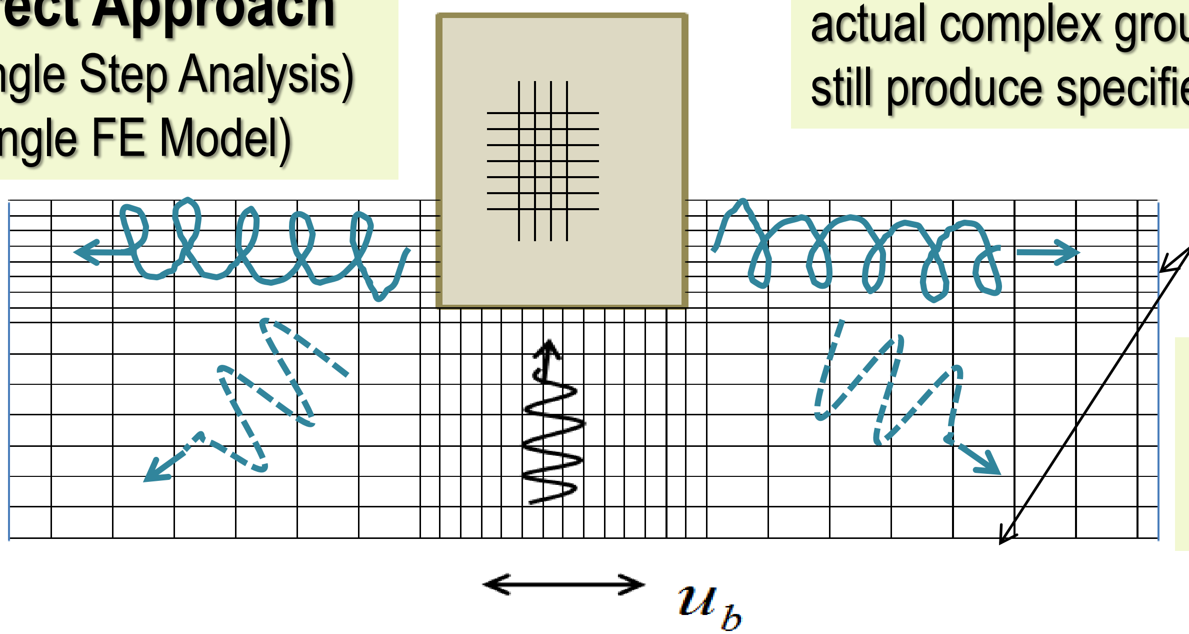

Conventional BCs
(stiffness, damping, soil motion)

Enormous amount of solid elements; 99% of FE elements are in soil media

Linearized SSI Analysis Superposition Theorem

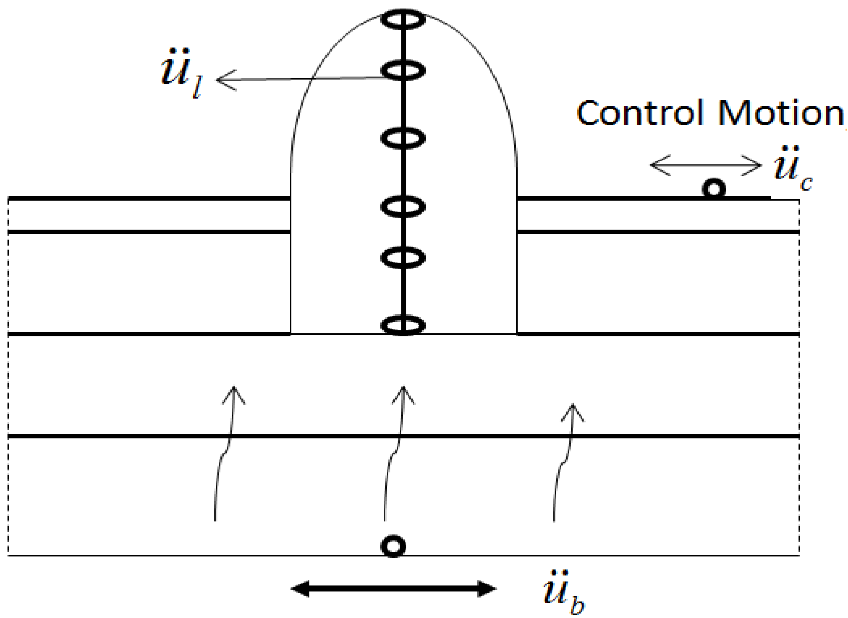

(a) Kinematic Interaction Analysis

Structure has stiffness but no mass.

Analysis leads to determination of motions at different points in structure relative to base control point.

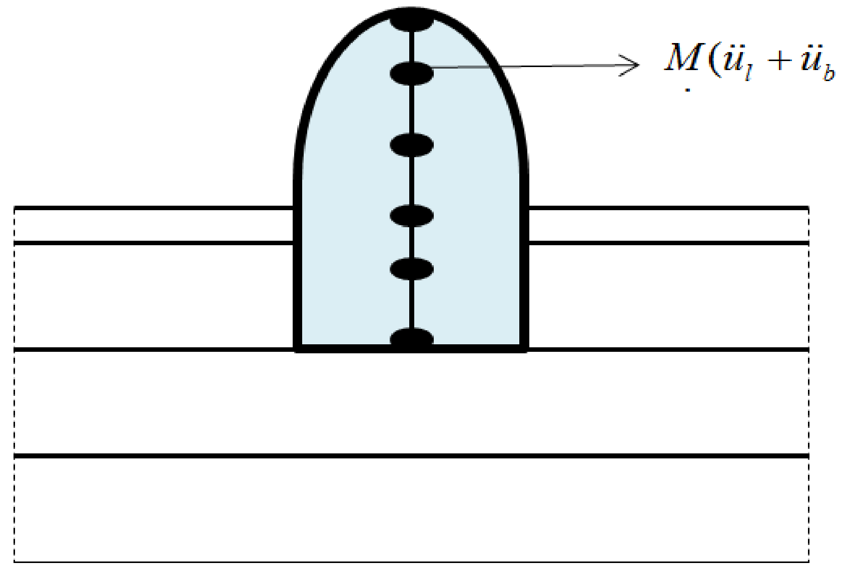

(b) Inertial Interaction Analysis

Motions computed in (a) are applied to masses in structure as shown above.

Analysis leads to computation of new motions at different points in structure.

SSI Substructuring Using Three Step Approach

Rigid Boundary SSI Substructuring (Kausel,1974)

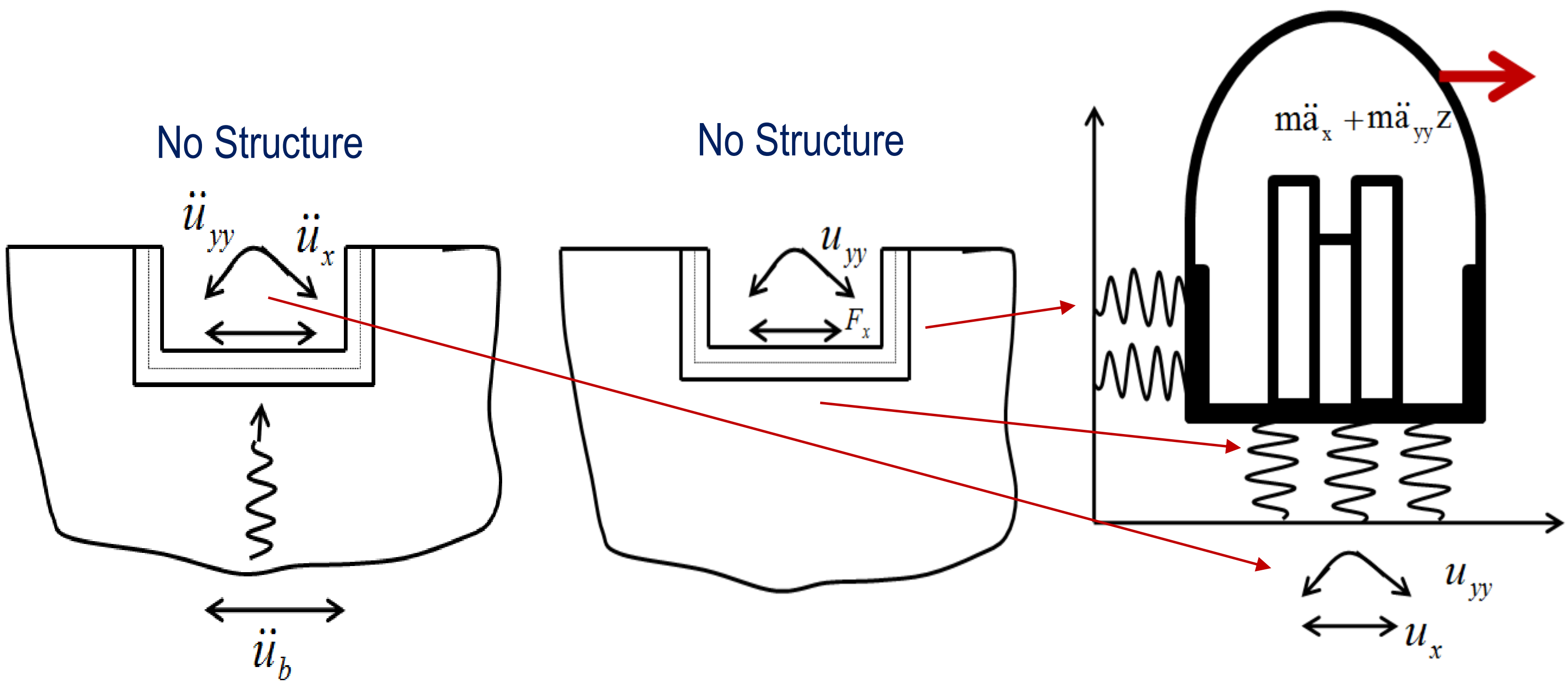

a) Kinematic SSI Analysis (Wave Scattering Problem Pb)

b) Impedance Computation (External Force Pb)

c) Inertial SSI Analysis (Structural Dynamics Pb)

Direct SSI Approach vs. SASSI Approach

Direct Approach (Time-Domain)

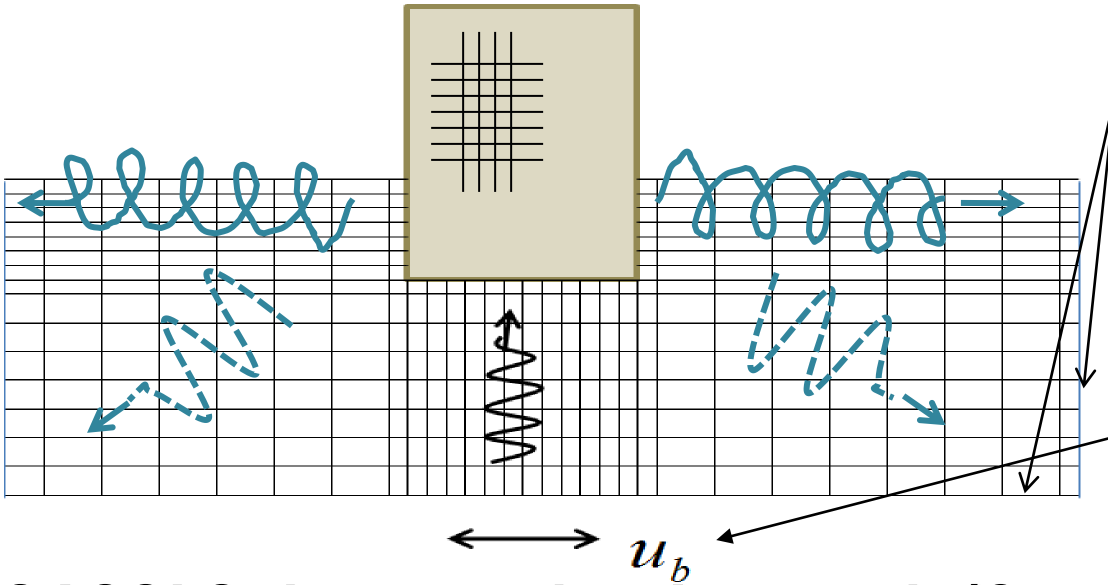

FE Model Boundaries
(stiffness, damping, soil motion)

99% of FE elements are in soil

Input motion

SASSI Substructuring Approach (Complex Frequency)

Structural dynamic analysis step includes *3D Structure FEM* and *Excavated Soil FEM*

Only *1D soil layering variation model* is used to compute the input motions and the soil impedance for SSI analysis via axisymmetric soil deposit modeling

1D Soil Layering FE Model
w/o Excavated Soil
(Free Field Analysis)

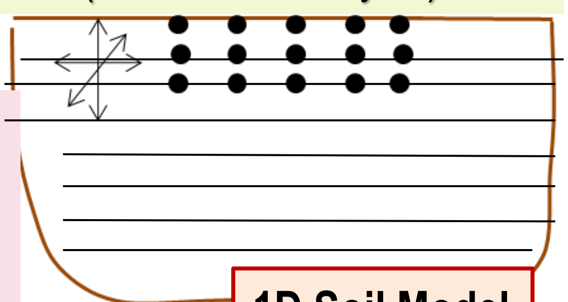

1D Soil Model

3D Structure w/ Excavated Soil
FE Model (SSI Analysis)

Free-field motion

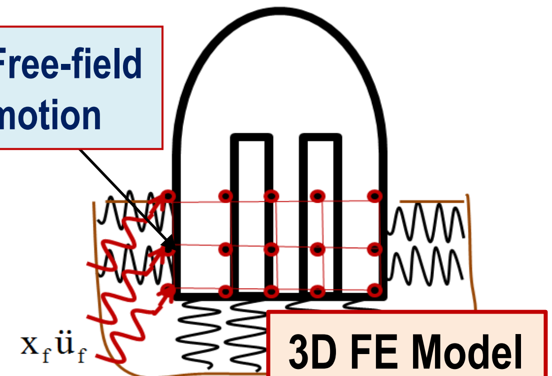

3D FE Model

Direct SSI Approach and SASSI Approach Models

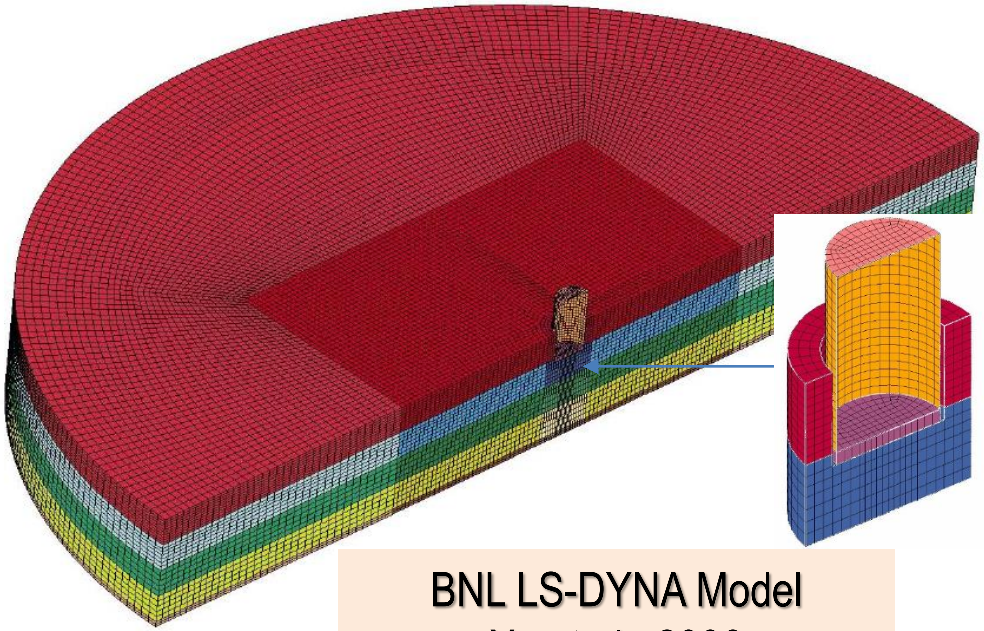

BNL LS-DYNA Model
Xu et al., 2006

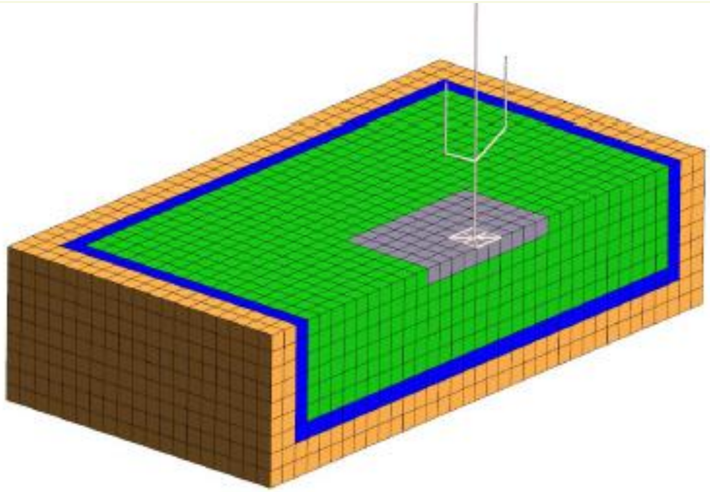

E-SSI Model (Low Frequency)
Neboja et al., 2015

Direct SSI Approach Model

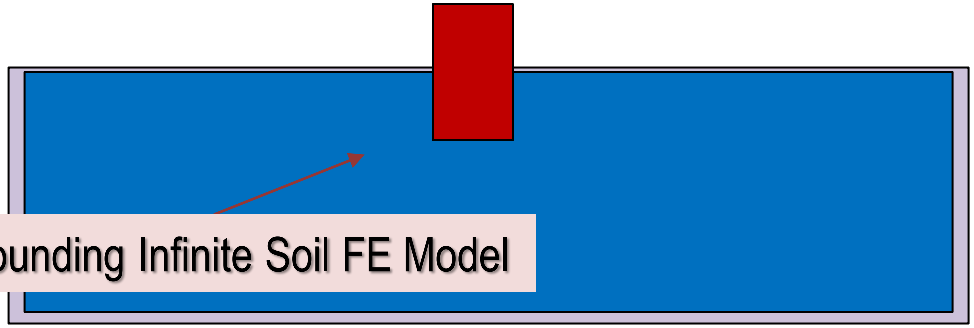

Surrounding Infinite Soil FE Model

SASSI Approach Model

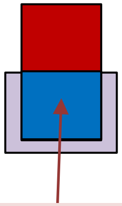

Excavated Soil FE Model

Flexible Volume (FV) Substructuring Method

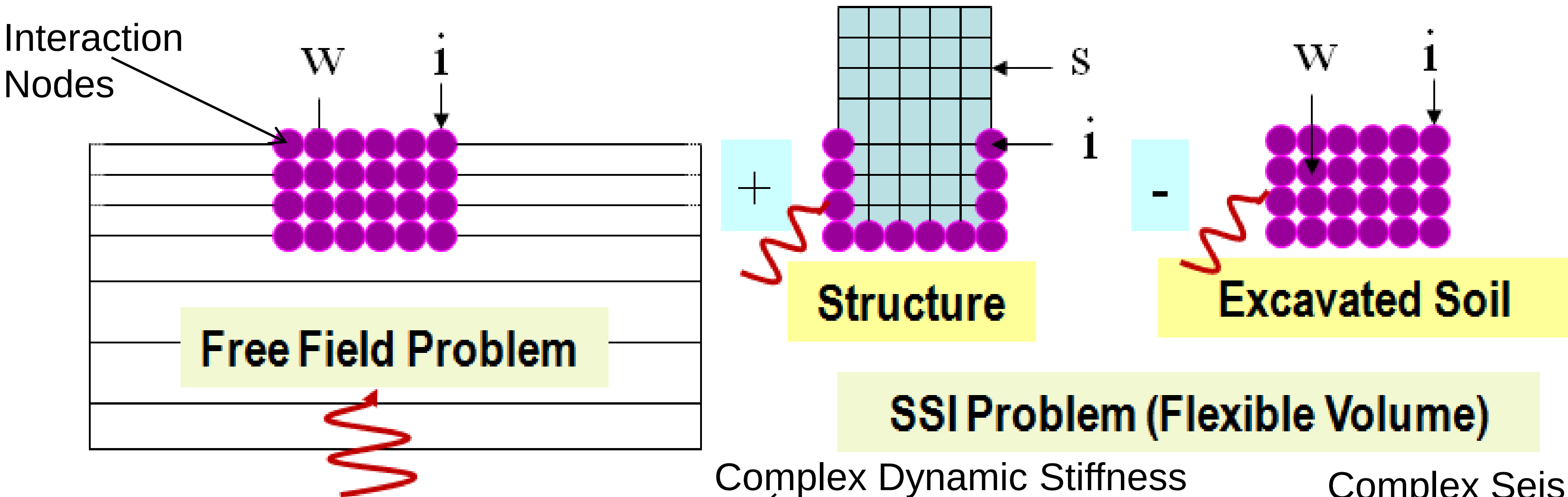

Complex Frequency Domain Formulation:

Complex Dynamic Stiffness

Complex Seismic Load Vector

$$\boxed{C(\omega)\,U(\omega) = Q(\omega)}$$

Complex Absolute Displacements

Complex Soil Impedance Terms

$$\begin{bmatrix} \mathbf{C}^{s}_{ii} - \mathbf{C}^{e}_{ii} + \mathbf{X}_{ii} & -\mathbf{C}^{e}_{iw} + \mathbf{X}_{iw} & \mathbf{C}^{s}_{is} \\ -\mathbf{C}^{e}_{wi} + \mathbf{X}_{wi} & -\mathbf{C}^{e}_{ww} + \mathbf{X}_{ww} & \mathbf{0} \\ \mathbf{C}^{s}_{si} & \mathbf{0} & \mathbf{C}^{s}_{ss} \end{bmatrix} \begin{Bmatrix} \mathbf{U}_{i} \\ \mathbf{U}_{w} \\ \mathbf{U}_{s} \end{Bmatrix} = \begin{Bmatrix} \mathbf{X}_{ii}\mathbf{U}'_{i} + \mathbf{X}_{iw}\mathbf{U}'_{w} \\ \mathbf{X}_{wi}\mathbf{U}'_{i} + \mathbf{X}_{ww}\mathbf{U}'_{w} \\ \mathbf{0} \end{Bmatrix}$$

REMARK: All Excavated Soil nodes are interaction nodes (include exact equations of motion)

SASSI Substructuring Uses 3D1D SSI Models

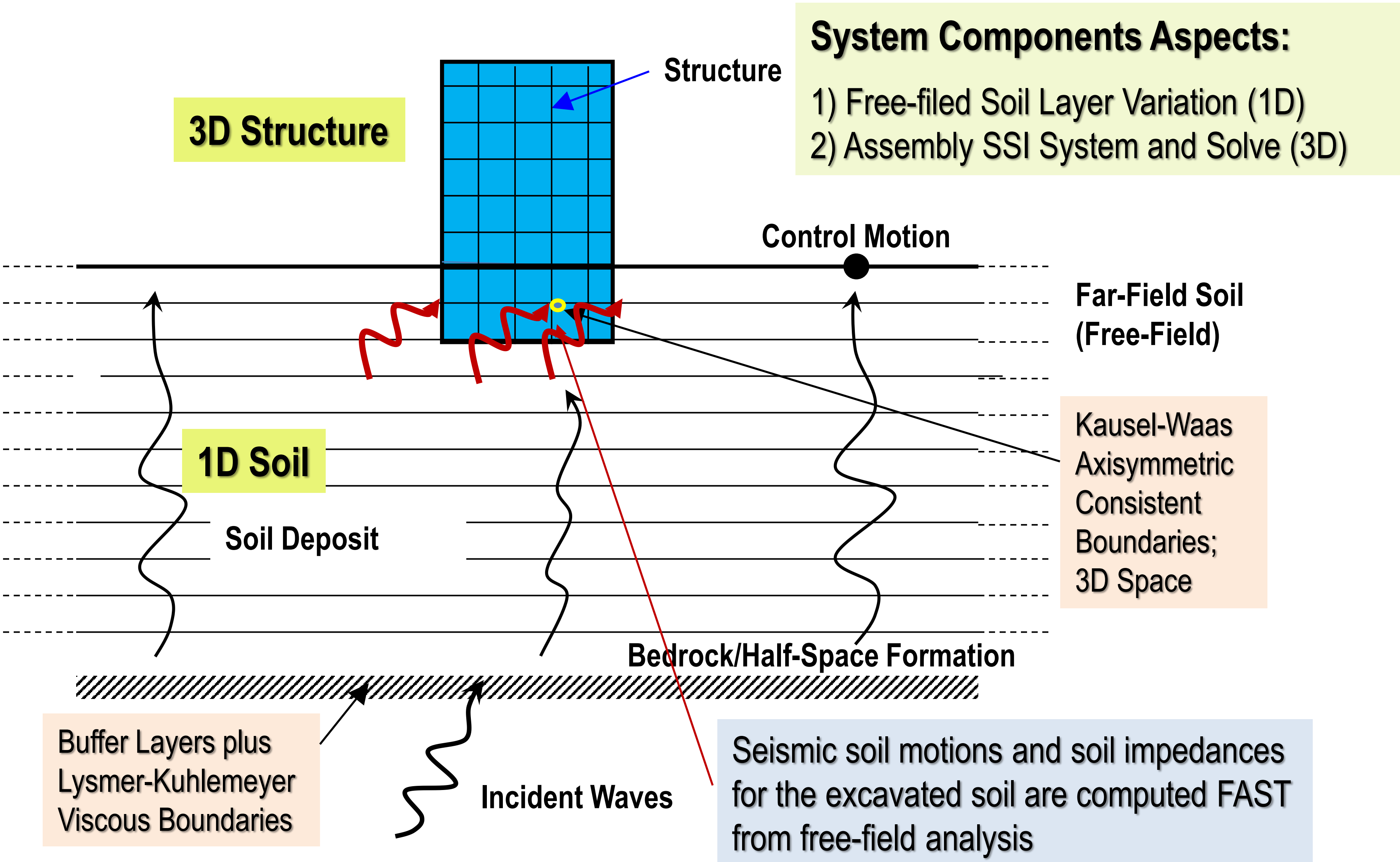

SSI Analysis Formulation in Complex Frequency

The equation of motion of the SSI system is:

$$[M]\{\ddot{u}\} + [C]\{\dot{u}\} + [K]\{u\} = -\{m\}\ddot{y}$$

$$[M]\{\ddot{u}\} + [K^*]\{u\} = -\{m\}\ddot{y}$$

Assume: $\ddot{y} = \ddot{Y}e^{i\omega t}$

Then: $\{u\} = \{U\}e^{i\omega t}$

$$\left([K^*] - \omega^2[M]\right)\{U\} = -\{m\}\ddot{Y}$$

Solve for complex transfer functions for each frequency:

$$\left([K^*] - \omega_s^2[M]\right)\{A_s\} = -\{m\}$$

Then the solution in frequency domain:

$$\{U_s\} = \{A_s\}\ddot{Y}$$

Use Fourier Transform for transient time histories, and the compute solution in time domain

$$u_j(t) = \mathrm{Re}\sum_{s=0}^{N/2} U_{j,s}e^{i\omega_s t}$$

Linearized Seismic SSI Analysis Implementation

Main Computational Steps:

Seismic SSI analysis is solved in the complex frequency domain.
Implementation include the following steps:

1. Solve the site response problem (SITE)
2. Solve the impedance problem (POINT, ANALYS)
3. Form the load vector (ANALYS)
4. Form the complex stiffness matrix (HOUSE, ANALYS)
5. Solve the system of linear equations of motion (ANALYS)
6. Compute SSI responses in time histories and maximum values (MOTION, RELDISP, STRESS)

Visco-Elastic Material Hysteretic Models in Physical Space and Complex Frequency Space

$$\boxed{\sigma(x,t)=\sigma^{*}(x)e^{i\omega t}}$$

$$\boxed{\varepsilon\left(x,t\right)=\varepsilon^{*}(x)e^{i\omega t}}$$

$$\boxed{\sigma^{*}(x)=D^{*}\varepsilon^{*}(x)}$$

$$\boxed{D^{*}=D\left(1+i\tan\delta\right)}$$

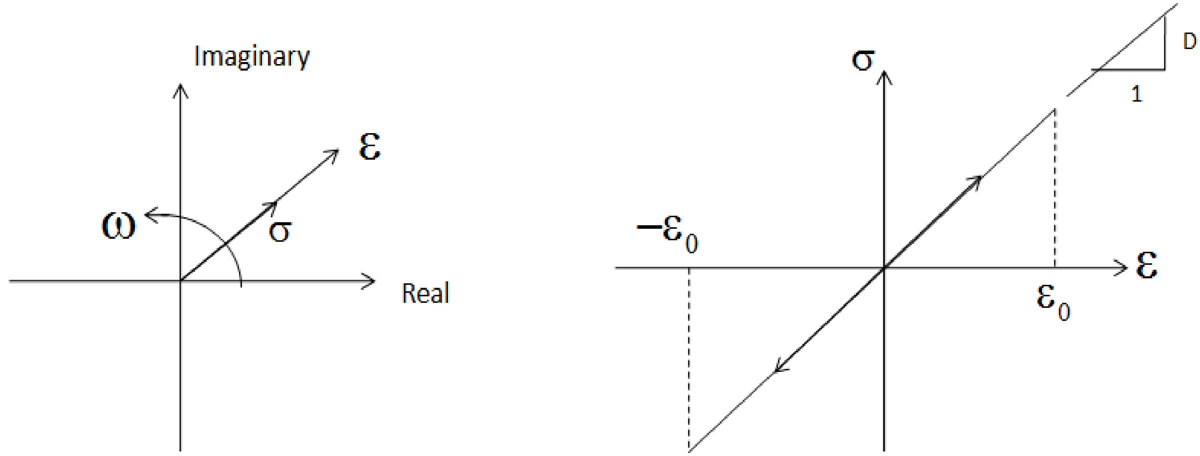

In complex frequency space

In physical space

Elastic Material Model

$$G^{*}=G(1-2\beta_s^2+2i\beta_s\sqrt{1-\beta_s^2})$$

$$M^{*}=M(1-2\beta_p^2+2i\beta_p\sqrt{1-\beta_p^2})$$

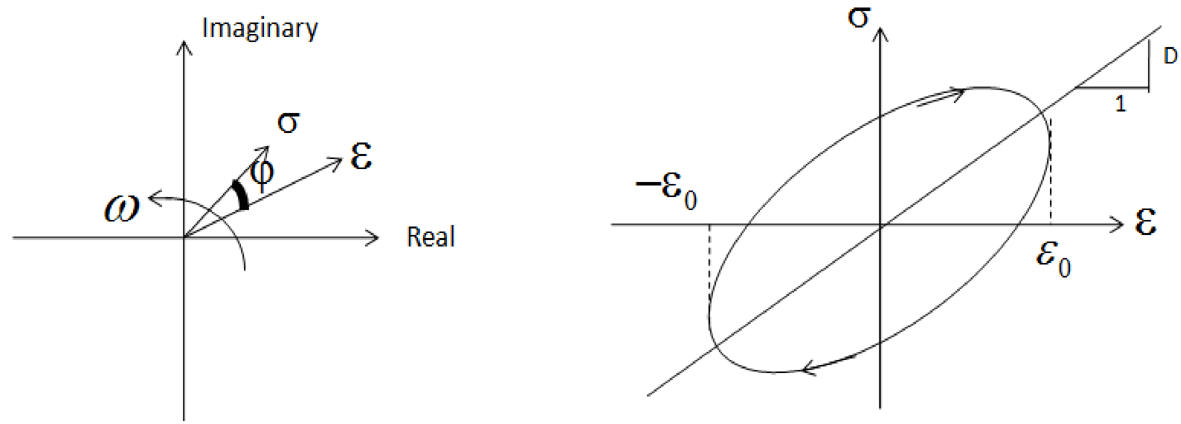

In complex frequency space

In physical space

Visco-Elastic Material Model

Linearized Hysteretic and Viscous Models

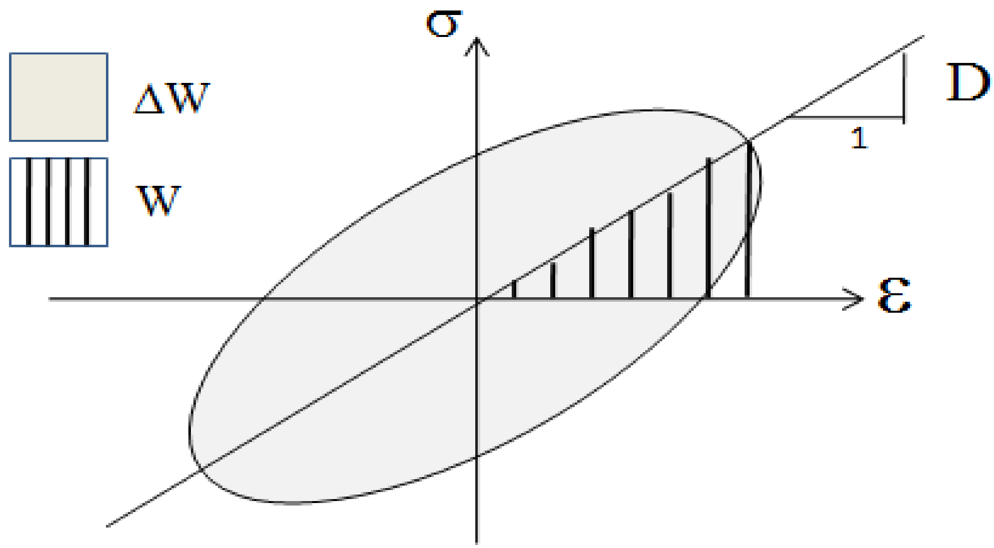

Damping (Imaginary Part)

Hysteretic Model (Frequency-Independent); structure and soil, LRB/FP

$$\tan\delta = \frac{\mathrm{Imag}(D^*)}{\mathrm{Real}(D^*)} = \frac{1}{2\pi}\frac{\Delta W}{W}$$

Viscous Model (Frequency-Dependent); HVD isolators

$$\tan\delta = \frac{\mathrm{Imag}(D^*)}{\mathrm{Real}(D^*)} = \frac{c(\omega)\omega}{\mathrm{Real}(D^*)}$$

Free-field Motion Input

Free-Field Response for Different Seismic Waves

Governing equations for the horizontal soil layering subjected to a system of plane incident body waves of SV and P type (that produces both normal and tangential stresses in soil layers).

The waves arrive at an arbitrary angle at the base of the soil layering from an underlying uniform half-space. The motions created by the incident plane body waves will produce displacements in 3D space, but these displacements will not vary in horizontal direction perpendicular to the wave propagation direction.

Assuming that this perpendicular direction is Y, the resulted motion will involve only the direction X and Z as shown in next slide (Chen, 1981)

Free-Field Motion in Time Domain

If the wave excitation is harmonic excitation and the soil is an isotropic viscoelastic medium, then, the equations of motion are:

For in-plane motion (SV and P):

$$(M^* - G^*)\frac{\partial \varepsilon}{\partial x} + G^* \nabla^2 u_X = \rho \frac{\partial^2 u_X}{\partial t^2}$$

$$(M^* - G^*)\frac{\partial \varepsilon}{\partial z} + G^* \nabla^2 u_Z = \rho \frac{\partial^2 u_Z}{\partial t^2}$$

For out-of-plane motion (SH waves):

$$G^* \nabla^2 u_Y = \rho \frac{\partial^2 u_Y}{\partial t^2}$$

Using the Helmholtz's theory, the in-place motions described by the partial differential equations (PDEs) can be considered in terms of the two wave potentials associated with P and SV wave motions denoted

$$\nabla^2\Phi = \frac{1}{V_P^{*2}}\frac{\partial^2\Phi}{\partial t^2} \qquad \nabla^2\Psi = \frac{1}{V_S^{*2}}\frac{\partial^2\Psi}{\partial t^2}$$

Assuming that the wave potential vary also harmonically the two coupled equations are separated in two independent equations:

$$\nabla^2\Phi + k_P^2 = 0 \qquad \nabla^2\Phi + k_S^2 = 0$$

The Real(k) indicates how fast the wave propagates at given frequency and Imag(k) indicates how fast wave amplitude decays with distance.

Thomson-Haskell's formulation for the motion of multilayered soil system overlaying an elastic halfspace produces very complicated equations of motions in which the wave number k enters in complex transcedental functions. A large simplification could be made if the displacement are assumed to vary linearly within each layer (Waas, 1972, Kausel, 1974).

Free-Field Models for Different Seismic Waves. Inclined SV Wave Propagation.

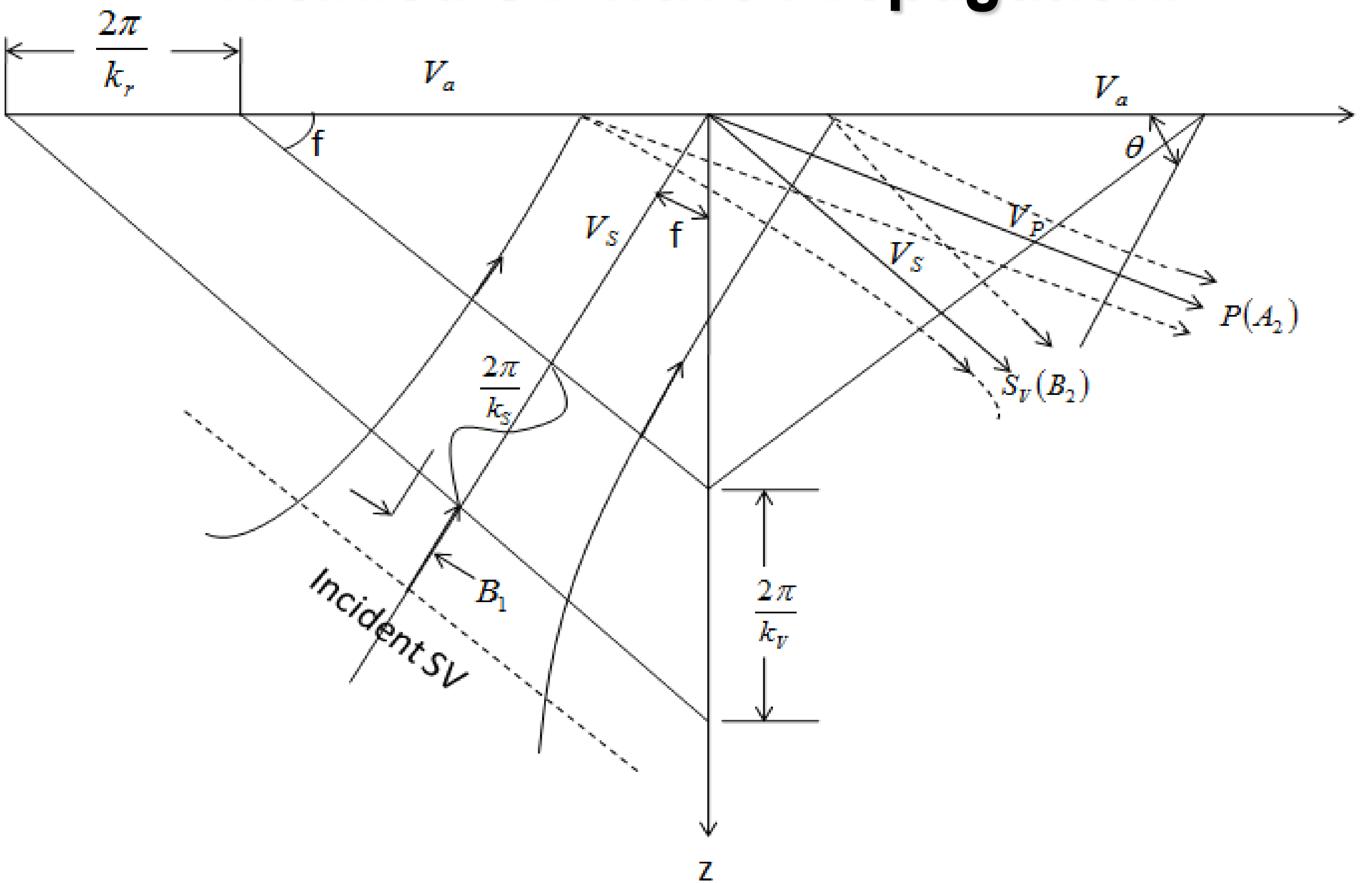

Incidence and Reflection of a SV Wave Arriving at a Free Surface

Layered Soil Model Via Thin Layer Method (TLM)

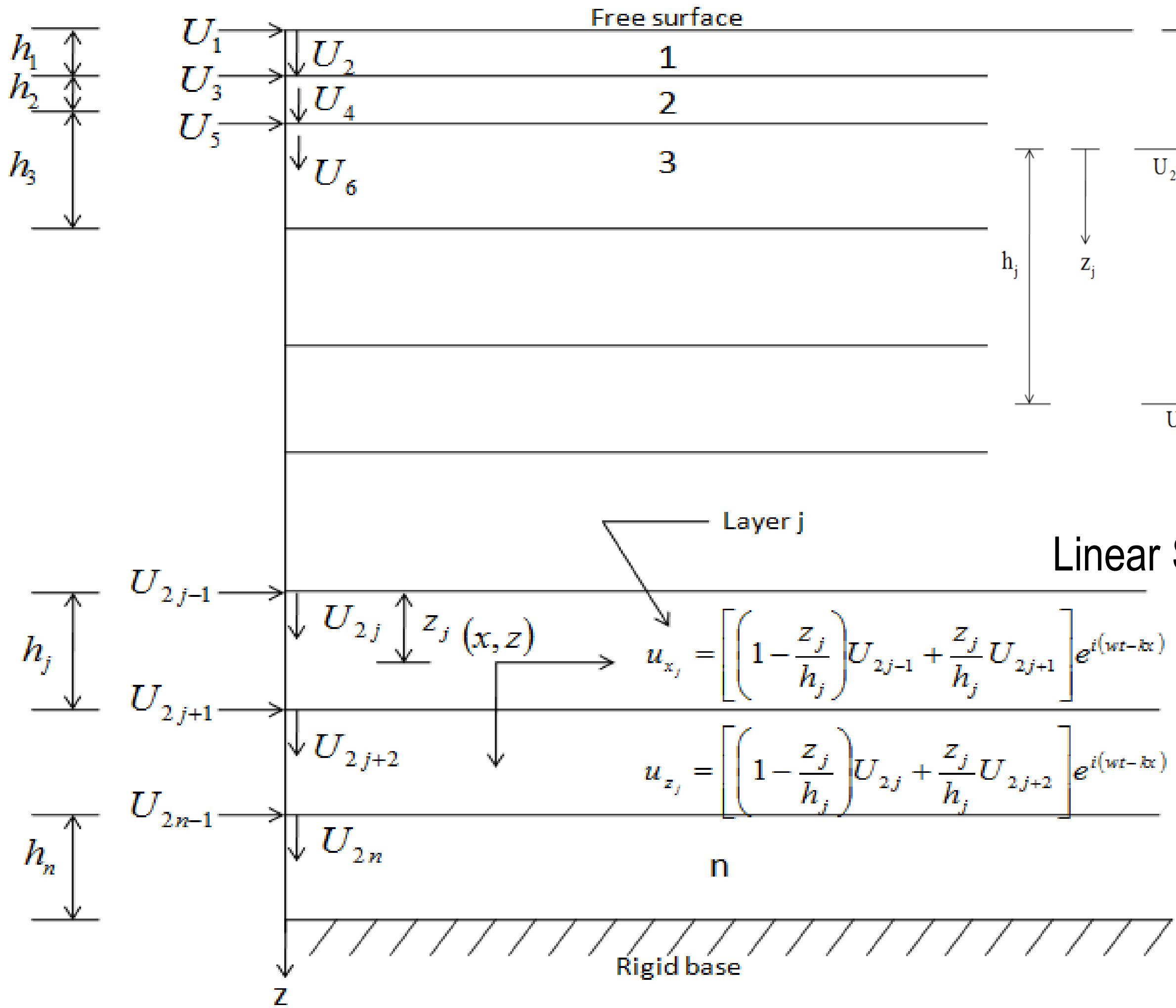

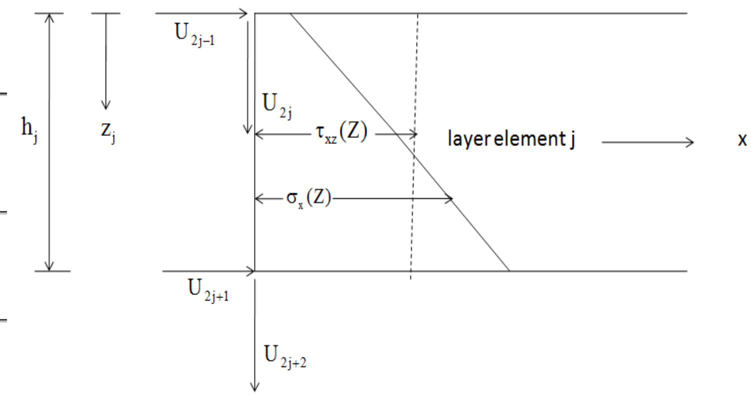

Linear Stress Variation Within Layer j

2n equations

Discrete Soil Layering System

Site Response Response for Seismic SV-P Waves

$$(Ak^2 + Bk + G - \omega^2 M)U = \begin{vmatrix} 0 \\ F_b \end{vmatrix}$$

TLM Solution

Solution to the above equation yields the displacement vector { U }.

The above matrix equation defines a *quadratic eigenvalue prob*lem.

Since the length of the finite element layer lengths do not appear in the matrices A, B, G and M indicates that wave radiation is considered without reflection.

The eigenvalues k are the possible wave numbers and the eigenvectors V are the corresponding mode shapes.

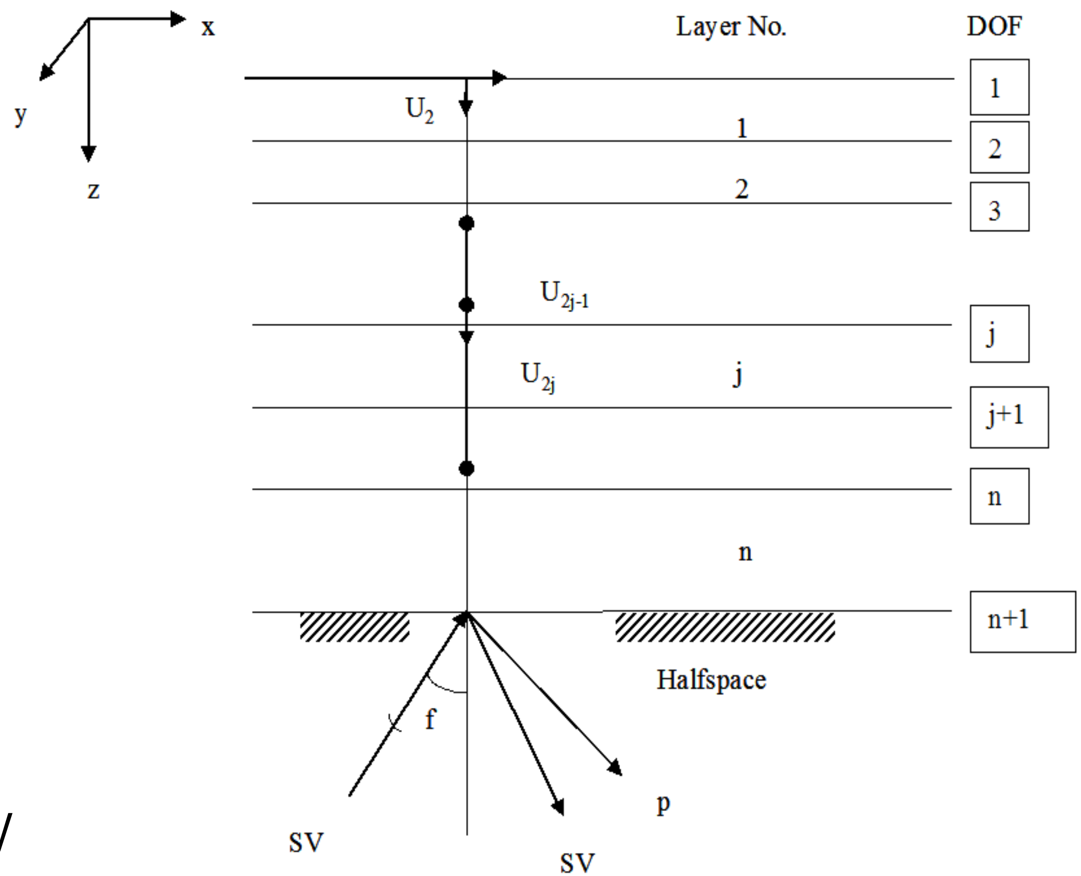

The n soil layer model for SV and P waves

Layered Soil Eigen Solution Iterative Algorithm

The quadratic eigenvalue problem has solution V if only and only if the determinant of the coefficient matrix vanishes. To get the solution of the quadratic eigenvalue problem an inverse iteration scheme with spectral shifting by Rayleigh coefficients and deflation via the Gram-Schmidt orthogonalization was applied.

Details in Wass, 1972, Chen, 1981, Kausel, 2006.

It should be noted that for soft nonuniform deep saturated soil deposit for which the Poisson coefficient is close to 0.50, say above 0.47 when a large number of soil layers is required, SITE module iterative algorithm for solving the soil layering eigenvalue problem might not converge correctly to the right solution, and this could further reflect in some spurious peaks in the complex amplitude SSI responses.

Free-Field Motion for Seismic SV-P Waves (cont.)

The k^2 and k matrices are diagonal matrices with complex wave numbers.

The layered soil system banded symmetric matrices A, B, G and M are assembled from the submatrices for each layer. Their size is 2n + 2.

The overall solution vector contains 2n + 2 displacement amplitudes for the n + 1 layer interfaces each having two degrees of freedom in the X and Z direction.

It should be noted that the solution is based on a continuum model theory in the horizontal direction and a discrete finite element in the vertical direction.

Free-Field Motion for Seismic SV-P Waves (cont.)

The site response complex displacement solution at a given frequency is expressed as

$$Ue^{-i\omega t} = \sum_{S=1}^{2n} \alpha_S V_S e^{i(\omega t - k_s x)}$$

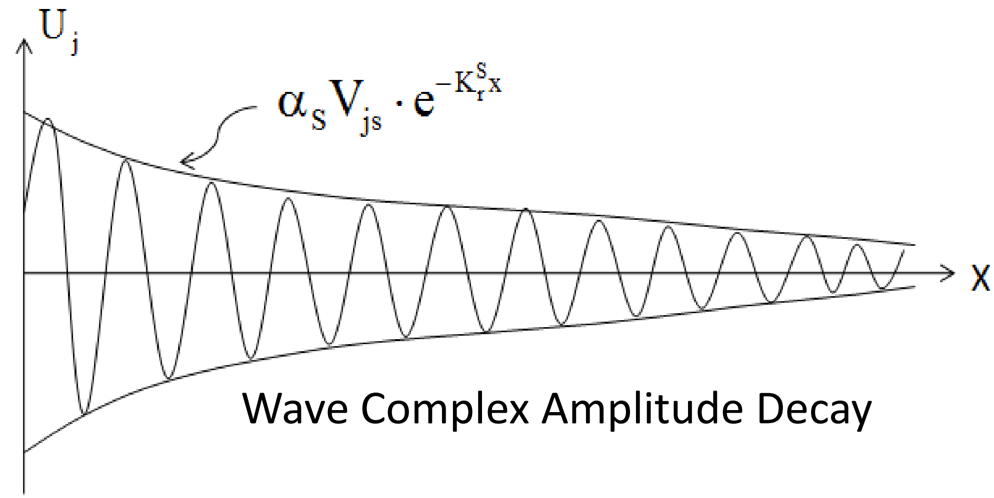

Or, for the complex amplitude displacement response

$$U = \sum_{S=1}^{2n} \alpha_S V_S e^{-ik_s x} = \sum_{S=1}^{2n} \alpha_S V_S e^{-k_{i,s} x} e^{-ik_{r,s} x}$$

where α_S are the mode participation factors and V_S are the mode shapes.
The complex wave number K has a real part $K_{r,s} = \omega / C_s$ and an imaginary part $K_{i,s}$ that characterizes the wave propagation speed (phase velocity) and the amplitude decay.

The negative ratio $-(K_i / K_r)$ is a measure of how fast the wave mode decays for a single wavelength.

Free-Field Motion for Vertically Propagating S and P Seismic Waves

For vertically propagating waves the quadratic eigenvalue problem reduces to a linear eigenvalue problem since matrices A and B are zero. Therefore the solutions for the SV and P waves are decoupled.

For vertically propagation waves the complex amplitude solution takes the form

$$U(z) = \sum \alpha_S V_S(z) e^{-ikx}$$

Note that the above equation defines the motion at any horizontal distance x and for all the points on layer interfaces within the soil model.

Once the location of control point is selected, the horizontal distance x can be obtained for all the interaction nodes.

Soil Layer Thickness Size Limitation for SSI Analysis (due to TML Formulation)

- For such elements the accuracy of the solution is function of the method used to compute the mass matrix and an accuracy better than 10 percent on wave amplitude is obtained if the element size **h** follows the relations shown below:

$$h \le \left| \begin{array}{l} 1/8\, \lambda_s \quad \text{for lumped mass matrix} \\ 1/5\, \lambda_s \quad \text{for consistent mass matrix} \\ \boxed{1/5\, \lambda_s \ \text{for mixed mass matrix}} \longleftarrow \end{array} \right.$$

- The wave length is obtained from

$$\lambda_s = \frac{V_s}{f_{max}}$$

Modeling of Semi-Infinite Halfspace Bedrock

The Variable Depth Method (Soil Buffer Layers)

The total depth H of the added layers varies with frequency and is set to:

$$H = 1.5\frac{V_s}{f}$$

The total thickness of the n layers is:

$$H = h_0 + \alpha^2 h_0 + --- + \alpha n h_0 = \frac{(\alpha^n - 1)h_0}{\alpha - 1}$$

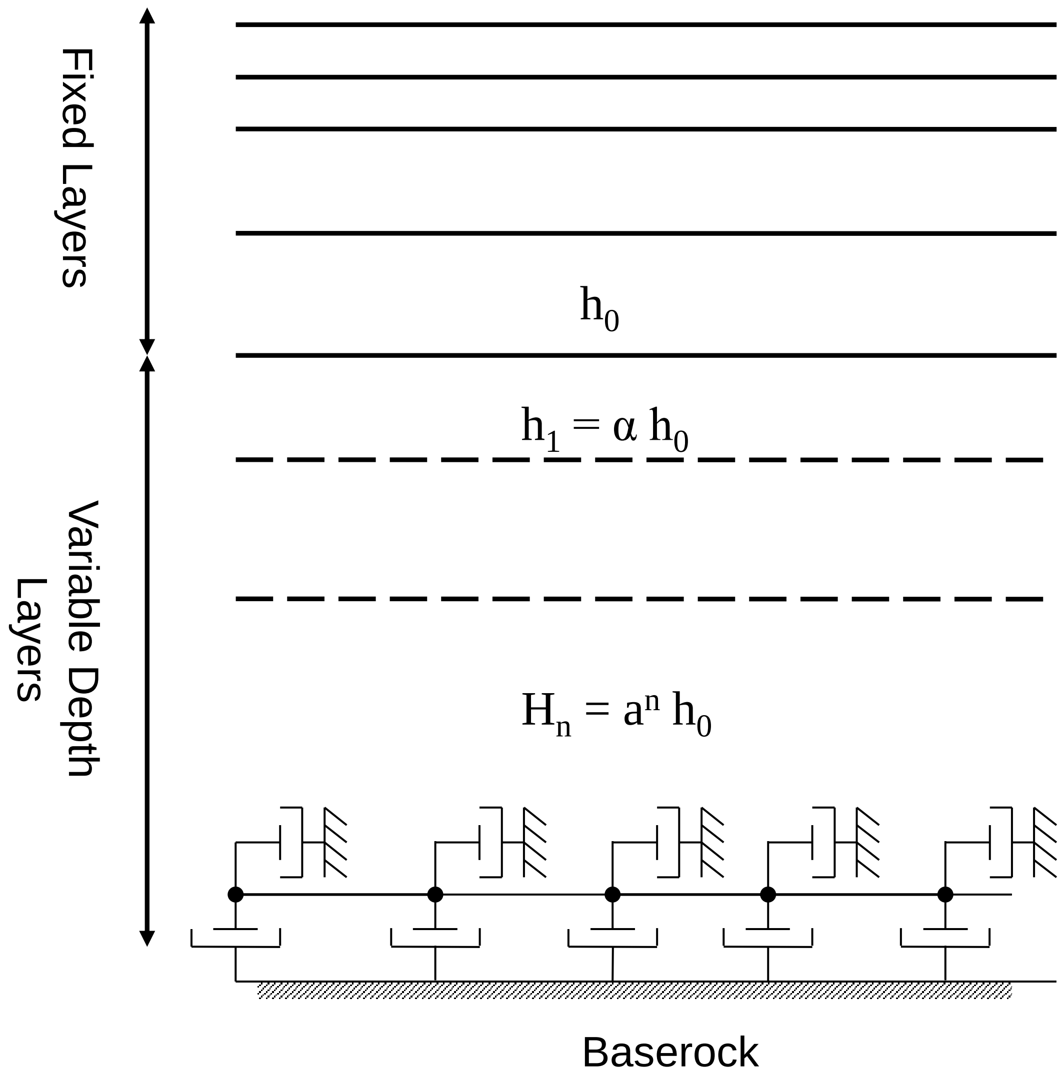

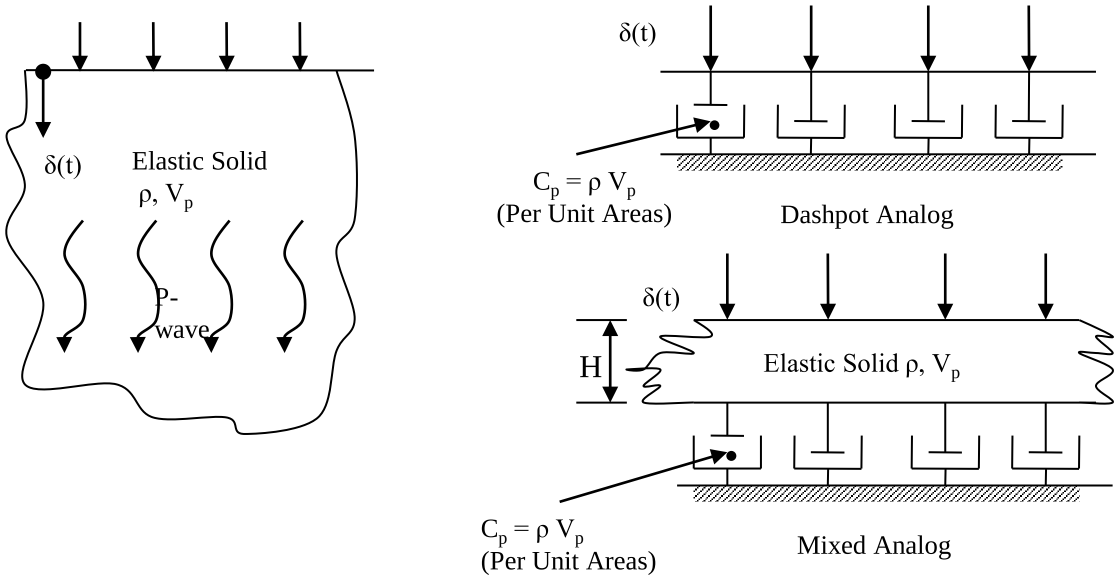

Vertically Loaded Halfspace

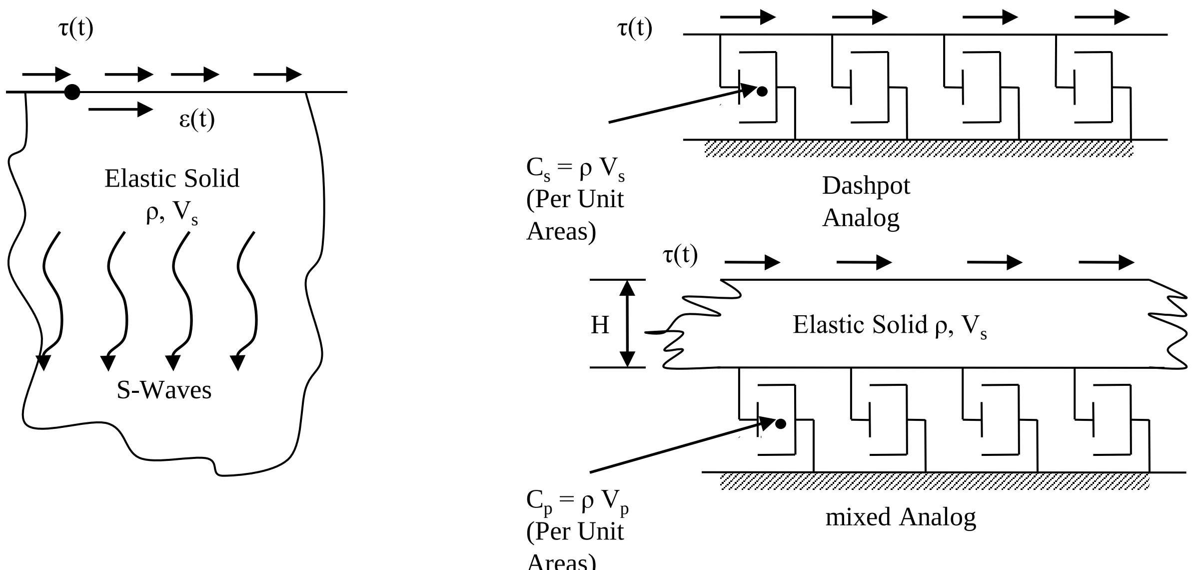

Horizontally loaded Halfspace

Free-Field Motion for Rayleigh Waves

For the generalized Rayleigh wave motion of the free-field equation is:

$$(Ak^2 + iBk + G - \omega^2 M)U = 0$$

The quadratic eigenvalue problem has solution V if only and only if the determinant of the coefficient matrix vanishes.

To get the solution of the quadratic eigenvalue problem an inverse iteration scheme with spectral shifting by Rayleigh coefficients and deflation via the Gram-Schmidt orthogonalization was applied.

The iterative algorithm was further modified for different incident waves, and to include at the soil layering base a viscoelastic half space.

The viscoelastic halfspace is simulated by combining the soil layer variable depth method with a Lysmer-Kuhlemeyer viscous boundary at the bottom of the model

The solution for Rayleigh waves has the same form as for body waves:

$$u = \sum_{S=1}^{2n} \alpha_s V_s e^{i(\omega t - k_s x)}$$

Free-Field Models for Rayleigh and Love Waves

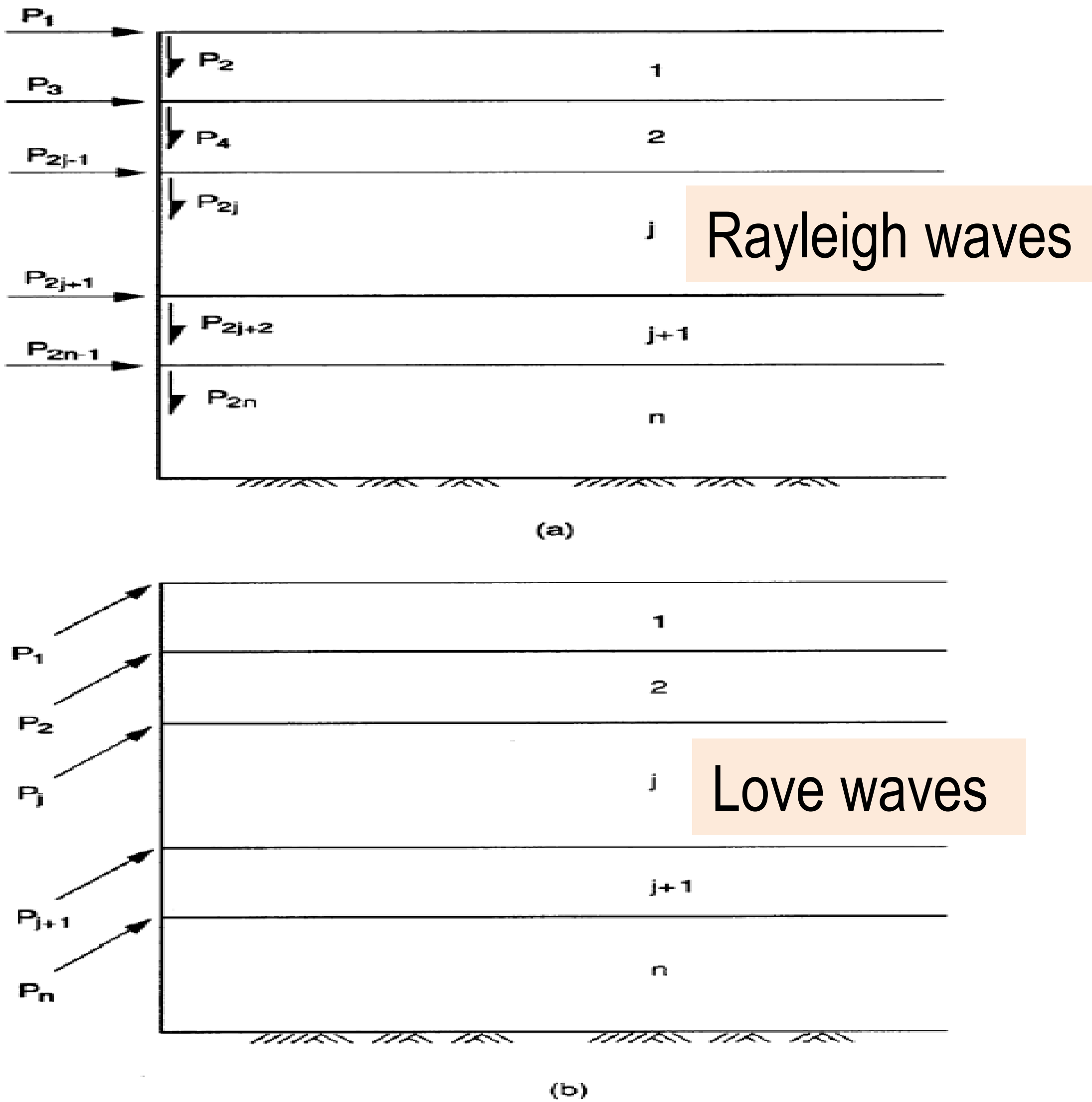

The n soil layer model for a) Rayleigh waves and b) Love waves

The solution for the Rayleigh and Love wave mode shapes with the associated wave numbers are also used for computing the transmitting boundary matrix for the wave motions moving out of the plane of the site model.

3D Scattered Wave Transmission and Soil Impedance Calculations

3D Consistent Boundary For Energy Transmission Using Axisymmetric Layered Soil Model

The problem of evaluating the dynamic flexibility matrix for a SSI problem reduces to the problem of finding the response of horizontally layered system to point loads at the layer interfaces. In 3D space this problem is an axisymmetric problem and can be solved using the axisymmetric FE model.

The model consists of a central cylinder with radius that is discretized in axisymmetric quadrilateral elements and is enclosed by an axisymmetric transmitting boundary.

The lower boundary of the soil layering is a viscoelastic halfspace that can de simulated using the variable depth and viscous boundary methods described before.

Consistent boundaries constitute perfect absorbers of any kind or waves impinging with arbitrary incidence. They can be placed next to embedded structures, so that size of FE model stays reasonably small.

3D Consistent Boundary For Energy Transmission Using Axisymmetric Layered Soil Model

Degrees of Freedom for Transmitting Boundary

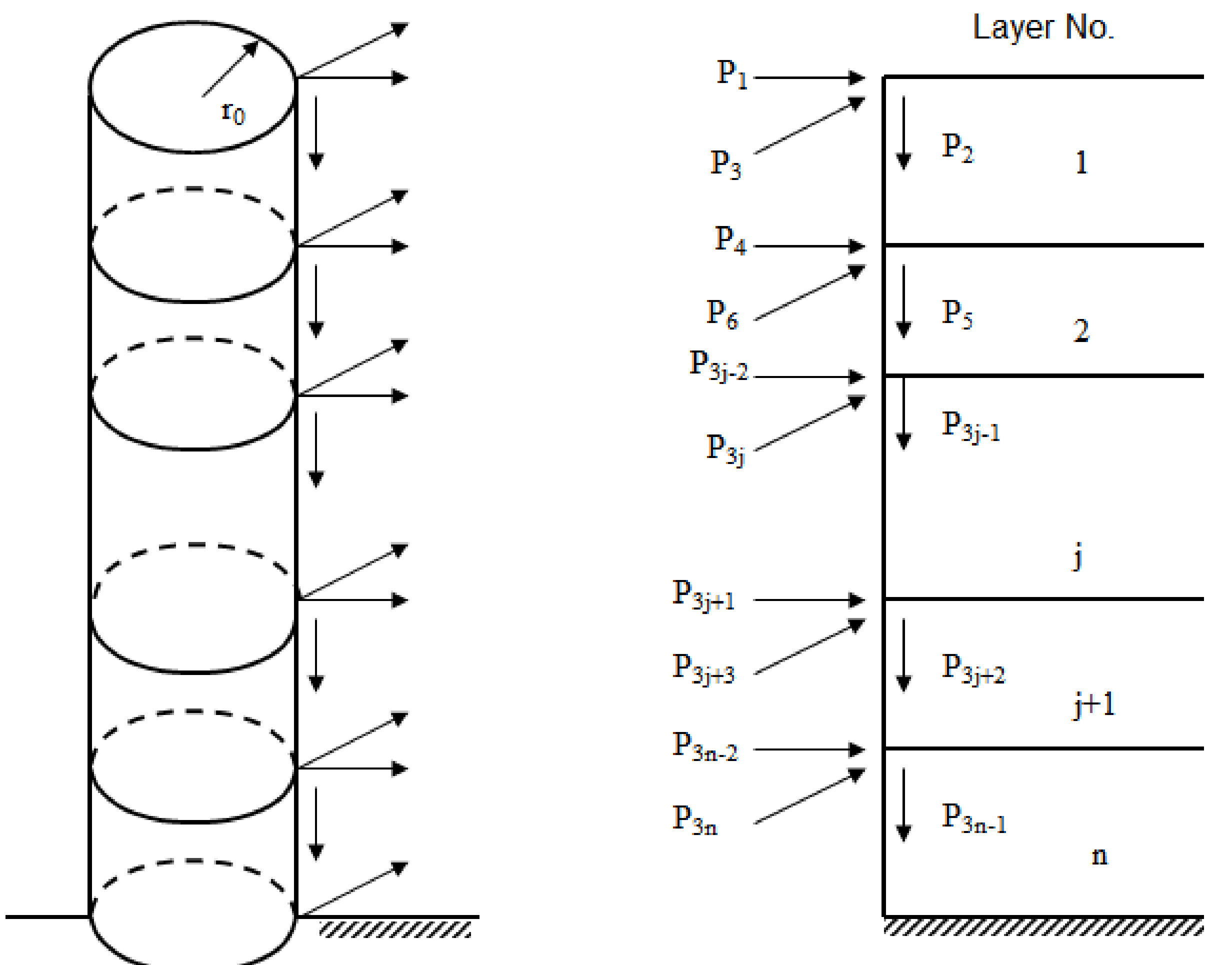

3n equations

(Kausel, 1974, 1981):

3D Consistent Boundary For Energy Transmission Using Axisymmetric Layered Soil Model (cont.)

Horizontal

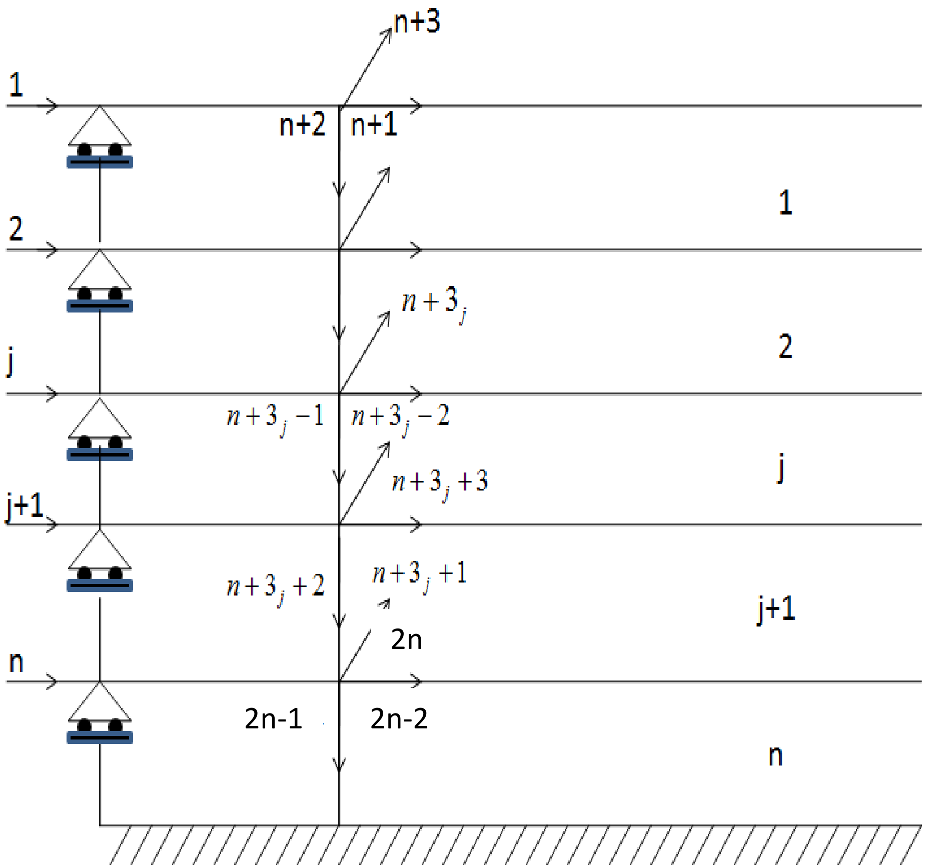

Boundary Conditions for Horizontal Loading

Vertical

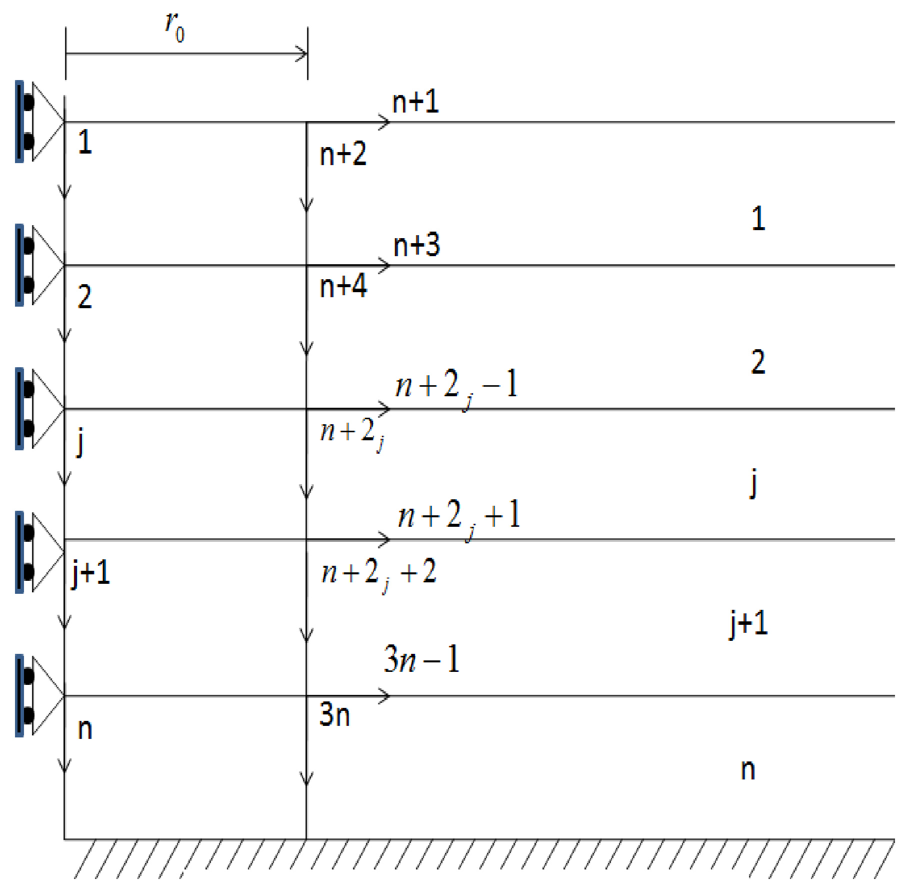

Boundary Conditions for Vertical Loading

Modal Matrices for Rayleigh & Love Waves

These 3n x 3n wave mode shape matrices are obtained for each mode l by assembling the elementary matrices for each layer interface j and Fourier harmonic n that are described as follows:

$$\Phi_{jl}(r) = \begin{bmatrix} -H_{n-1}(K_l r) & 0 & 0 \\ 0 & H_n(k_l r) & 0 \\ 0 & 0 & -H_{n-1}(k_l r) \end{bmatrix} \begin{bmatrix} V_{j,l} \\ V_{j+1,l} \\ V_{j+2,l} \end{bmatrix}$$

Rayleigh waves

$$\Psi_{jl}(r) = \begin{bmatrix} H_n(k_l r) & 0 & 0 \\ 0 & -H_{n-1}(k_l r) & 0 \\ 0 & 0 & H_n(k_l r) \end{bmatrix} \begin{bmatrix} V_{j,l} \\ V_{j+1,l} \\ V_{j+2,l} \end{bmatrix}$$

Love waves

where j = 1, 3n-2, 3.

Free-Field Modal Matrices for j-th Layer Interface

The 3n x 3n mode shape be matrix at the j-th layer interface for radius r is

$$W_{jl}(r) = \begin{bmatrix} H_n^{'}(k_l r) & 0 & \frac{n}{r} H_n(k_l r) \\ 0 & H_n(k_l r) & 0 \\ \frac{n}{r} H_n(k_l r) & 0 & H_n^{'}(k_l r) \end{bmatrix} \begin{bmatrix} u_{j,l} \\ u_{j+1,l} \\ u_{j+2,l} \end{bmatrix}$$

Then the axisymmetric displacement solution for Fourier harmonic n is:

$$u_n(r) = \sum_{i=1}^{3n} \alpha_i H_n(k_i r) V_i = W(r)\Gamma$$

where the V are the projections of Rayleigh and Love wave mode shapes in the cylindrical system. Also, if u is known for $r = r_0$, $\Gamma = W(r = r_0)^{-1} u(r = r_0)$

The notations $H_n^{'}(Kr) = \frac{\partial H_n(Kr)}{\partial r}$ and $H_n(Kr)$ are the complex Hankel transforms functions of order n related to the Fourier harmonic expansion order of the 2nd kind.

Computation of Layered Soil Flexibility Matrix

For each node dof the flexibility is computed using an axisymmetric model that includes a central zone with radius of cylindrical elements enclosed by an axisymmetric consistent boundary.

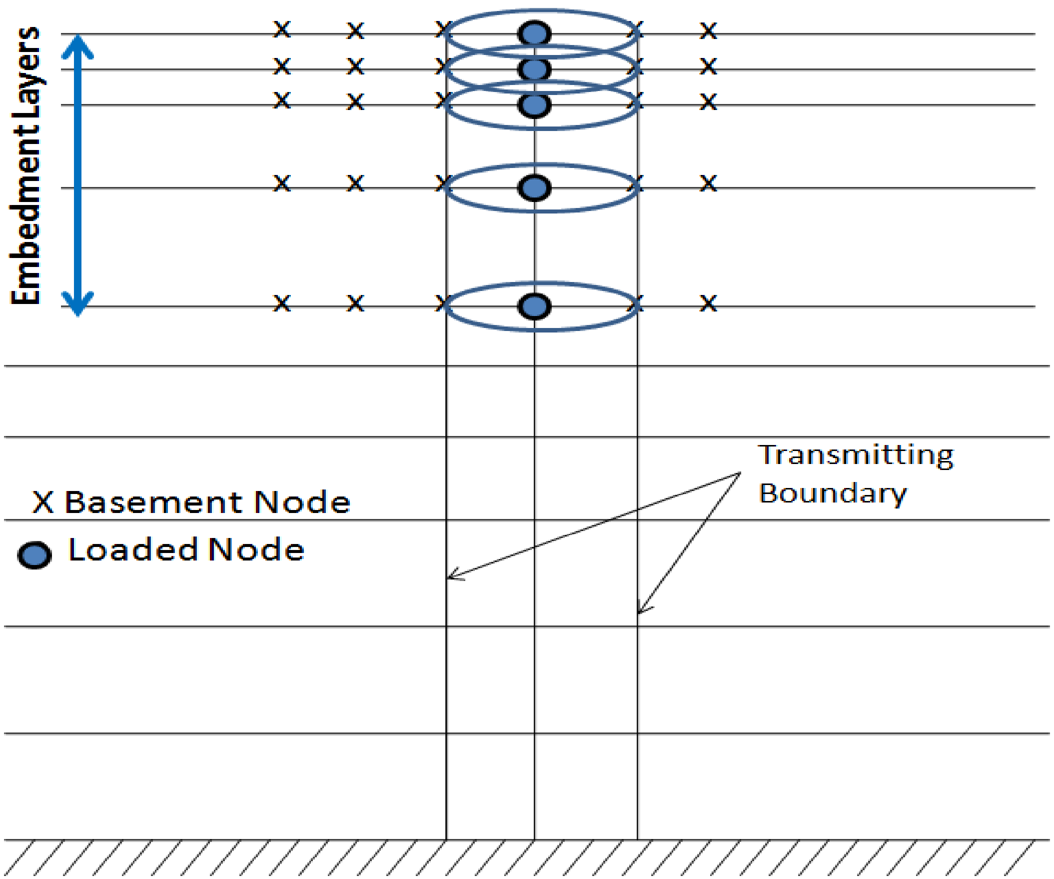

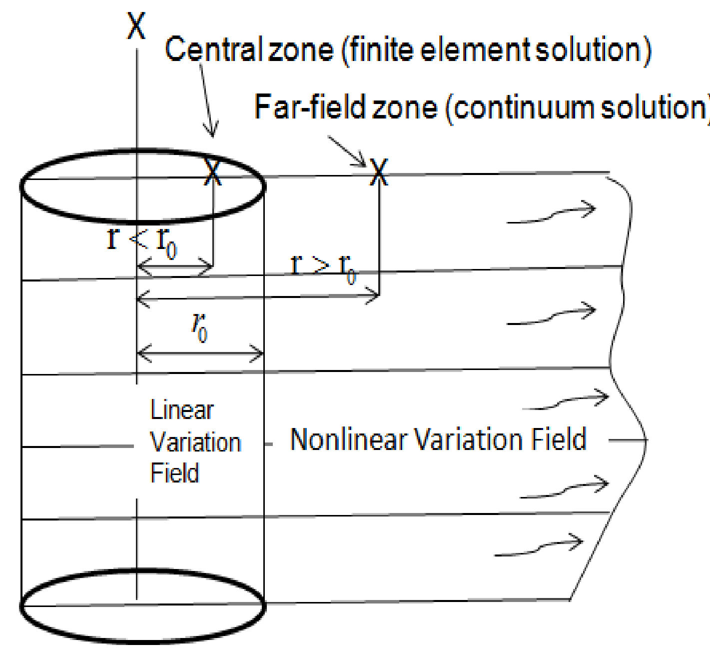

Column Load Pattern for SSI Interaction Nodes

3D Transmitting Boundary Matrix Computed for Point Loads in 3D Free-Field Layered Soil Space

It is important to relate the forces to the displacements on the layered boundary of a half-space from which the cylindrical core with radius r has been removed. The dynamic stiffness of the layered system is computed in terms of the Rayleigh and Love wave mode shapes by integrating layer stresses under harmonic loads and sum them up. For all the soil layers, the dynamic boundary forces for $r = r_0$ can be computed for any frequency .

$$\{P\}_m = [R]_m \{U\}_m$$

Love waves

Rayleigh waves

The stiffness matrix takes the following form:

$$[R]_m = r_0 \{[A][\psi]_m [K^2] + ([D] - [E] + m[N][\phi]_m [K] - m(\frac{m+1}{2}[L] + [Q])[\psi]_m [W(r_0)]^{-1}\}$$

(Waas, 1972, 1985, Kausel, 1974, 1981)

Layered Soil Impedance Matrix Computation

In this method, the flexibility matrix need be computed for all the interacting nodes using the methods described above.

The impedance matrix is obtained by inverting the flexibility matrix, i.e.,

$$\mathbf{X}_{\mathbf{ff}} = \mathbf{F}_{\mathbf{ff}}{}^{-1}$$

- The inversion of the matrix is computationally intensive and needs to be performed for every frequency of analysis.
- An efficient in-place inversion routine is used to invert the flexibility matrix which is a full matrix in the direct method of analysis.
- For total number of i interacting nodes, the resultant impedance matrix of the order of 3i x 3i for three-dimensional problems.

Layered Soil Impedance Matrix Computation

Computational Steps:

1. Compute Flexibility Matrix (complex soil displacement amplitudes under unit amplitude harmonic forces at each frequency)

2. Compute Impedance Matrix (complex soil stiffness amplitudes)
   - Flexible Volume Method (FV, uses all excavation interaction nodes)
   - Flexible Interface Method (FV-EVBN or MSM, ESM, SM, FFV, uses only excavation interface nodes)

3. Equivalent Global Impedances (Optional, Old option).
   NOT RECOMMENDED. These are not foundation impedances!

FE Modeling and FVS-Based SSI Approaches

Typical Nuclear Island ACS SASSI Modeling (Using 3D FE Models)

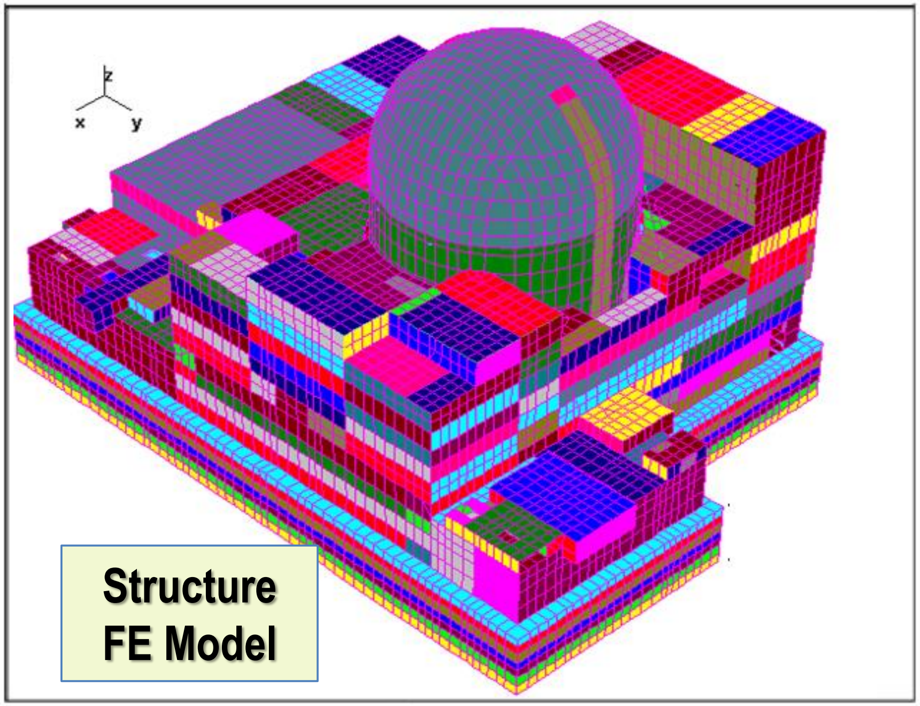

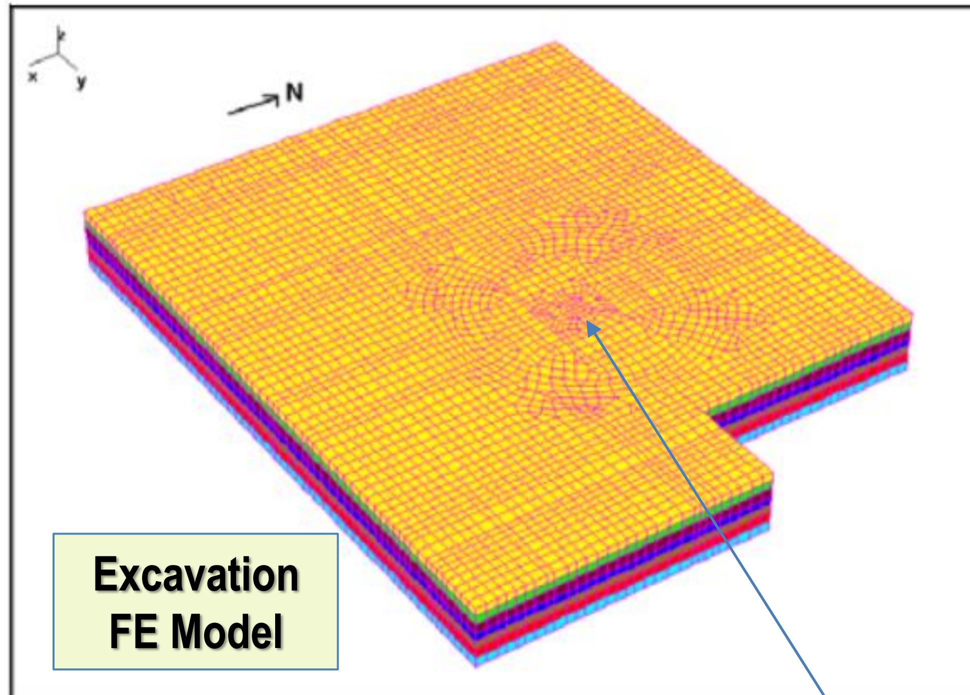

US-APWR RB SSI Model

Ghiocel et. al., 2013, SMIRT22

ACS SASSI Nonlinear Soil Behavior Using Iterative Equivalent-Linear SSI Analysis (3D and 2D Models)

US-APWR ACS SASSI MODEL

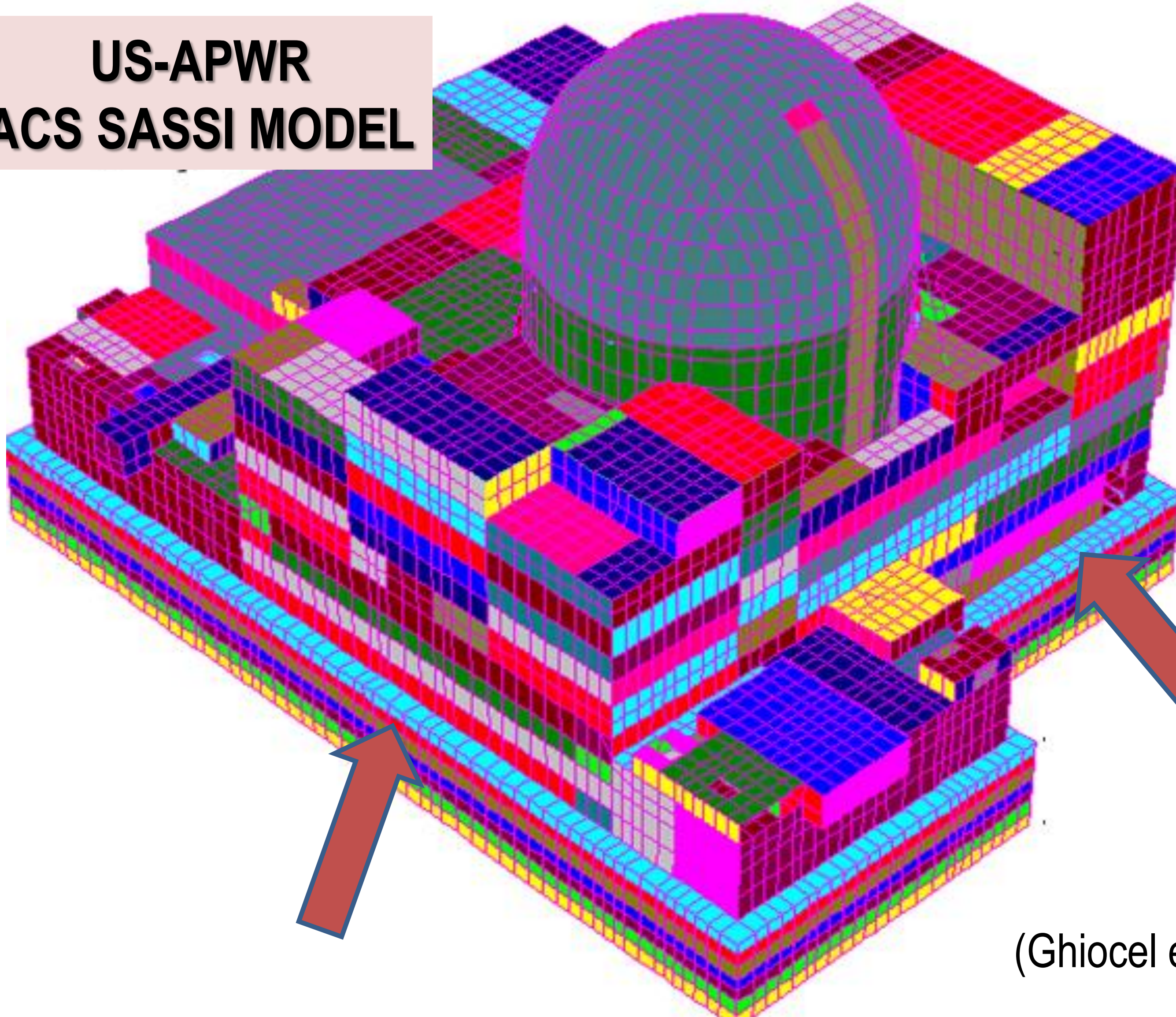

Iterative EQL

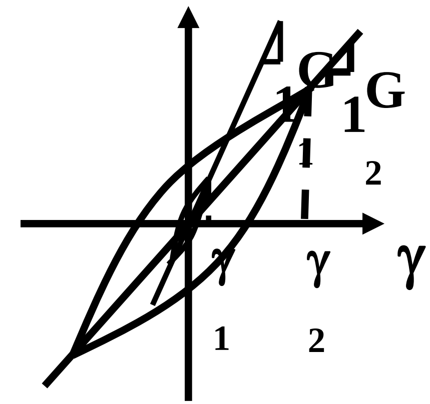

Nonlinear soil solid elements

(Ghiocel et. al., 2013, SMIRT22)

Standard vs. Improved FE Modeling for SSI

"*Standard*" SASSI Modeling

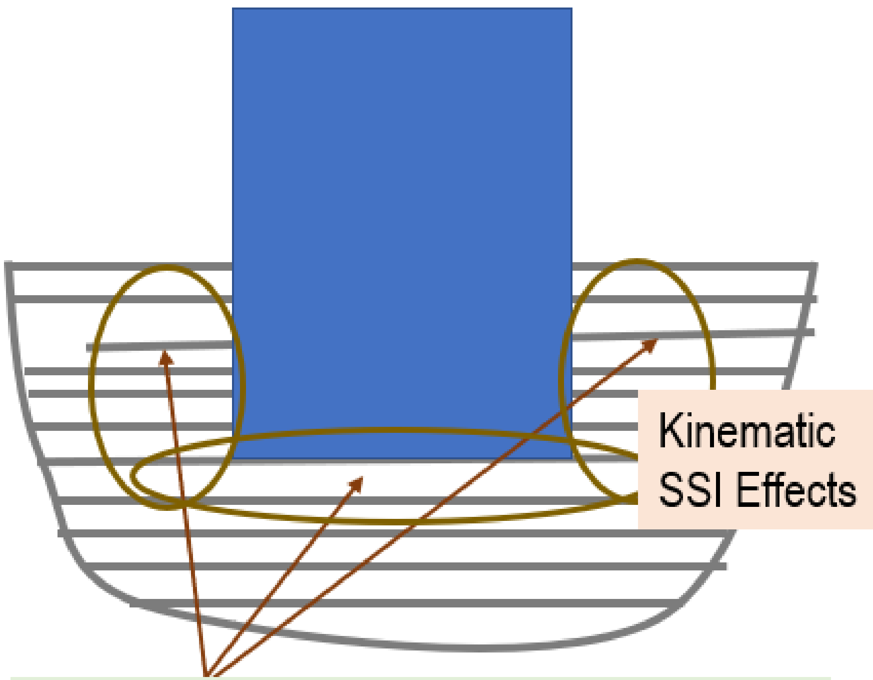

Typically, SSI model uses in the vicinity of foundation iterated strain-compatible soil layer properties computed using iterative 1D wave propagation equivalent-linear approach, *EQL via SHAKE methodology*. Kinematic SSI effects are neglected.

"*Improved*" SASSI Modeling

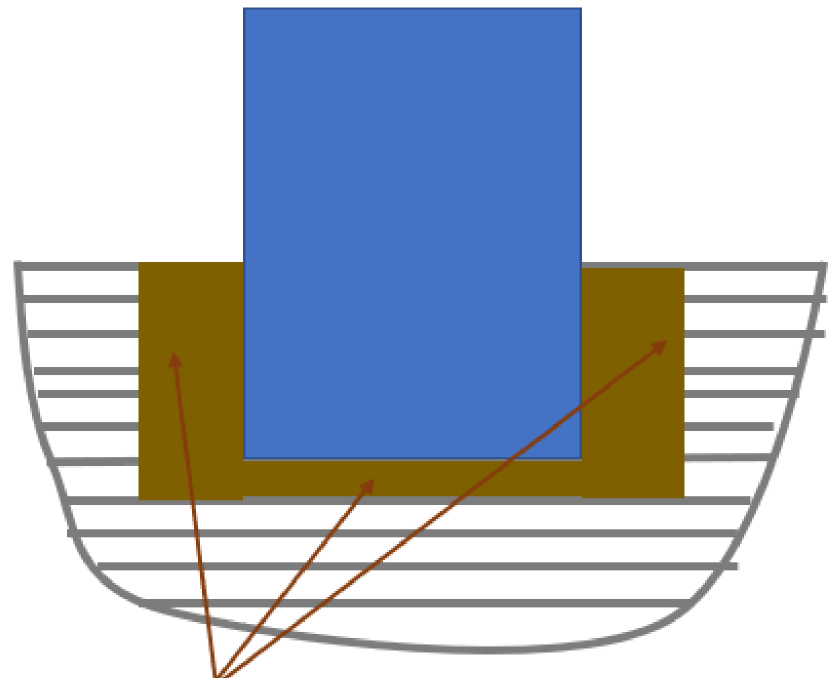

SSI model uses in the vicinity of foundation iterated strain-compatible soil layer properties computed using iterative 3D SASSI equivalent-linear approach to capture kinematic SSI effects, *EQL via fast SASSI iterations.*

SASSI Flexible Volume for Embedded Structures

Flexible Volume Substructuring Approaches

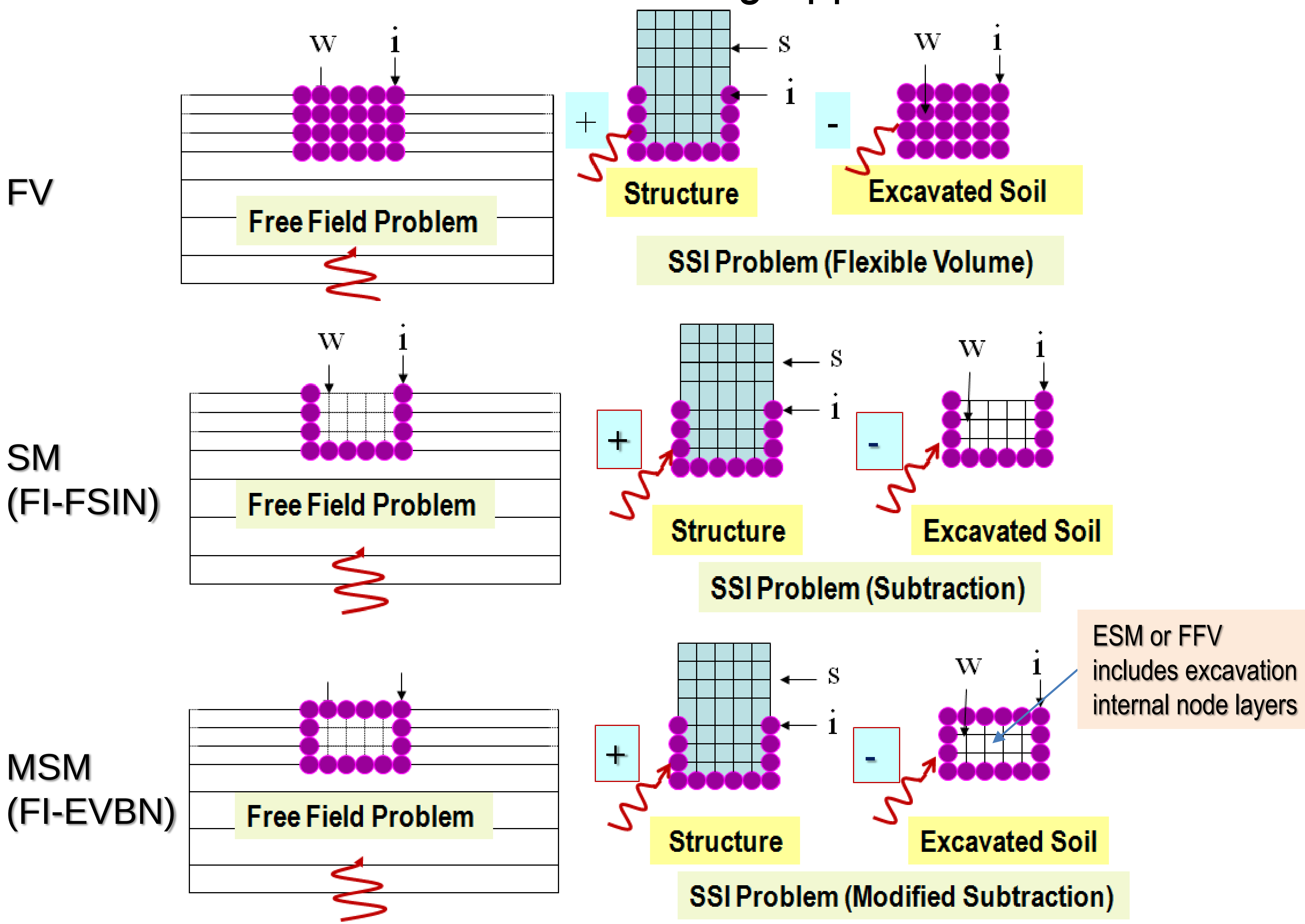

Excavated Soil Vibration Using FVM, SM and MSM

Effects of Ground Surface Constraints on Scattered Surface Wave Solution

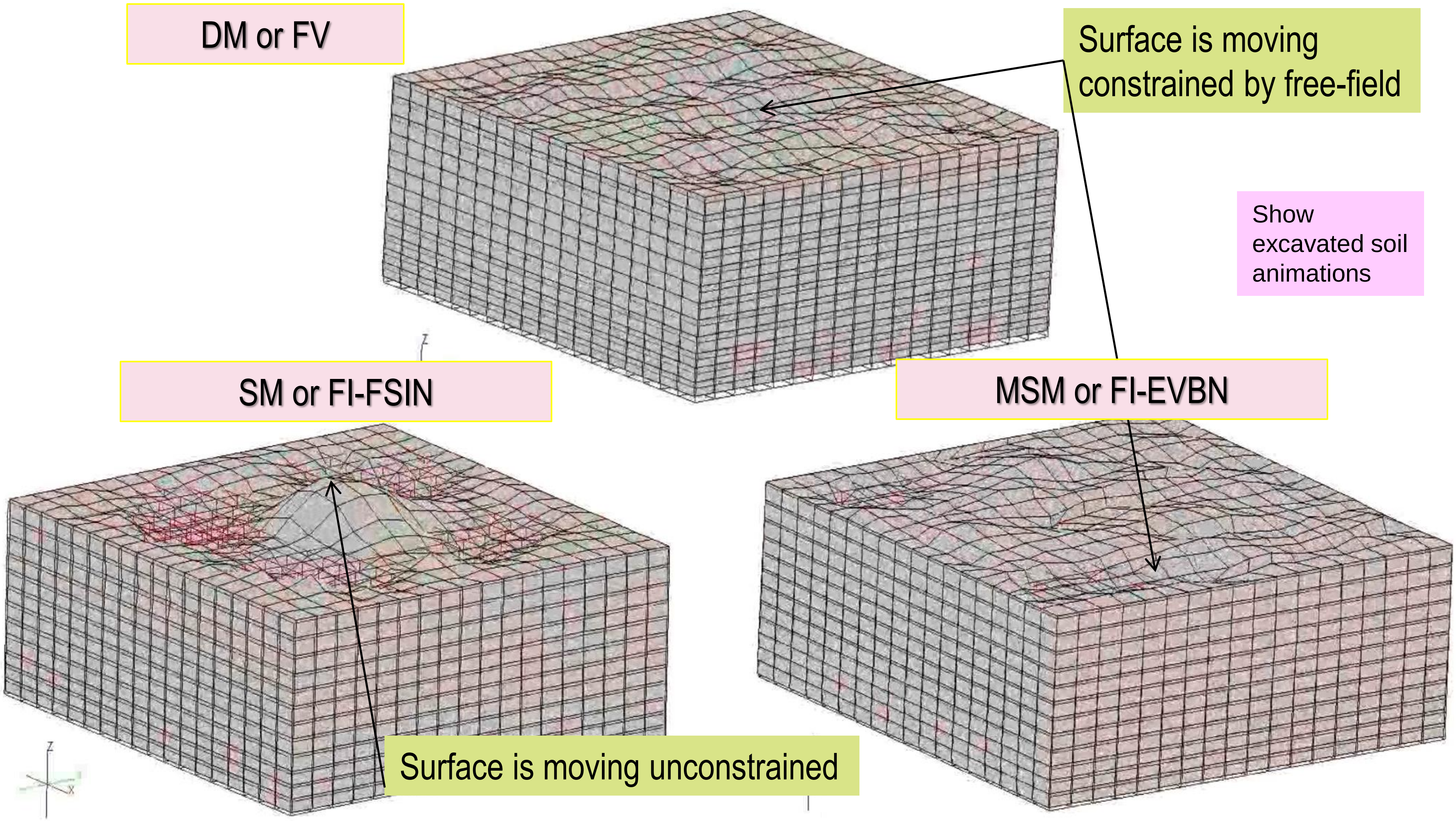

MSM Approach Failure for Deeply Embedded NI

Direction X

Direction Z

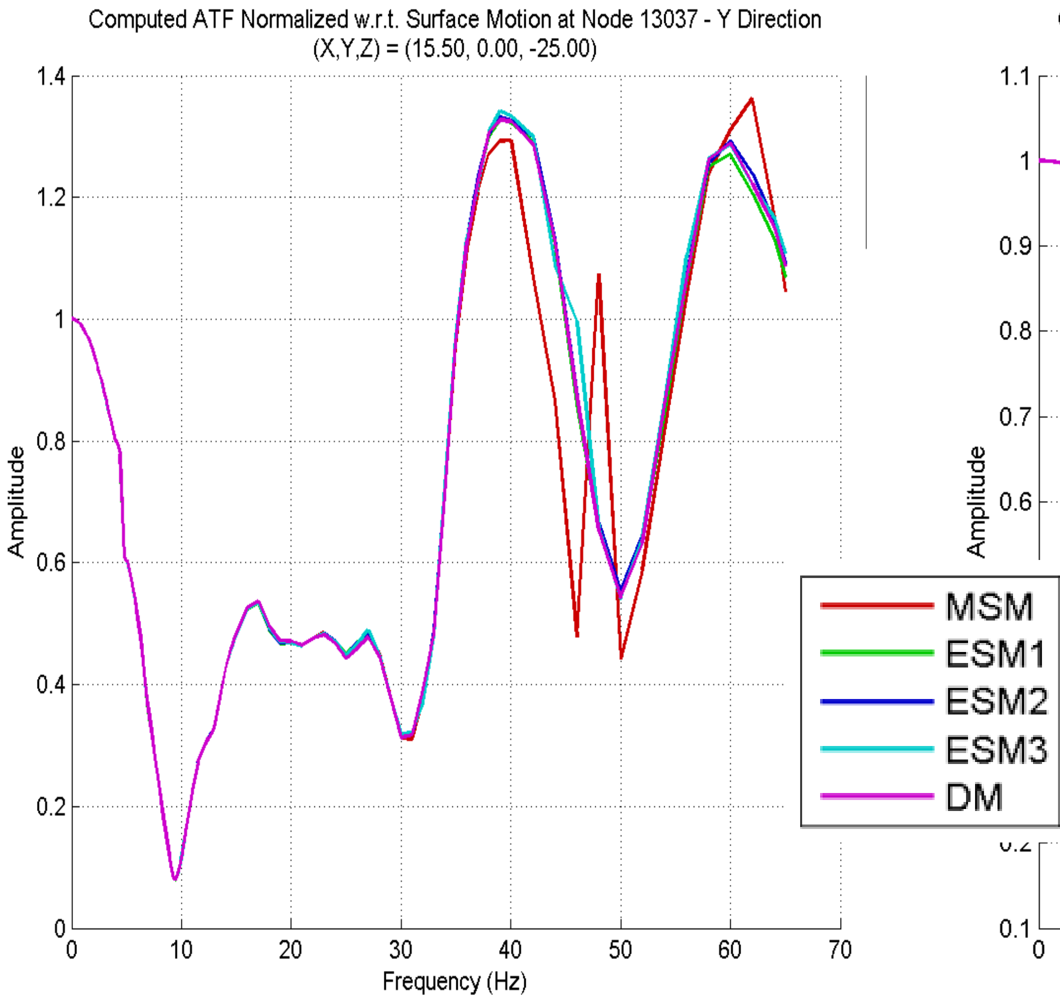

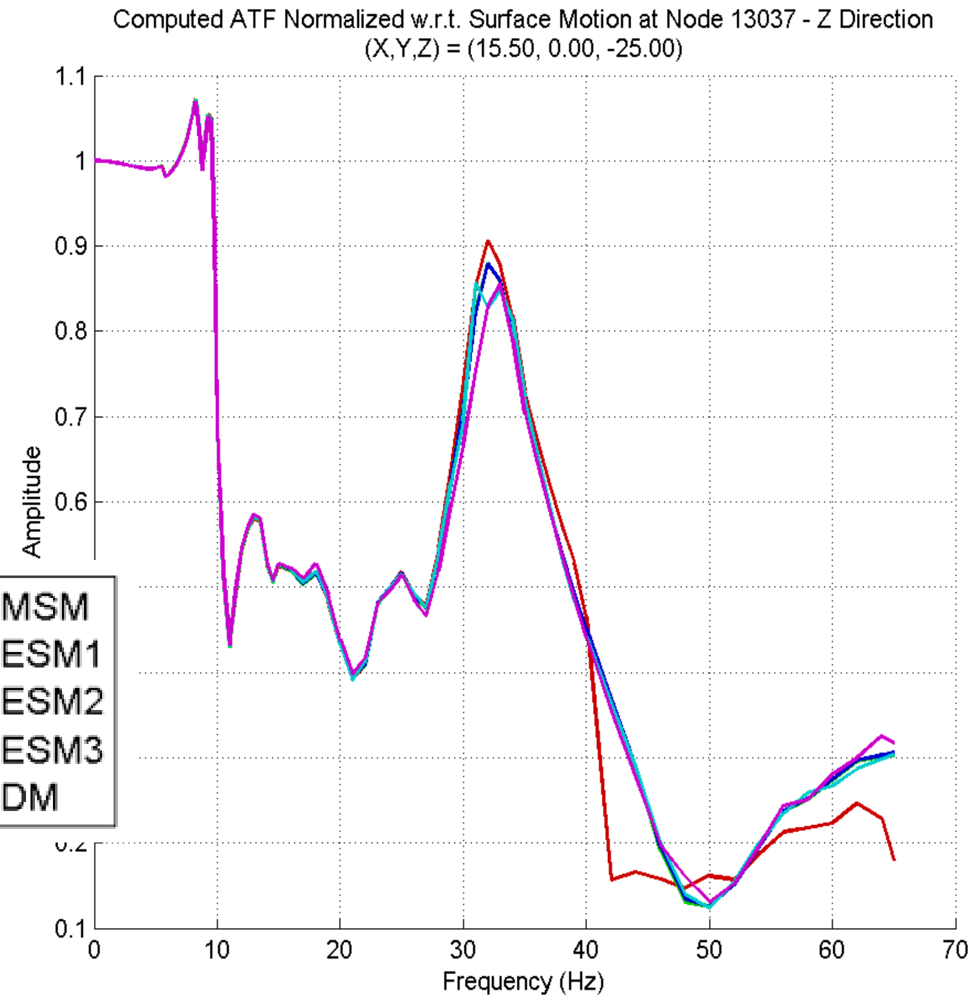

Fully Embedded SMR Methodology Study

Volume Size: 120 ft x 80 ft x 80 ft

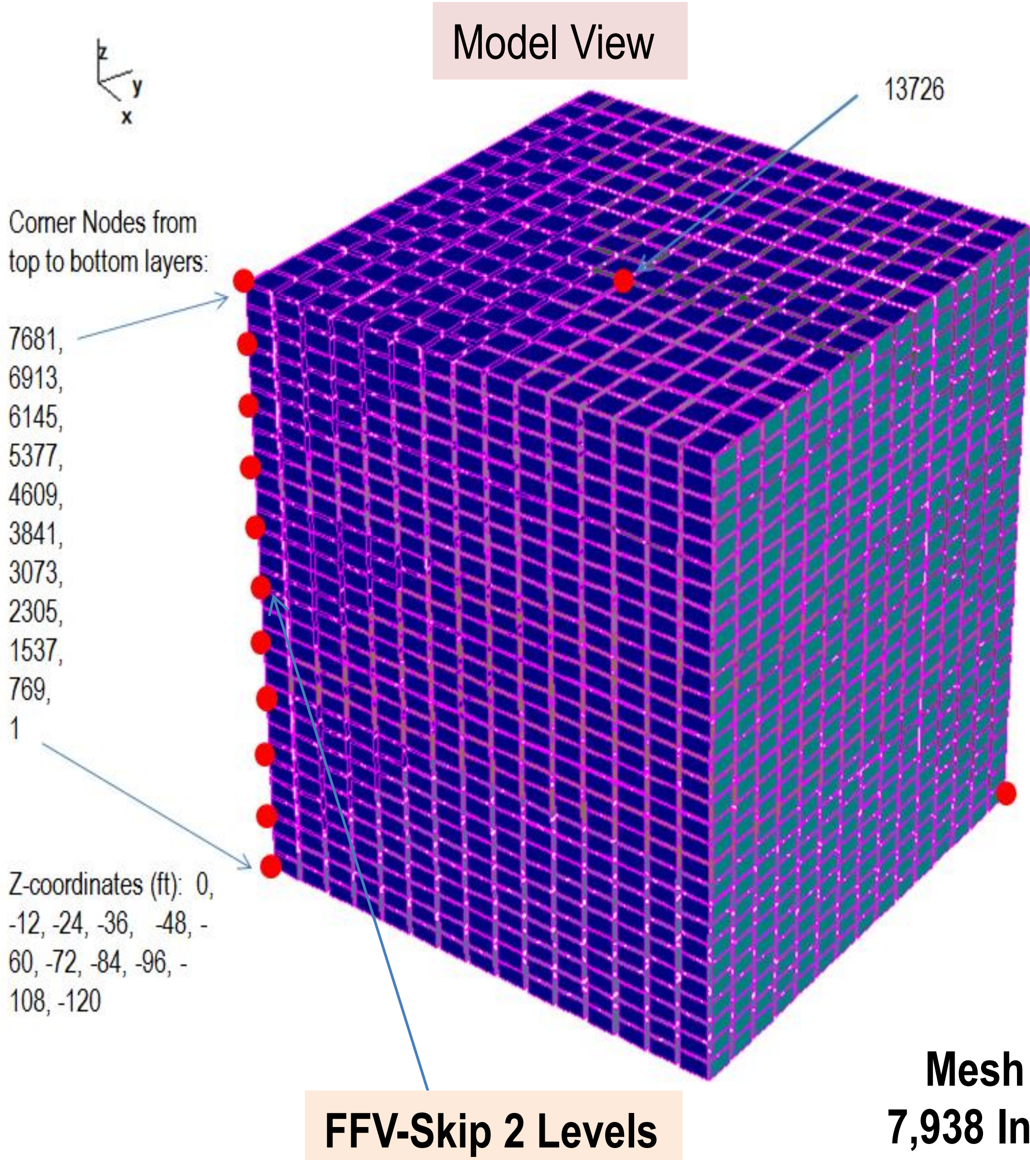

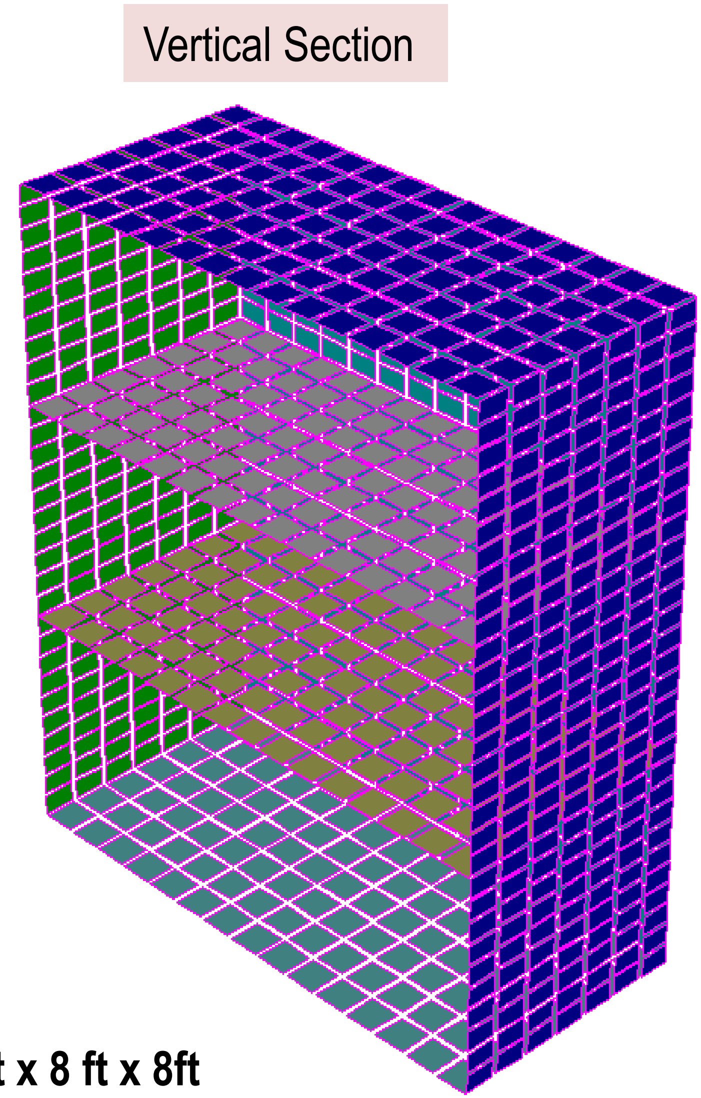

Mesh 4 ft x 8 ft x 8ft
7,938 Interaction Nodes

Excavation Study on SASSI FV Substructuring Methods

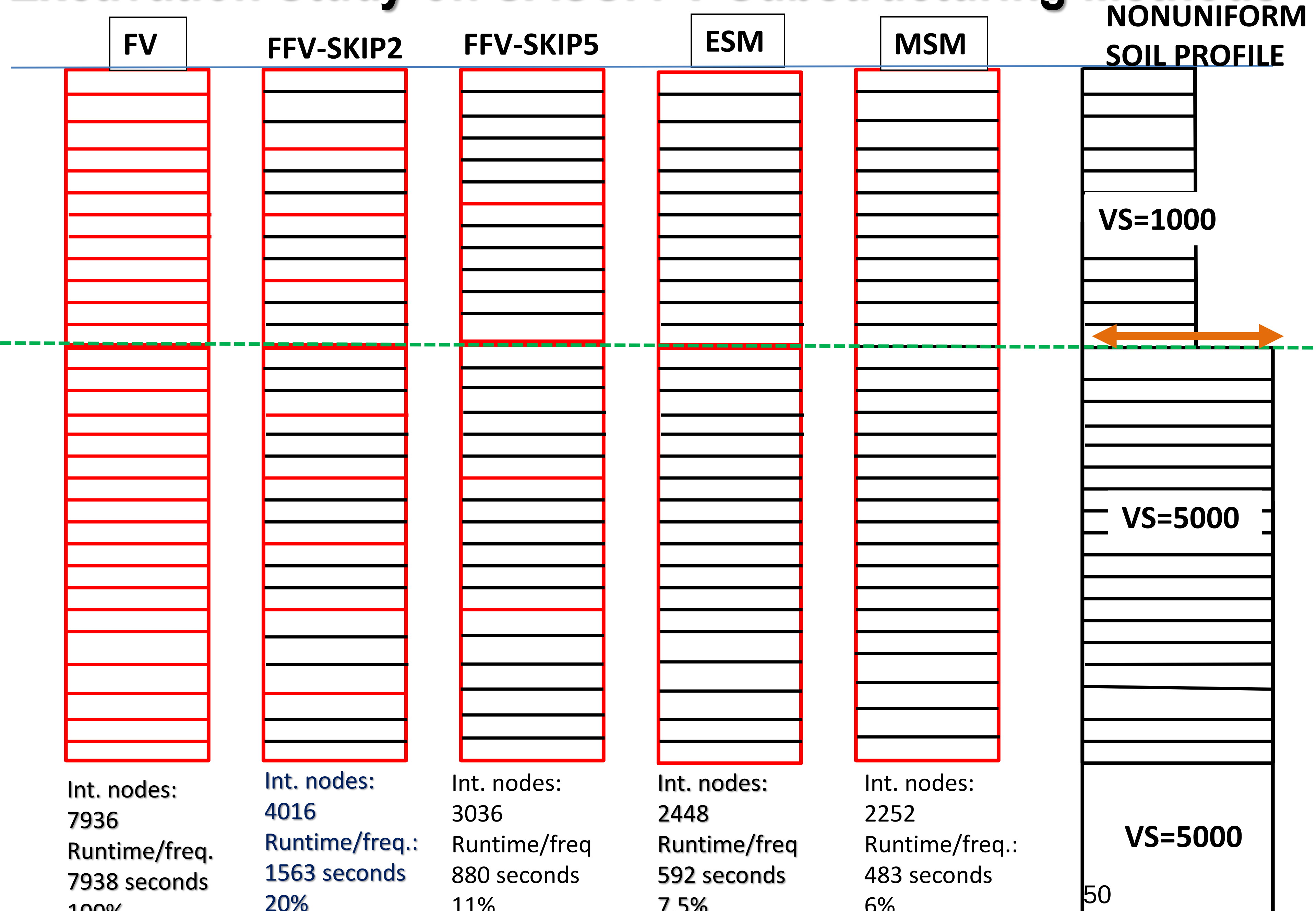

Comparative ATF at -120 ft Depth (Foundation Level)

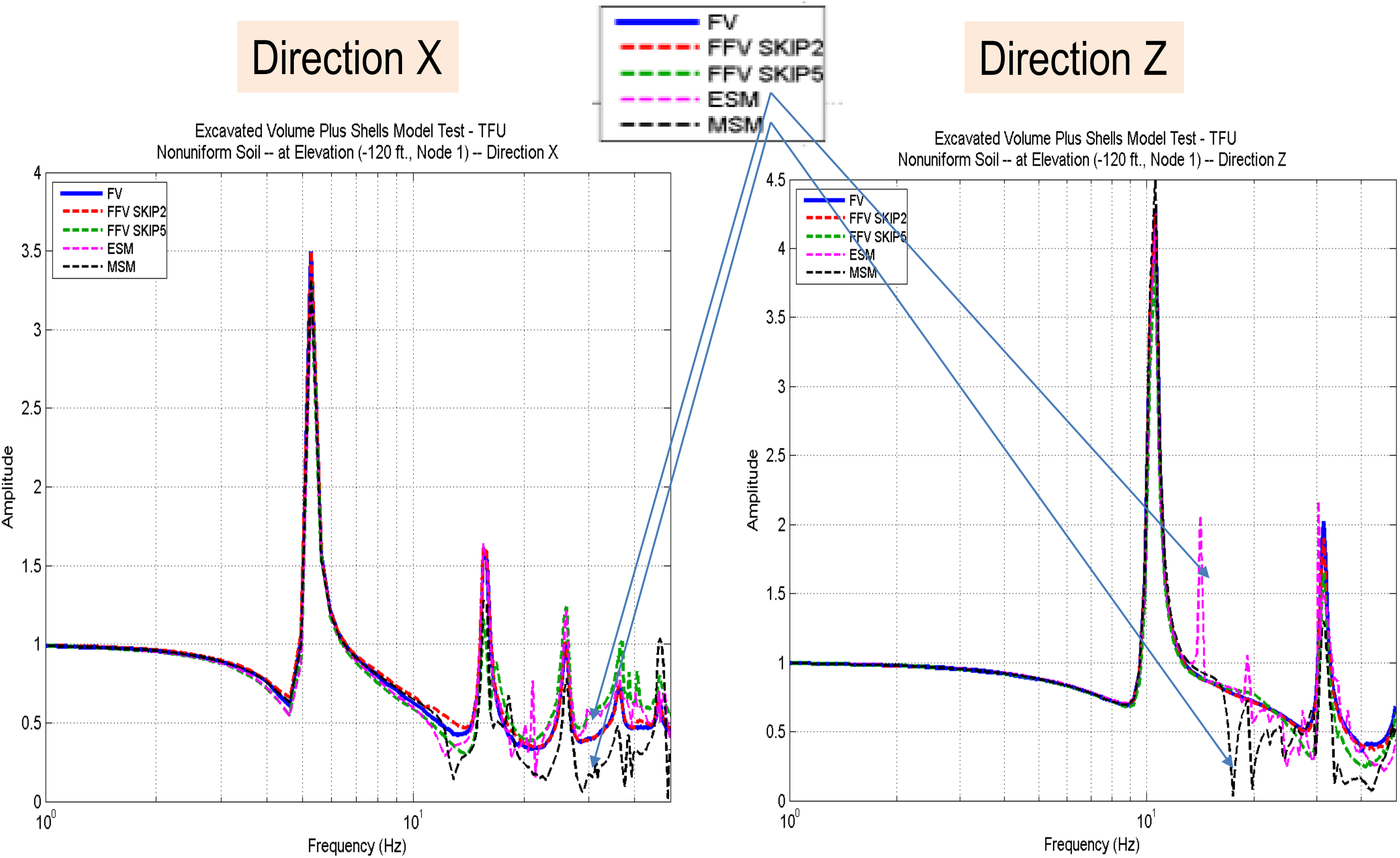

Comparative ATF at -32 ft Depth (1/4 of Embedment)

Direction X

Direction Z

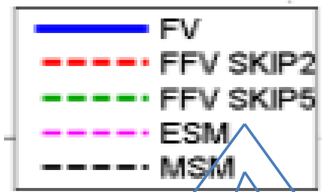

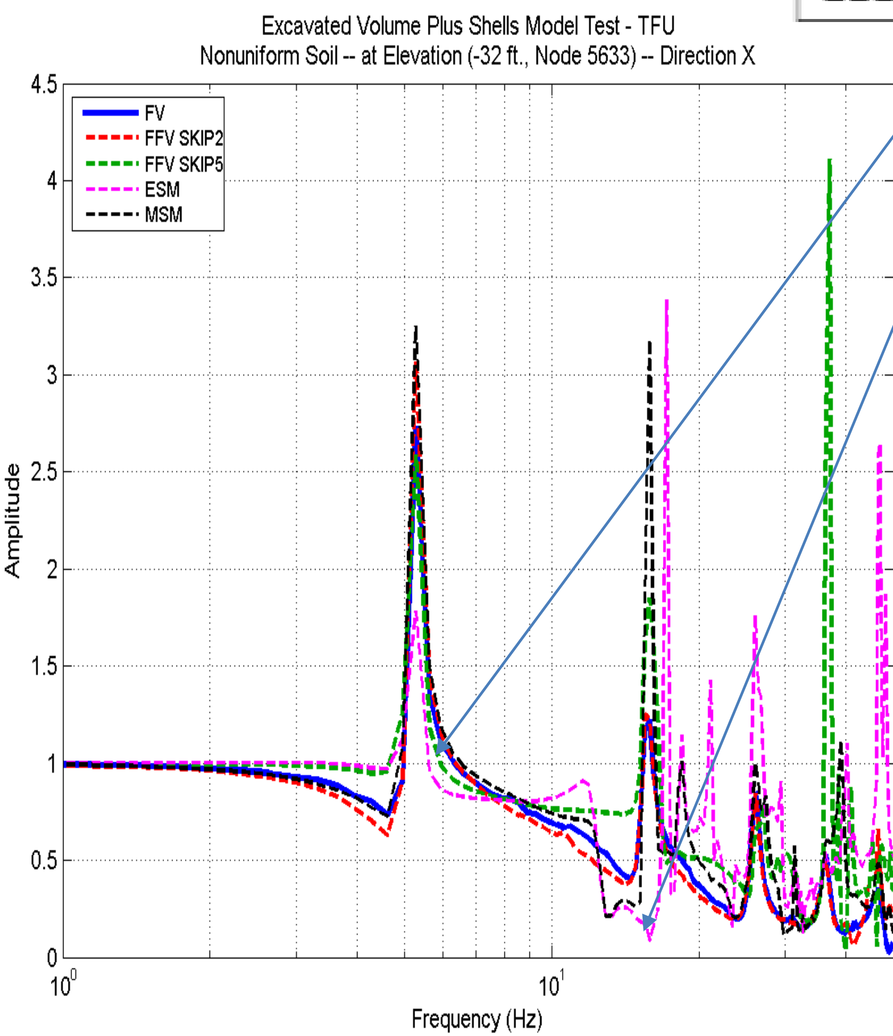

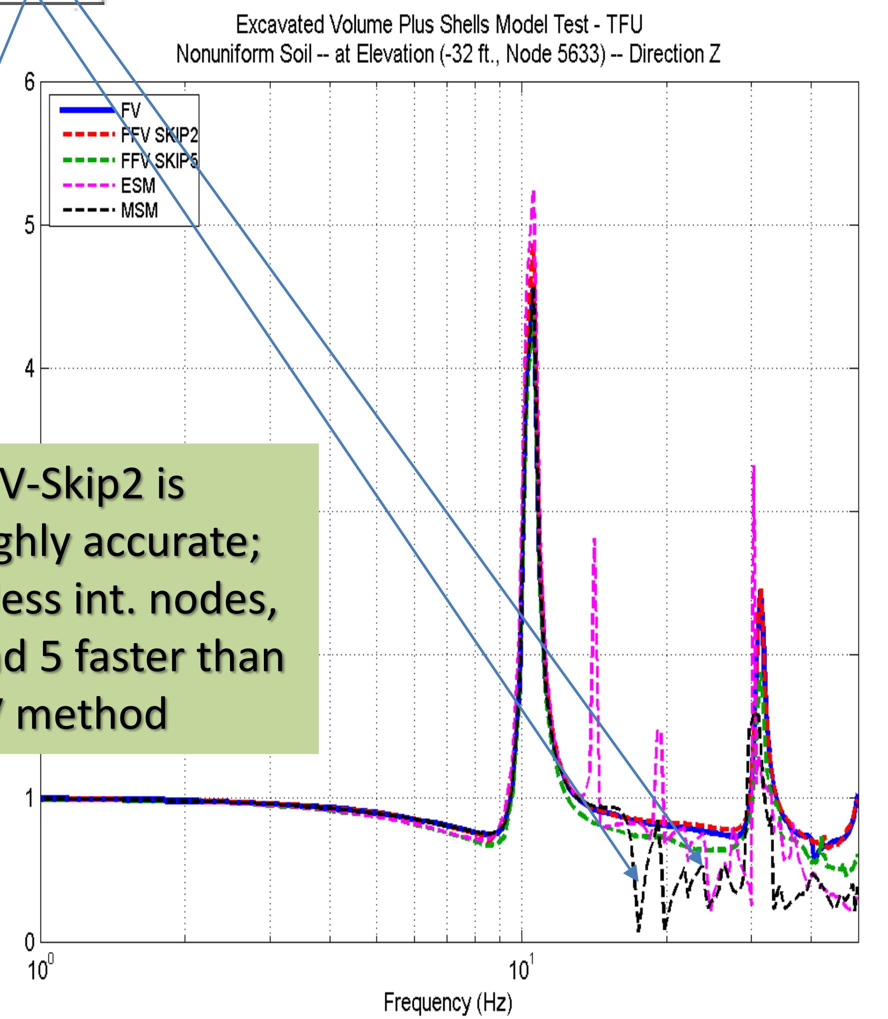

FFV-Skip2 is highly accurate; 5 less int. nodes, and 5 faster than FV method

Fast SSI Analysis for DES Using Excavated Soil Reduced-Order Model (FVSROM and FVROM-INT)

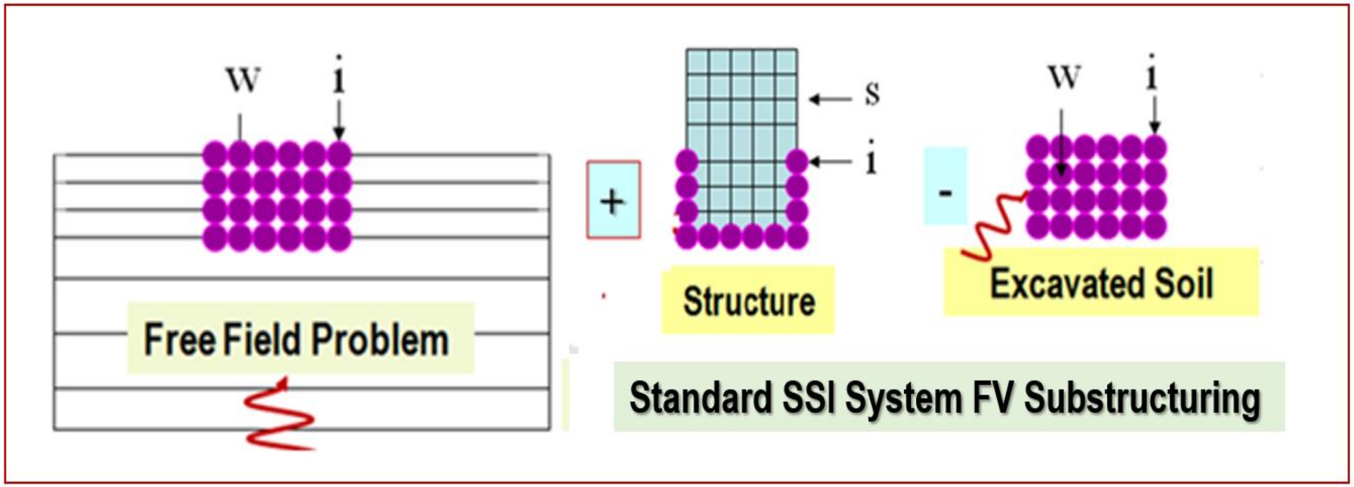

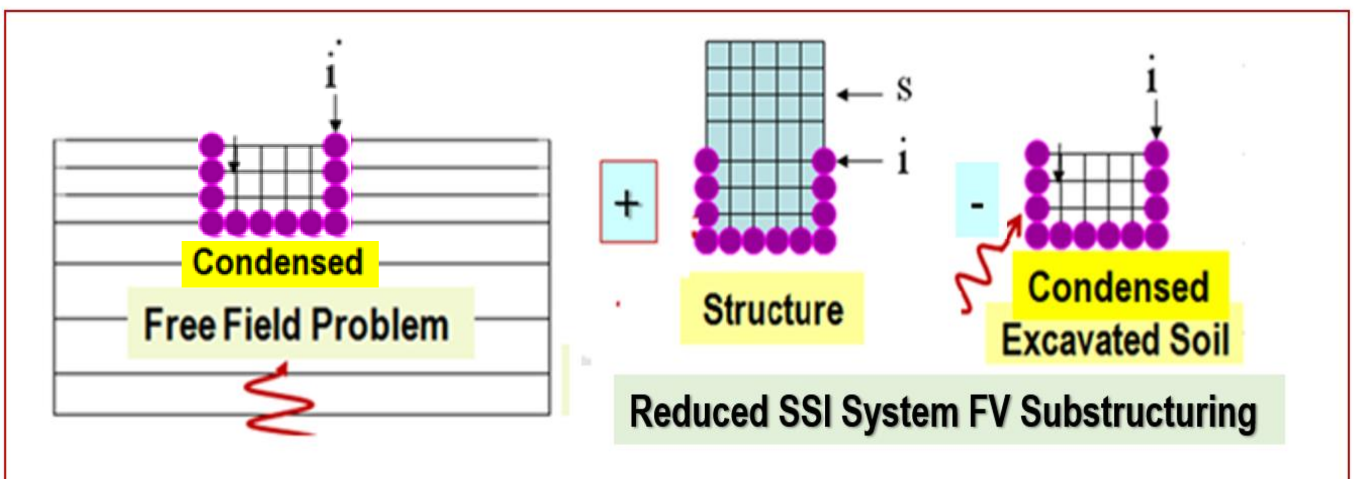

The excavated soil dynamic matrix is a frequency-dependent large-size full complex matrix.

Due to its lack of sparseness, the inclusion of this matrix in the SSI solution affects largely the numerically efficiency of the FV substructuring as defined in the original SASSI approach.

Using a frequency-dependent matrix condensation scheme, the size of this large-size matrix can be hugely reduced, and by this large speedups of SSI solution are obtained.

Fast SASSI Analysis Using Excavated Soil Reduced-Order Modeling (FVSROM-INT)

Step 1

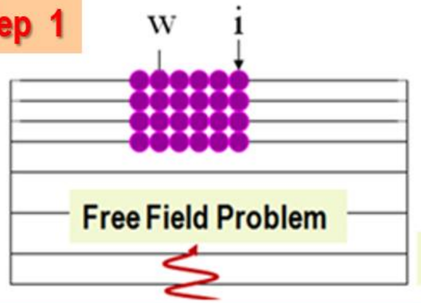

Identify Key Frequencies Based on Free-Field Excavated Soil Dynamics

Perform the site response analysis by *running the SOIL module* to identify a reduced set of key frequencies for the excavated soil dynamics in free-field. Both the frequency-dependence of the excavated soil impedance matrix and its associated seismic load vectors are considered. The *dense SSI frequencies* for the SITE module which will be used for final SSI analysis are automatically *adjusted* based on the *key frequencies.*

Step 2

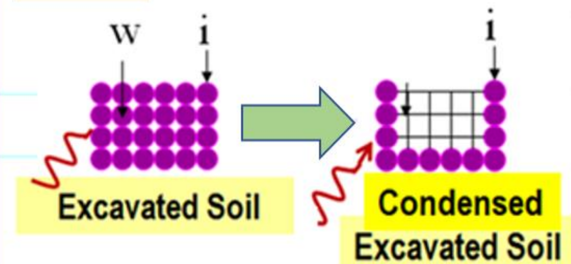

Condense Soil Matrix for Key Frequencies and Interpolate for All Frequencies

The frequency-dependent excavated soil dynamic matrix is condensed for the foundation-soil interface nodes for *key frequencies only*. This is accomplished by *running ANALYS option "Condense Impedance" (Mode 7).* Then, the reduced excavation dynamic matrix and seismic load vector are interpolated *for all dense SSI frequencies* by *running the CNDS_INTERP module*. Reduced soil matrices can be also exported to ANSYS for performing a SSI harmonic analysis via SASSI methodology.

Step 3

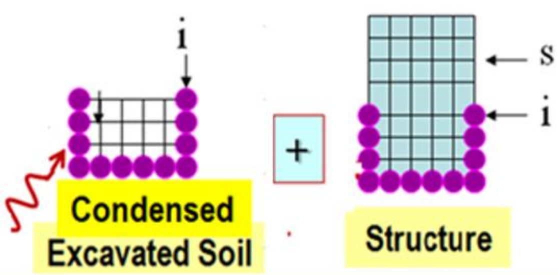

Compute SSI Solution Using Reduced Excavation Matrix for All Frequencies

The interpolated reduced excavation dynamic matrix and seismic load vectors computed *for all SSI frequencies* are assembled with the structure model, and the SSI solution is obtained for each frequency. This is accomplished by *running ANALYS option "SSI with Condensation" (Model 8).* The final SSI solution running time and the soil impedance file sizes are much smaller since the number of interaction nodes is minimal. Speed ups of 5-15 times are expected for detailed deeply embedded models.

SSI Flexible Volume Application for DES/SMR

ASCE 4-16 Chapter 5:

- MSM is a highly accurate and robust SSI approach for large-size embedded foundations, as nuclear island (NI) complex foundations. MSM is much more robust than SM.
- MSM could break down for deeply embedded structures. Use ESM.
- MSM needs to be validated against FVM for quarter excavation models

ACS SASSI NQA V4 Options:

- Use FFV (or ESM) with interaction nodes on excavation internal node layers. FFV is still computationally intensive
- *Use new FVSROM-INT which reduces the interaction nodes to only the foundation-soil interface nodes (as in SM!). Speedups of 4 - 8 times vs. FFV.*

  Currently, applied to NuScale SMR, GEH SMR, HOLTEC SMRs.

Embedded RB Complex ACS SASSI Analysis for Direct SSI (FFV) vs. Reduced SSI (FVSROM)

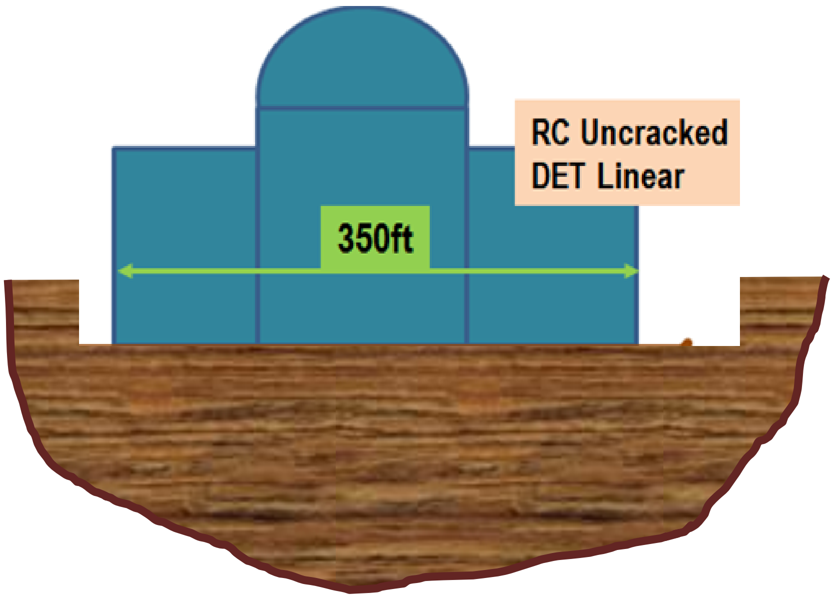

RB Complex SSI Model Information:

- Number of Nodes: About 80,000
- Number of Interaction Nodes: About 8,000
- Embedment Depth: 45 ft
- Excavation includes 6 Embedment Layers
- Direct SSI Approach: Fast FV with 4 out of 7 interaction node layers

Seismic SSI Analysis Runtime:

ACS SASSI Direct Runtime: 733 units

ACS SASSI with Condensation Runtime: 176 units

Speed Up due to Condensation: 4.2

Larger speed ups up to 5-8 times or even more are expected for larger-size SSI models with deep embedment and larger number of interaction nodes.

ATFs for Direct SSI (FFV) and FVROM-INT SSI

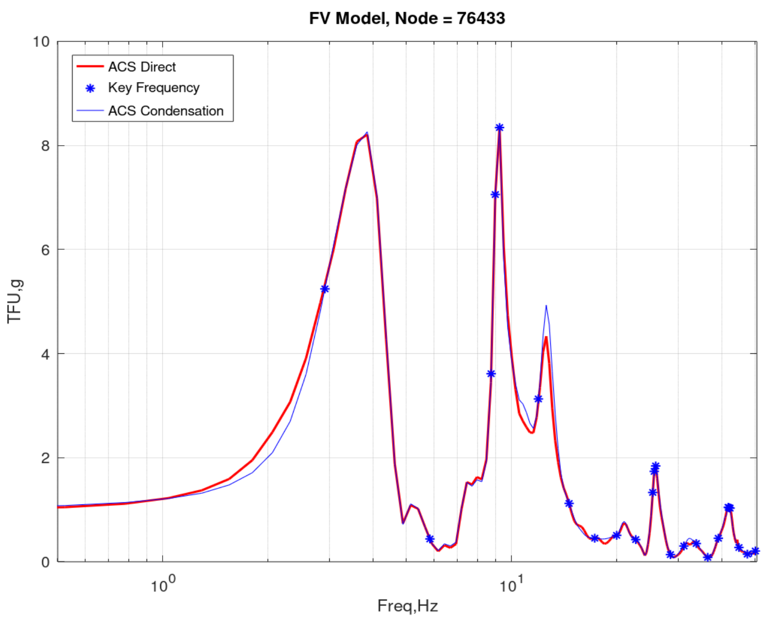

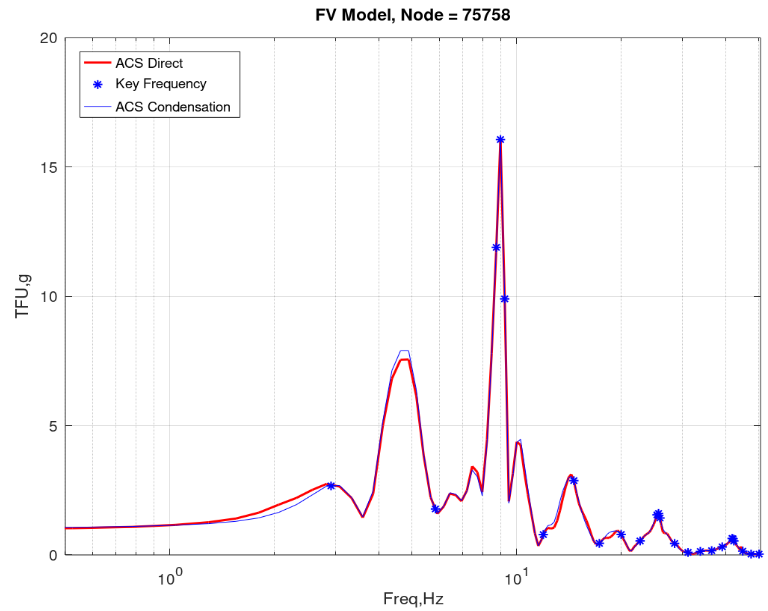

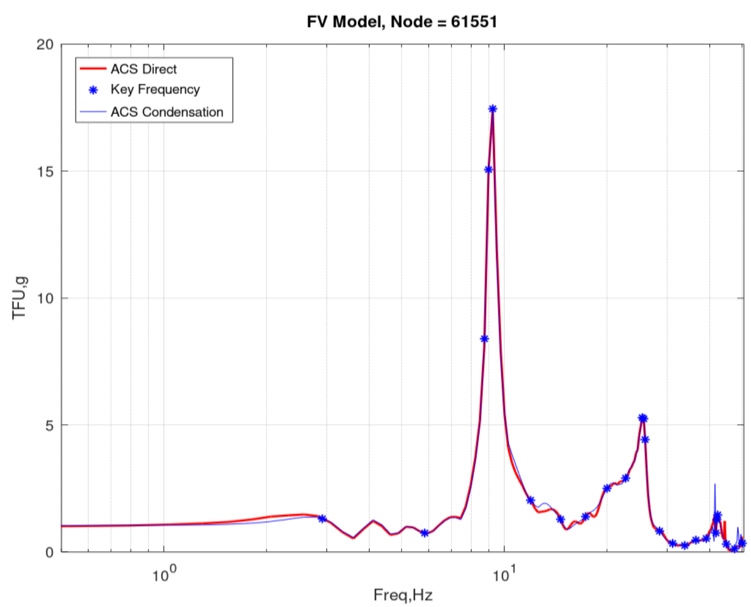

Usually, 15-25 key frequencies are sufficient for accurate reduced excavation soil impedance matrix interpolation and SSI responses

FE Mesh Issues

Excavation Volume Mesh Nonuniformity Study

Volume Size: 200 ft x 100 ft x 100 ft

140 ft Embedded SMR Model

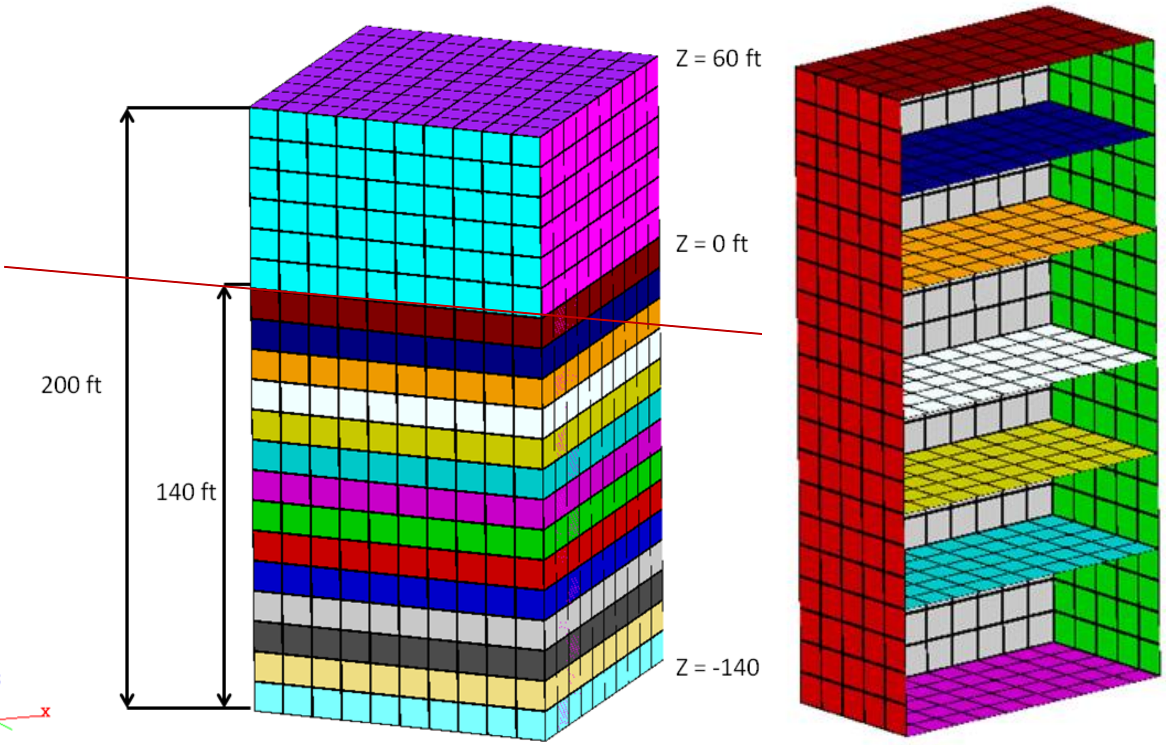

SMR size: 100 ft x 100 ft X 200 ft
Embedment: 140 ft
Mesh size: 10 ft X 10 ft X 10 ft
Number of Nodes: 2,580
Interaction Nodes: 1,815

Vs Soil Profile (fps)

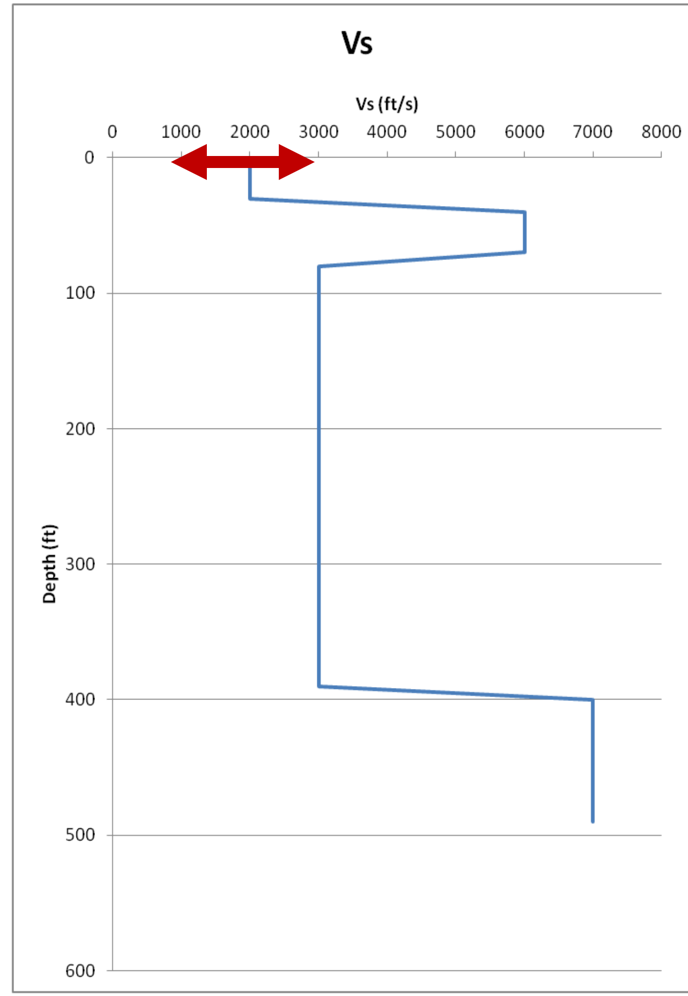

140 ft Embedment SMR Excavation Volume Meshes

Uniform Model

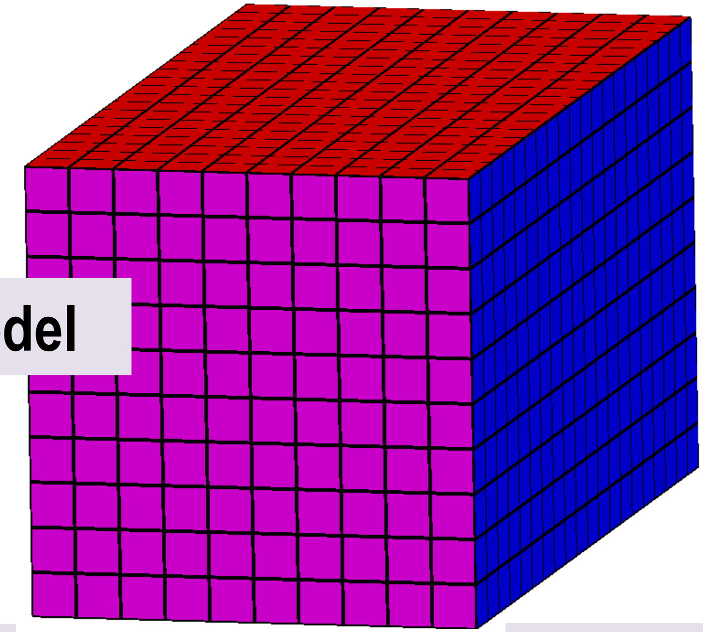

For nonuniform meshes the average radius values are used.

Non-uniform Model

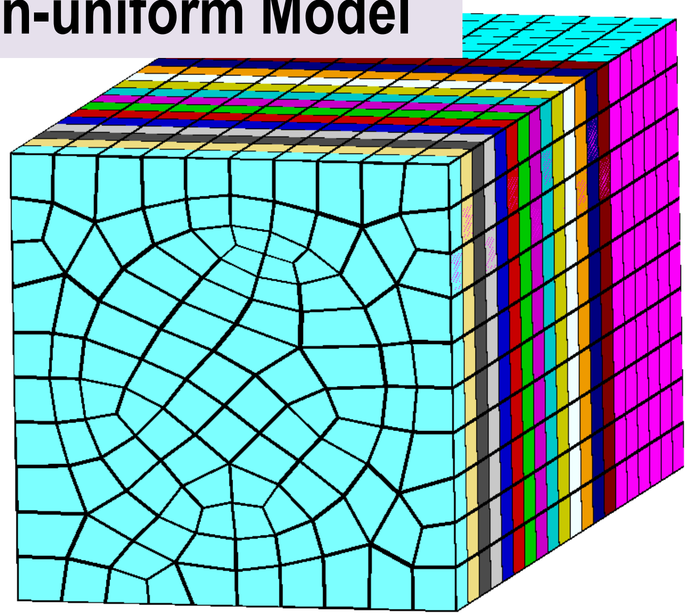

Refined Non-uniform Model

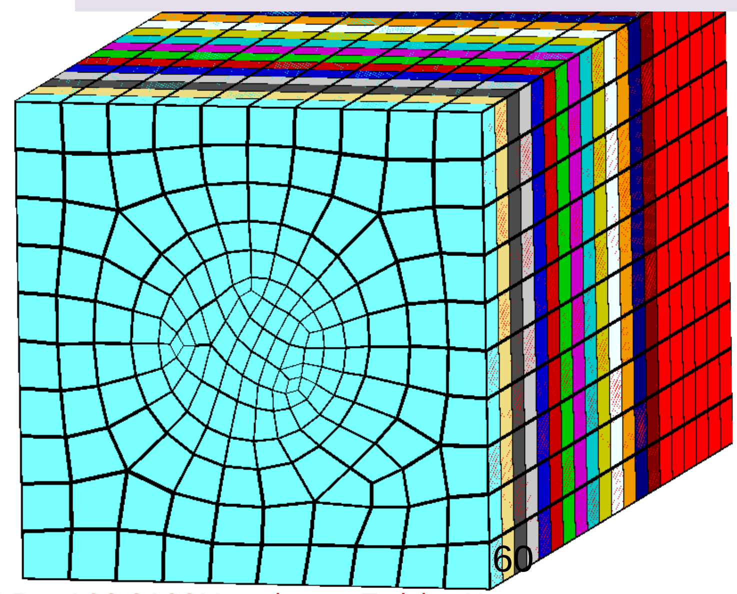

Effects of Excavation Volume FE Meshing. Uniform Mesh vs. Nonuniform Mesh

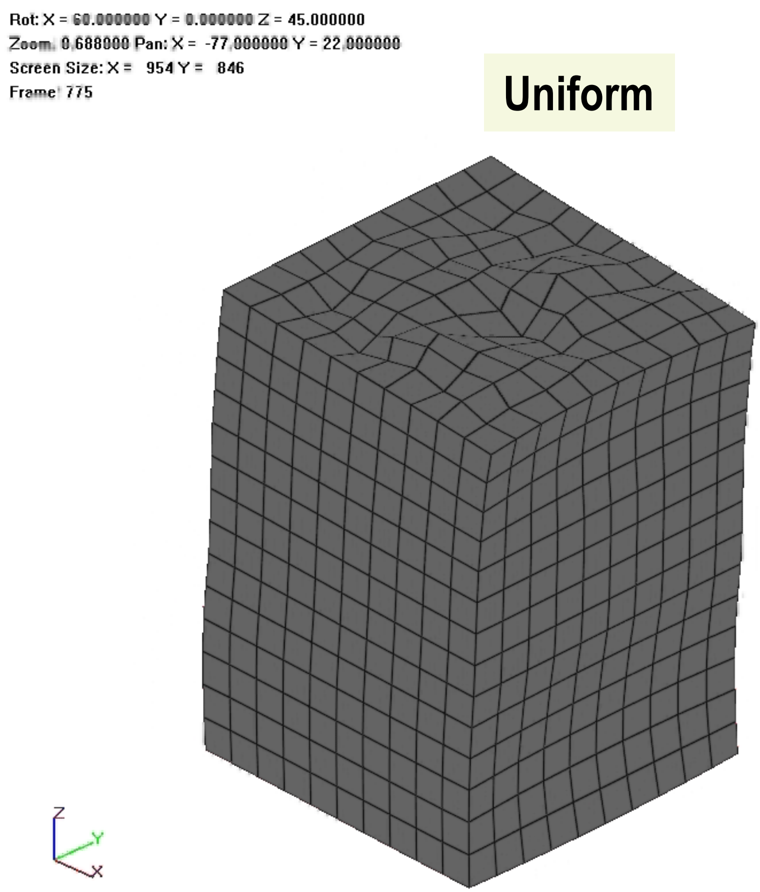

HORIZONTAL

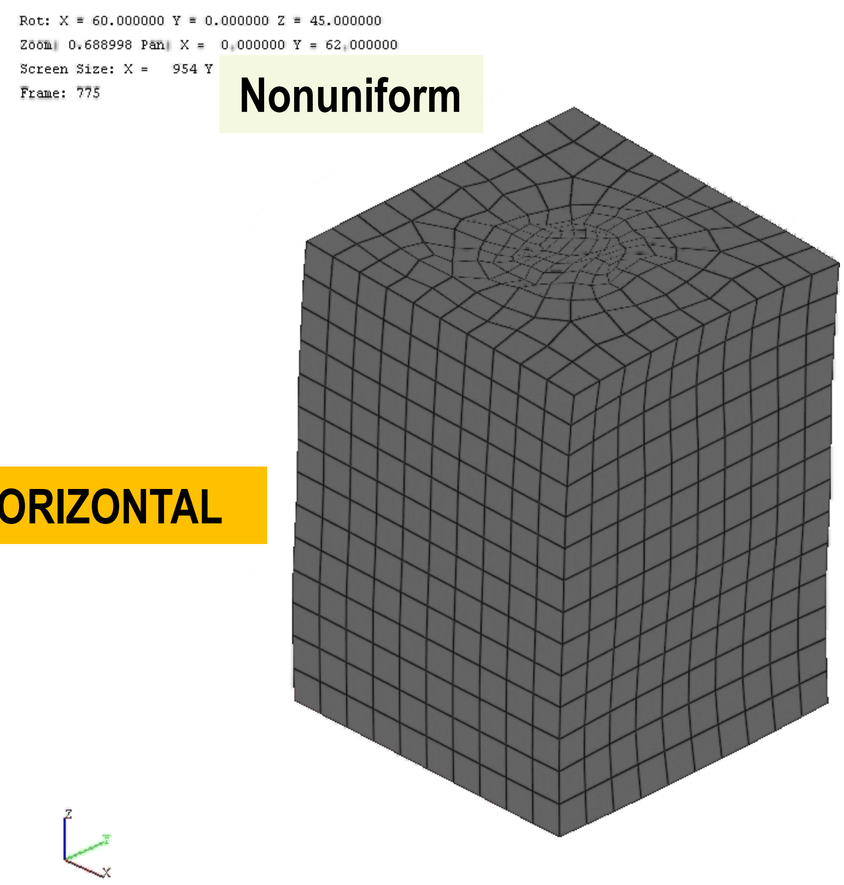

Regular uniform mesh excavation FE models capture accurately the high-frequency wave scattering effects.

Effects of Excavation Volume FE Meshing. Uniform Mesh vs. Nonuniform Mesh

Uniform

Nonuniform

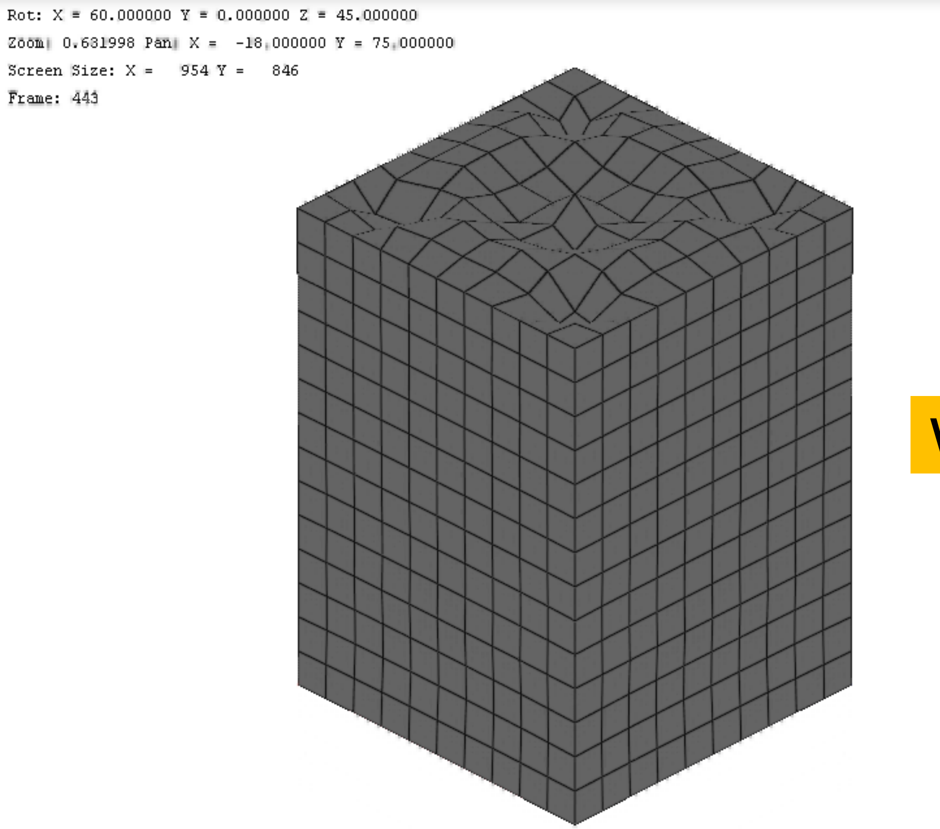

VERTICAL

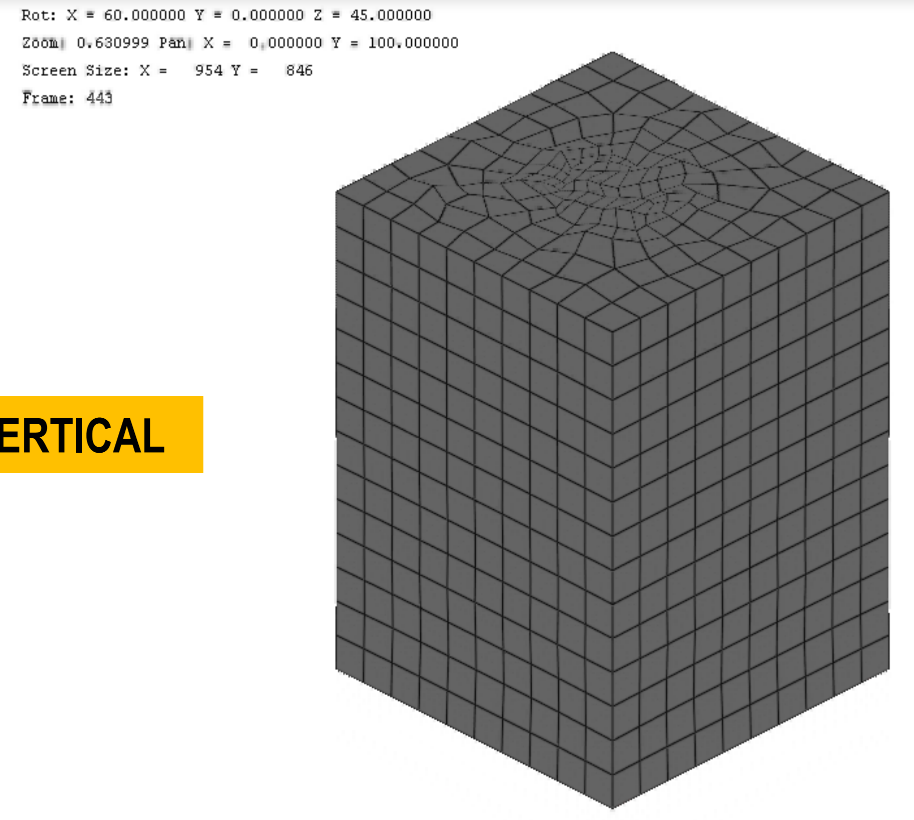

Regular uniform mesh excavation FE models capture accurately the high-frequency wave scattering effects.

ANIMATION

BROOKHAVEN NATIONAL LABORATORY

BNL-102434-2013

Seismic Soil-Structure Interaction Analyses of a Deeply Embedded Model Reactor – SASSI Analyses

J. Nie, J. Braverman, M. Costantino

October 2013

Therefore, it is recommended to pursue further improvements in the frequency domain codes in parallel to the ongoing research to develop and benchmark the time domain codes. Some of the key improvements are listed below:

(1) Re-establish/develop a modern, modularized (pluggable for incorporating future capabilities), and parallel code base for SASSI;
(2) "Profile" the code (i.e., analyze the efficiency of various parts of the code) and optimize the code to expedite the execution speed;
(3) Implement/automate certain capabilities based on industry guidelines for using SASSI (e.g., addressing the need for regular excavated soil mesh for any reasonable finite element structural model, approximating local soil nonlinearity, automating the treatment of soil layering, implementing advanced data management, etc.);
(4) Investigate the number-theoretic (e.g., GLP) enhanced subtraction method (ESM, which was proposed and briefly tested in this study); and
(5) Incorporate methods to consider uncertainties in soil properties.

Transition Mesh Zones Are Necessary to Get A Regular Mesh Excavation FE Model

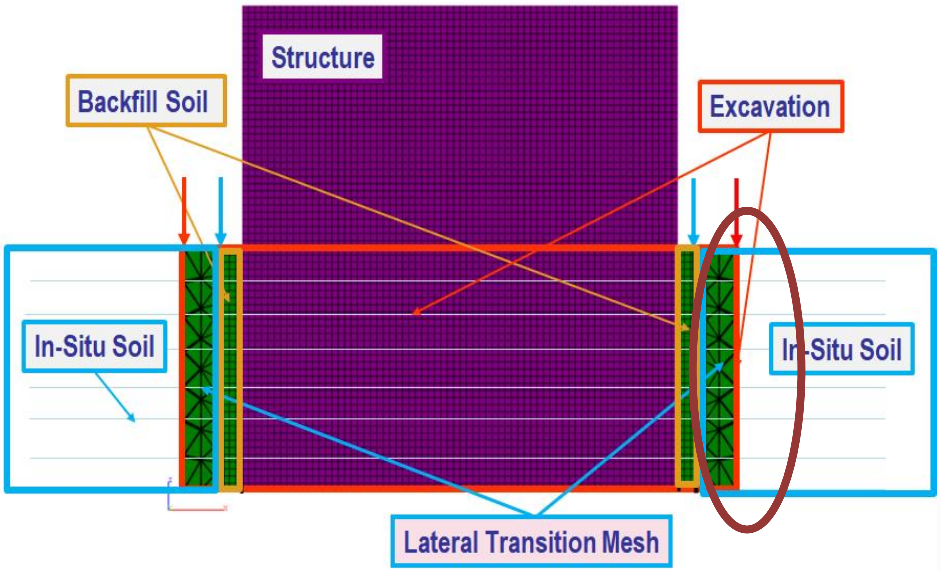

Regular uniform mesh excavation FE models capture accurately the high-frequency wave scattering effects. Also ensures much more efficient SSI runs.
See conclusions of the *Brookhaven National Lab Report BNL-102434-2013 by USNRC BNL Consultants*.

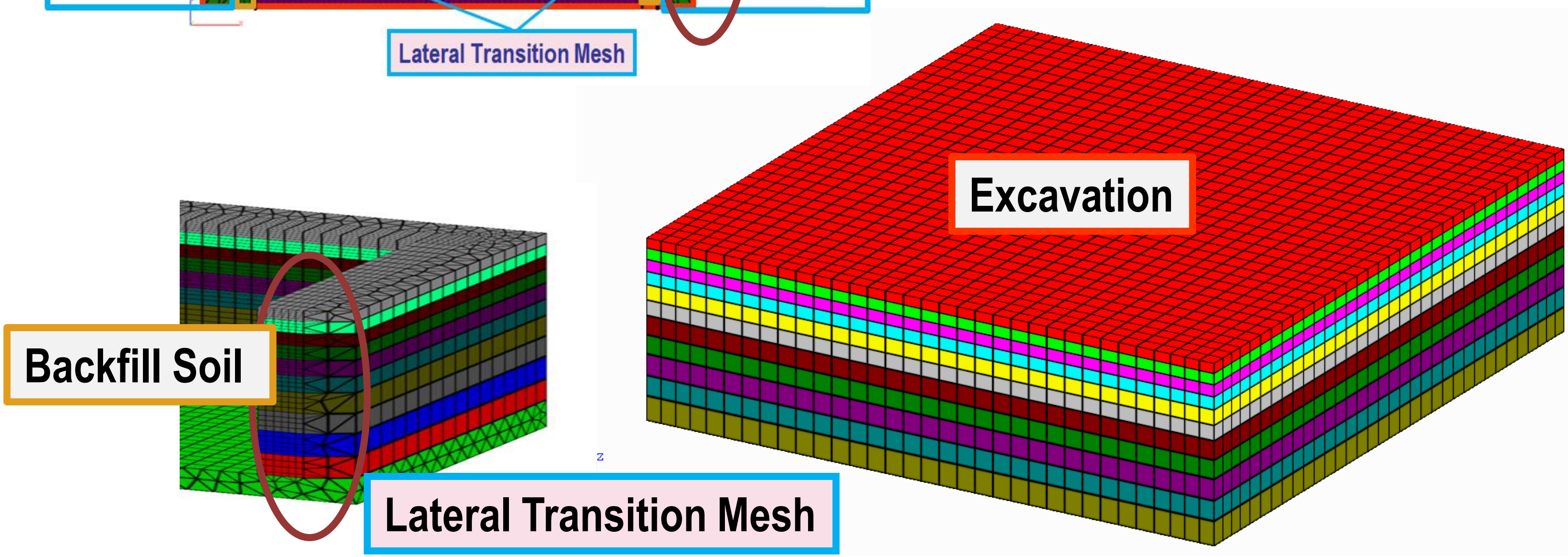

RB Complex Pile Foundation Example Includes More Then 200,000 FE Mesh Nodes (10,000/level)

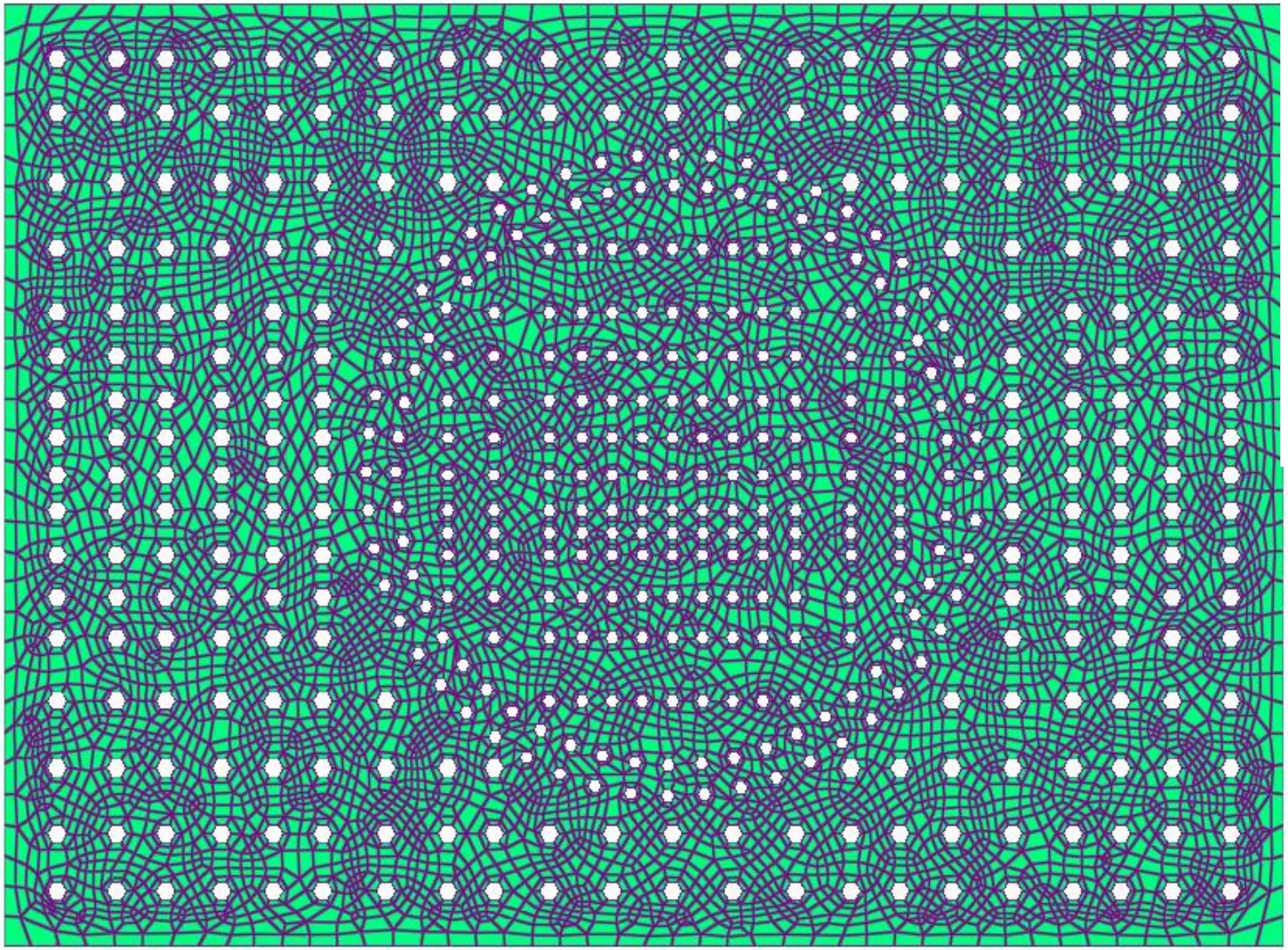

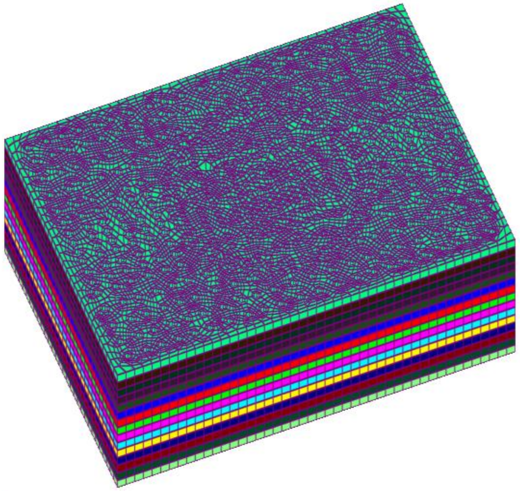

SSI runtime was about 2,600 sec. per frequency on a 128 GB RAM MS Windows PC

2. ACS SASSI Motion Incoherency Modeling

Theoretical and Implementation Aspects

Incoherent SSI Analysis in ACS SASSI

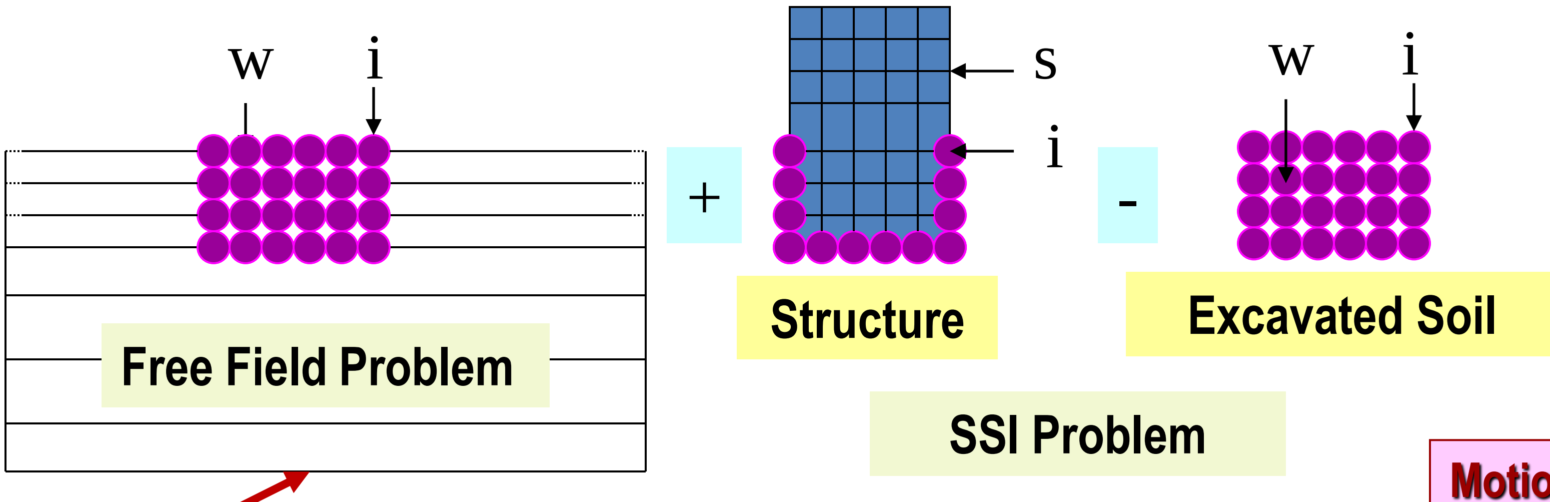

Flexible Volume Method (using all excavated volume nodes)

$$\begin{bmatrix} \mathbf{C}^{e}_{ii} - \mathbf{C}^{e}_{ii} + \mathbf{X}_{ii} & -\mathbf{C}^{e}_{iw} - \mathbf{X}_{iw} & \mathbf{C}^{s}_{is} \\ -\mathbf{C}^{e}_{wi} + \mathbf{X}_{wi} & -\mathbf{C}^{e}_{ww} + \mathbf{X}_{ww} & \mathbf{0} \\ \mathbf{C}^{s}_{si} & \mathbf{0} & \mathbf{C}^{s}_{ss} \end{bmatrix} \begin{Bmatrix} \mathbf{U}_{i} \\ \mathbf{U}_{w} \\ \mathbf{U}_{s} \end{Bmatrix} = \begin{Bmatrix} \mathbf{X}_{ii}\mathbf{U}'_{i} + \mathbf{X}_{iw}\mathbf{U}'_{w} \\ \mathbf{X}_{wi}\mathbf{U}'_{i} + \mathbf{X}_{ww}\mathbf{U}'_{w} \\ \mathbf{0} \end{Bmatrix}$$

Motion Incoherency affects free-field motion at interaction nodes

$$\boxed{C(\omega)\,U(\omega) = Q(\omega)}$$

where $C(\omega) = K - \omega^2 M$

Incoherent SSI Analysis in Complex Frequency

The complex frequency response is computed as follows:

- Coherent SSI response:

Structural transfer function given input at interaction nodes

Coherent ground transfer function at interface nodes given control motion

$$U_s(\omega) = H_s(\omega) * H_g^c(\omega) * U_{g,0}(\omega)$$

Complex Fourier transform of control motion

- Incoherent SSI response:

Incoherent ground transfer function given coherent ground motion and coherency model (random spatial variation in horizontal plane)

$$U_s(\omega) = H_s(\omega) * S_g^i(\omega) * H_g^c(\omega) * U_{g,0}(\omega)$$

Complex Fourier transform of relative spatial variations of soil motion at interaction nodes = stochastic wave field

$$S_g(\omega) = [\Phi(\omega)][\lambda(\omega)]\{\eta_\theta\}$$

Eigen**modes** of coherency kernel (deterministic part)

Random **phases** (stochastic part)

How Many Modes Should Be Considered for SRSS Approaches? SS Considers All!

Low Frequency/Large Wavelengths/Only Few Low Order Incoherency Modes

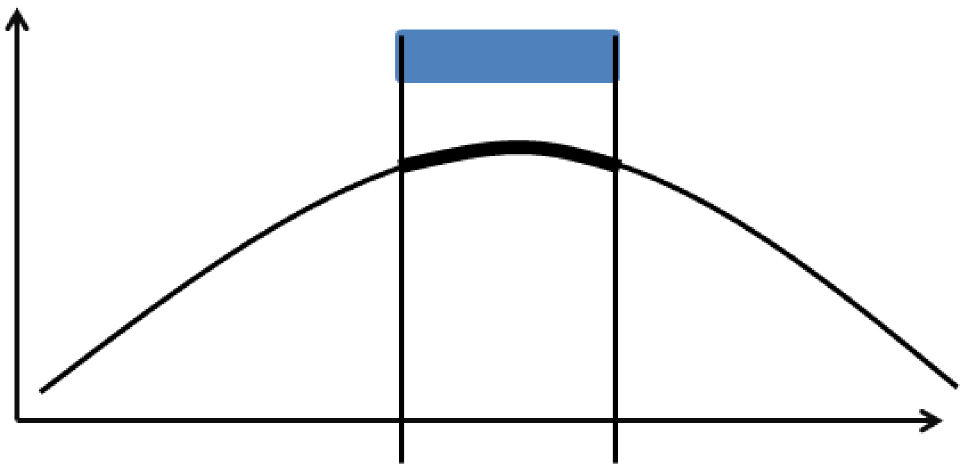

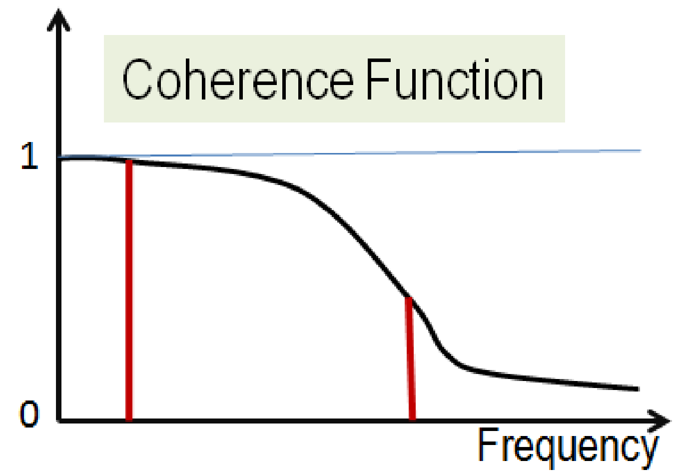

High Frequency/Short Wavelengths/Low and High Order Incoherency Modes

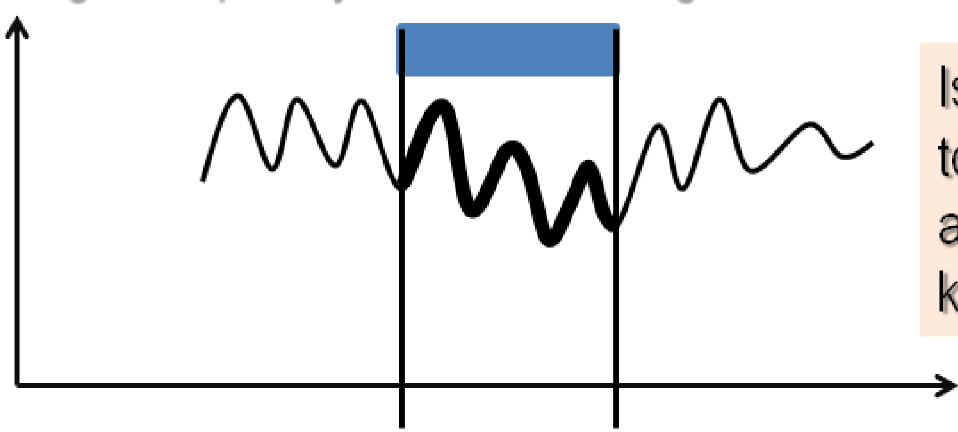

Is the foundation sufficiently rigid
to neglect high order modes
at high frequency due to
kinematic interaction effects?

Cumulative Modal Contribution for 10 Modes

2007 Abrahamson Rock Site Model

```
*** CUMULATIVE MODAL MASS/VARIANCE(%) ***

Frequency =     0.098     Horizontal =  100.00%   Vertical =  100.00%
Frequency =     1.562     Horizontal =  100.00%   Vertical =   99.97%
Frequency =     3.125     Horizontal =   99.94%   Vertical =   99.75%
Frequency =     4.688     Horizontal =   99.69%   Vertical =   99.20%
Frequency =     6.250     Horizontal =   98.90%   Vertical =   98.09%
Frequency =     7.812     Horizontal =   97.01%   Vertical =   96.00%
Frequency =     9.375     Horizontal =   93.55%   Vertical =   92.59%
Frequency =    10.938     Horizontal =   88.54%   Vertical =   87.93%
Frequency =    12.500     Horizontal =   82.47%   Vertical =   82.46%
Frequency =    14.062     Horizontal =   75.90%   Vertical =   76.67%
Frequency =    15.625     Horizontal =   69.31%   Vertical =   70.92%
Frequency =    17.188     Horizontal =   63.02%   Vertical =   65.45%
Frequency =    18.750     Horizontal =   57.20%   Vertical =   60.37%
Frequency =    20.312     Horizontal =   51.92%   Vertical =   55.74%
Frequency =    21.875     Horizontal =   47.19%   Vertical =   51.55%
Frequency =    23.438     Horizontal =   42.99%   Vertical =   47.79%
Frequency =    25.000     Horizontal =   39.26%   Vertical =   44.40%
Frequency =    26.562     Horizontal =   35.96%   Vertical =   41.37%
Frequency =    28.125     Horizontal =   33.04%   Vertical =   38.65%
Frequency =    29.688     Horizontal =   30.42%   Vertical =   36.20%
Frequency =    31.250     Horizontal =   28.04%   Vertical =   34.00%
Frequency =    32.812     Horizontal =   25.81%   Vertical =   32.01%
Frequency =    34.375     Horizontal =   23.63%   Vertical =   30.21%
Frequency =    35.938     Horizontal =   21.37%   Vertical =   28.57%
Frequency =    37.500     Horizontal =   18.93%   Vertical =   27.09%
Frequency =    39.062     Horizontal =   16.31%   Vertical =   25.74%
```

Spectral Factorization of Coherency Matrix Using Limited Number of Incoherency Modes

Spectral factorization uses the diagonal eigenvalue matrix and the eigenvector matrix of coherency matrix at any given frequency

$$\boldsymbol{\Sigma}(\omega) = \boldsymbol{\Phi}(\omega)\boldsymbol{\Lambda}^2(\omega)\boldsymbol{\Phi}^T(\omega)$$

To check the eigen-expansion convergence the norm of the trace of the eigen-value matrix $\boldsymbol{\Lambda}^2$ that is equal to the original matrix $\boldsymbol{\Sigma}$.

$$\sum_{j=1}^{N} \lambda_j^2 = N \quad \text{or} \quad \sum_{j=1}^{N} \frac{\lambda_j^2}{N} 100 = 100\%$$

For m < N eigen-modes their cumulative contribution to the total variance of the motion amplitude should be greater than 90% (similar criterion with 90% cumulative modal mass in dynamics)

$$\sum_{j=1}^{m} \upsilon_j = \sum_{j=1}^{m} \frac{\lambda_j^2}{N} 100 > 90\%$$

ACS SASSI Stochastic Simulation includes all incoherency modes! Exact!

Incoherent Seismic Wave Field Modeling

- Assuming that motion is a Gaussian vector process, then it is fully defined in frequency domain by

local variability

spatial correlation

$$S_{Uj,Uk}(\omega) = [S_{Uj,Uj}(\omega) S_{Uk,Uk}(\omega)]^{1/2} \Gamma_{Uj,Uk}(\omega)$$

Thus, for two arbitrary points in horizontal plane, j and k, the coherency spectrum or coherence is defined by

$$\Gamma_{Uj,Uk}(\omega) = \frac{S_{Uj,Uk}(\omega)}{[S_{Uj,Uj}(\omega) S_{Uk,Uk}(\omega]^{1/2}}$$

- The "plane-wave coherency" function for SSI analysis is defined as a complex function (Abrahamson, 1991-2007) including "spatial incoherency" (amplitude) and "wave passage" (phase) effects

$$\Gamma_{U\ Ui,Uk}(\omega) = \Gamma_{PWUi,Uk}(\omega) \exp\,[i\omega(X_{D,i} - X_{D,k})/V_D]$$

amplitude variability **phase shift**

P-W Coherency Functions for Different Soil Sites

Coherence Function from many records in different dense arrays:

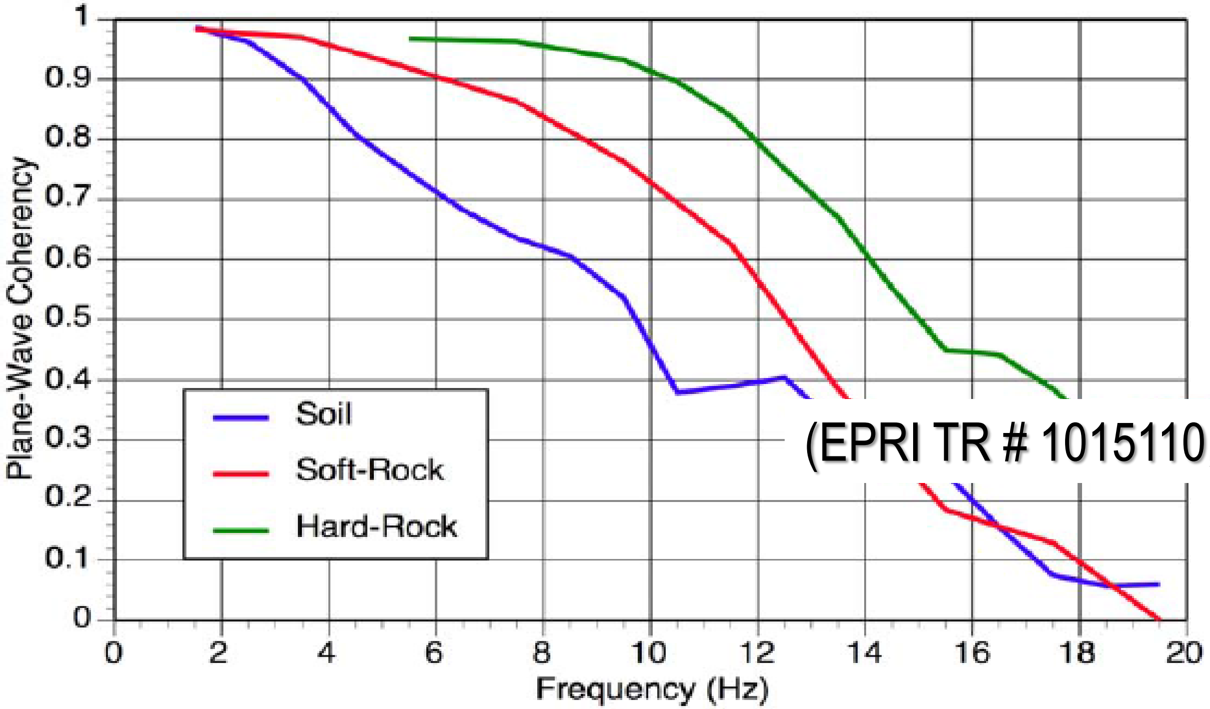

(EPRI TR # 1015110, December 2007)

Abrahamson Coherence Function (Fitted) Analytical Form:

$$\gamma_{pw}(f,\xi)=\left[1+\left(\frac{f\ \ Tanh(a_3\xi)}{a_1 f_c(\xi)}\right)^{n1(\xi)}\right]^{-1/2}\left[1+\left(\frac{f\ \ Tanh(a_3\xi)}{a_2}\right)^{n2}\right]^{-1/2}$$

Abrahamson Generic Coherence Functions for Rock & Soil Sites

HORIZONTAL

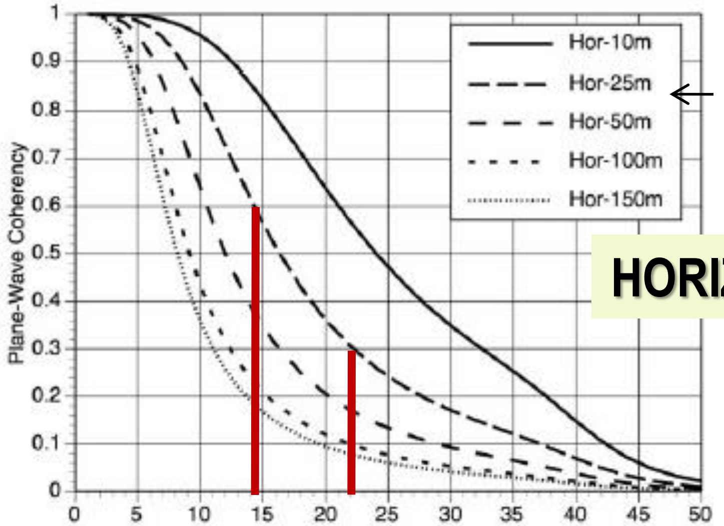

HARD-ROCK

Figure 6-1
Plane-Wave Coherency for the Horizontal Component

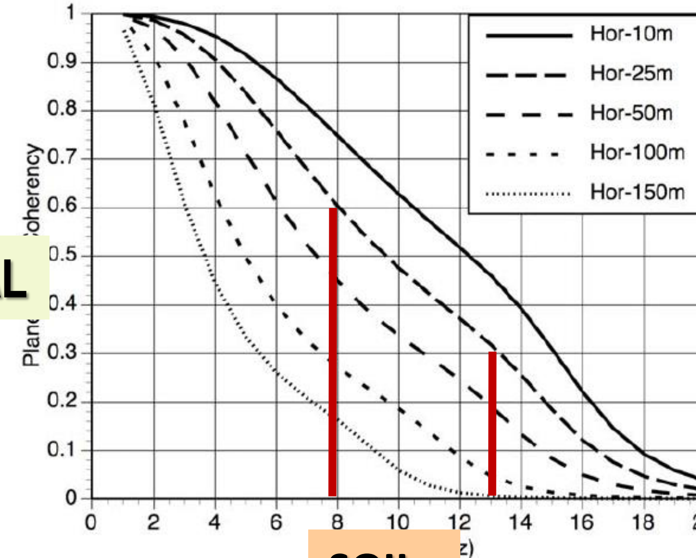

SOIL

Figure 7-1
Plane-Wave Coherency for the Horizontal Component for Soil Sites

VERTICAL

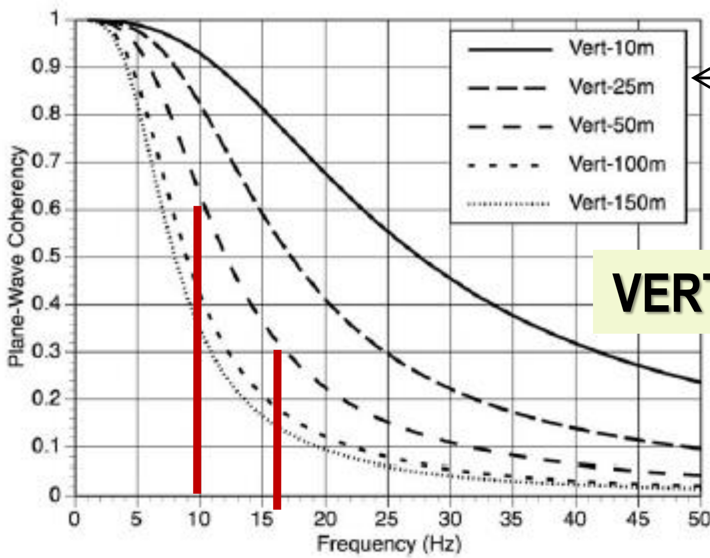

Figure 6-2
Plane-Wave Coherency for the Vertical Component

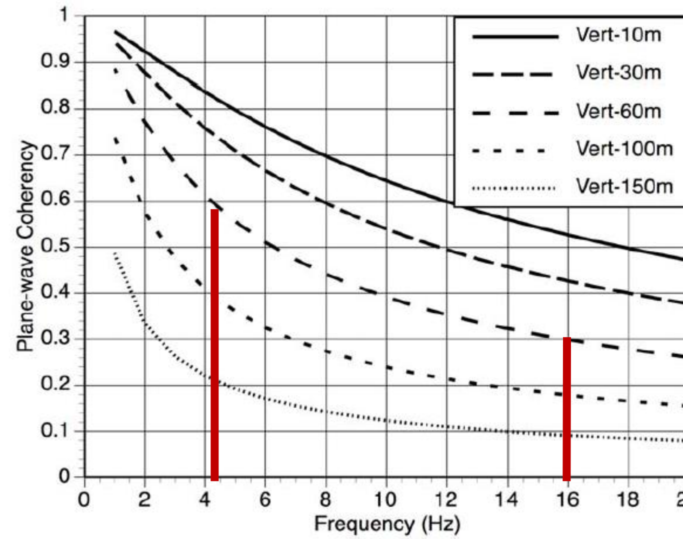

Figure 7-2
Plane-Wave Coherency for the Vertical Component for Soil Sites

(EPRI TR # 1015110, December 2007)

2007 EPRI Validation Study on Seismic Incoherent SSI Approaches

(EPRI Report # 1015111)

EPRI AP1000 Stick Model: 3 Stick Models with A Common Rigid Basemat

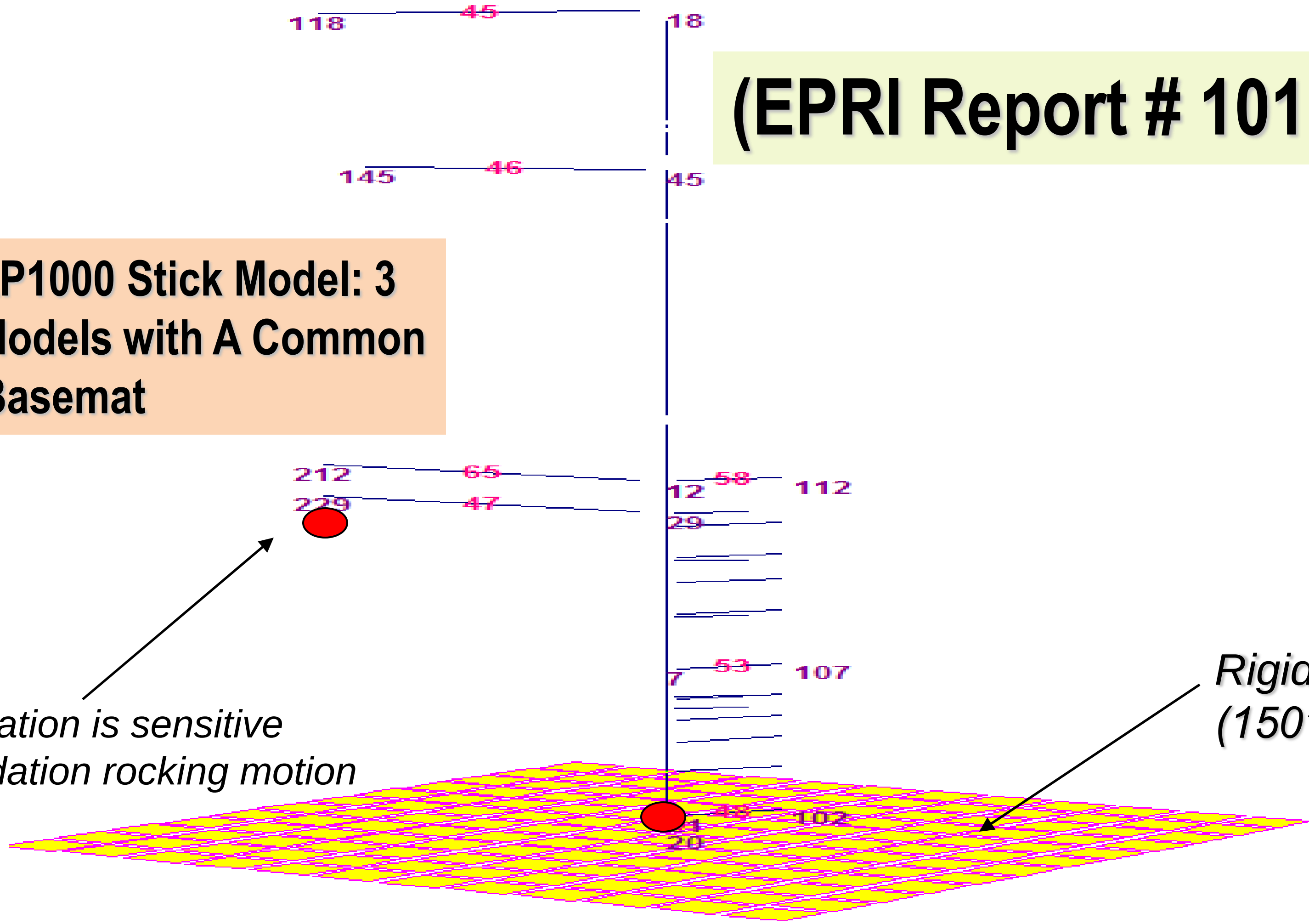

Z translation is sensitive to foundation rocking motion

Rigid Mat (150'x150')

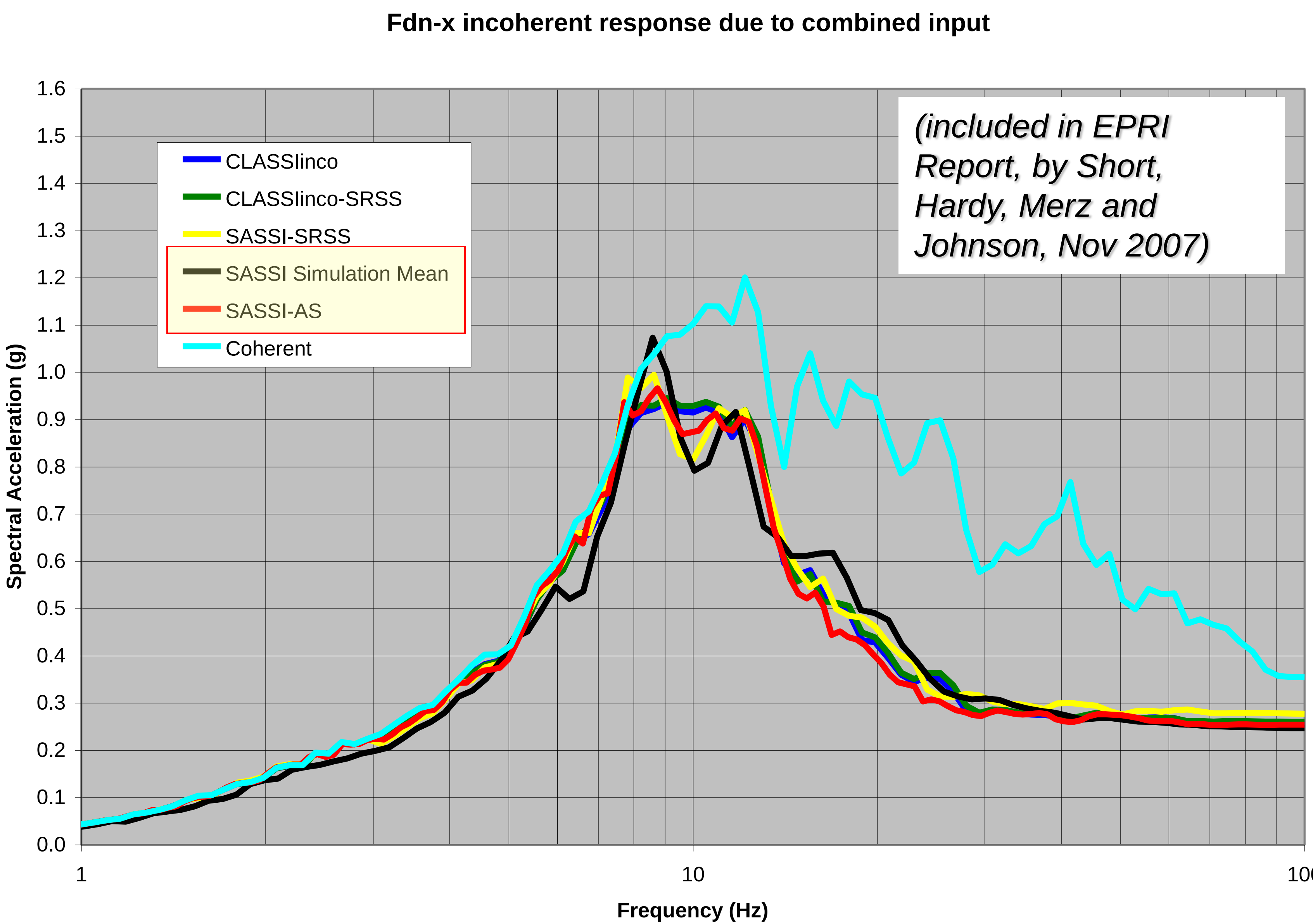

Center of Foundation (Node 1) Response Spectra – X Direction
CLASSIinco, CLASSIinco-SRSS, Bechtel SASSI-SRSS, ACS SASSI Simulation Mean and AS

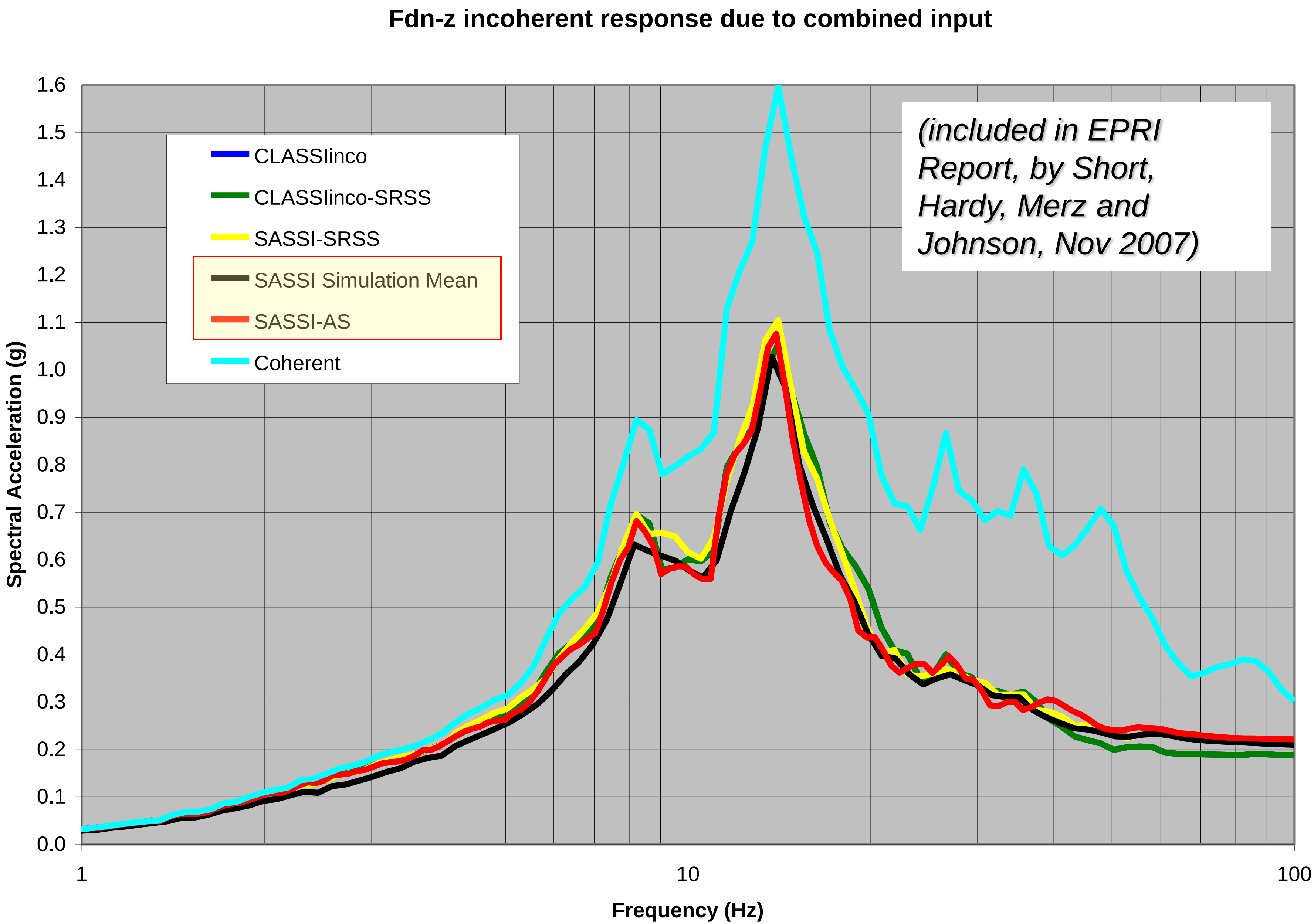

Center of Foundation (Node 1) Response Spectra – Z Direction
CLASSIinco, CLASSIinco-SRSS, Bechtel SASSI-SRSS, ACS SASSI Simulation Mean and AS

Mean RS for 5, 10, 15 and 20 Stochastic Samples For 3 Stick Model with Rigid Basemat (EPRI Studies, 2007)

Random FRS Samples

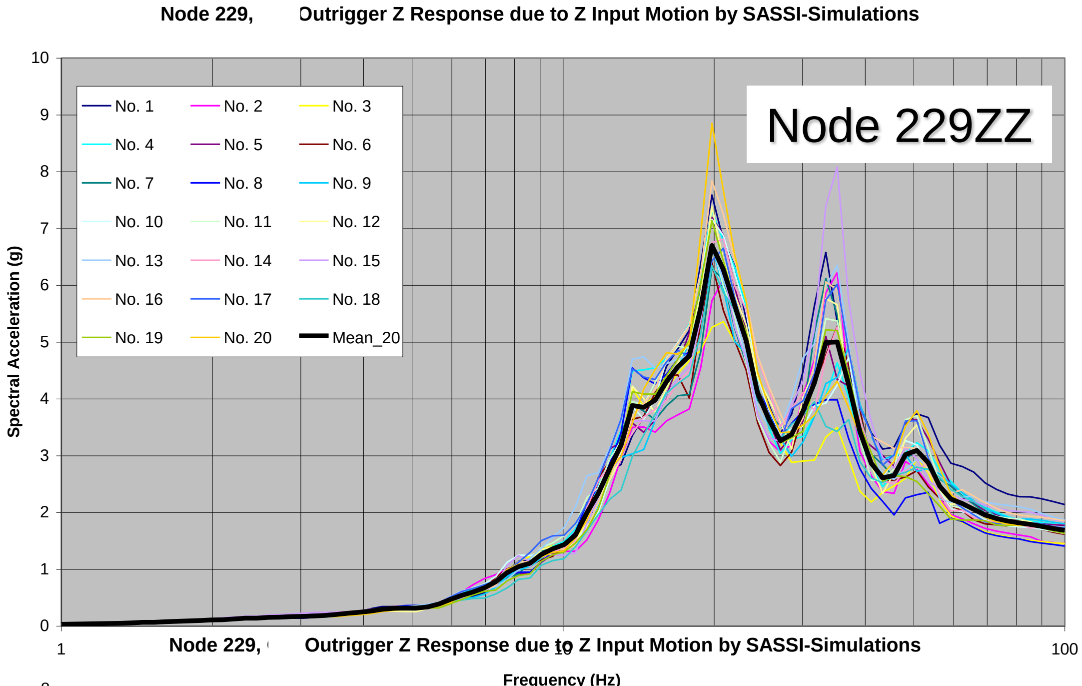

Mean FRS

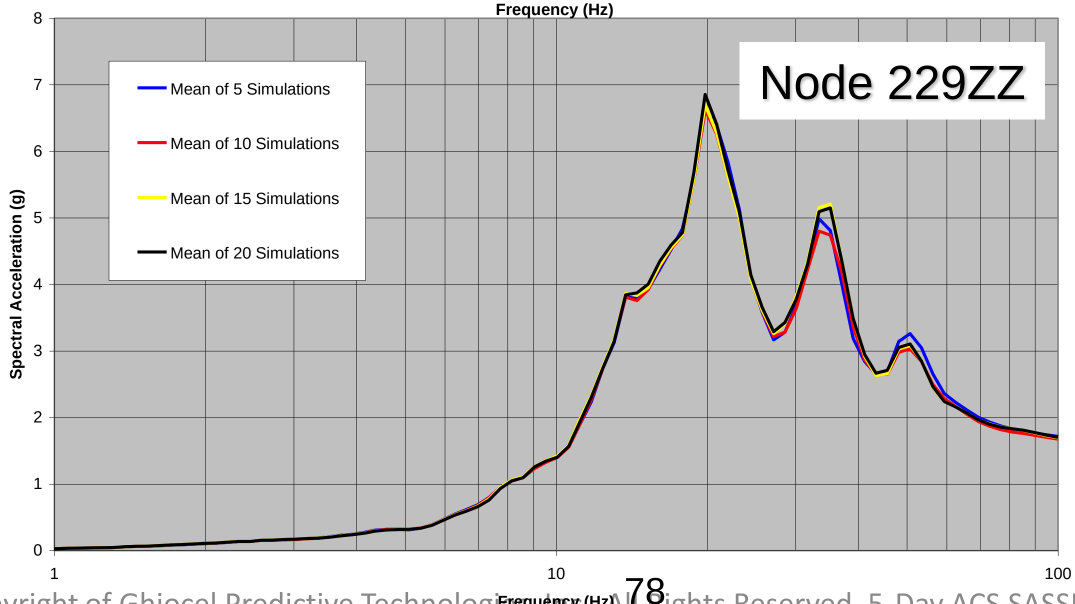

(included in EPRI Report, Figs. 4.1 and 4.2, page 4-5, by Short, Hardy, Merz and Johnson, Sept 2007)

We also compared with results from 50 random Samples – not shown.

EPRI Conclusions on Incoherency Effects Based on AP1000 Stick Model (EPRI Report # 1015111, Nov 30, 2007)

The qualitative effects of motion incoherency effects are:

i) for horizontal components, there is a reduction in excitation translation concomitantly with an increase of torsion and a reduction of foundation rocking

ii) for vertical components, there is a reduction in excitation translation concomitantly with an increase of rocking excitation.

Benchmarked SASSI-Based "Consensus" Approaches:

1) Stochastic Simulation – As reference approach (*with phase adjustment*)
2) SRSS TF Approach (with ATF zero-phases and includes 10 modes)
3) AS Approach (with phase adjustment)

Other remarks:

- No evaluation of the effects of zeroing the ATF phases
- No guidance for flexible or embedded foundations
- No guidance for the piping/equipment multiple history analysis with incoherent inputs
- No specific guidance is provided for evaluation of incoherent structural forces

Stochastic Simulation Incoherent SSI Approach

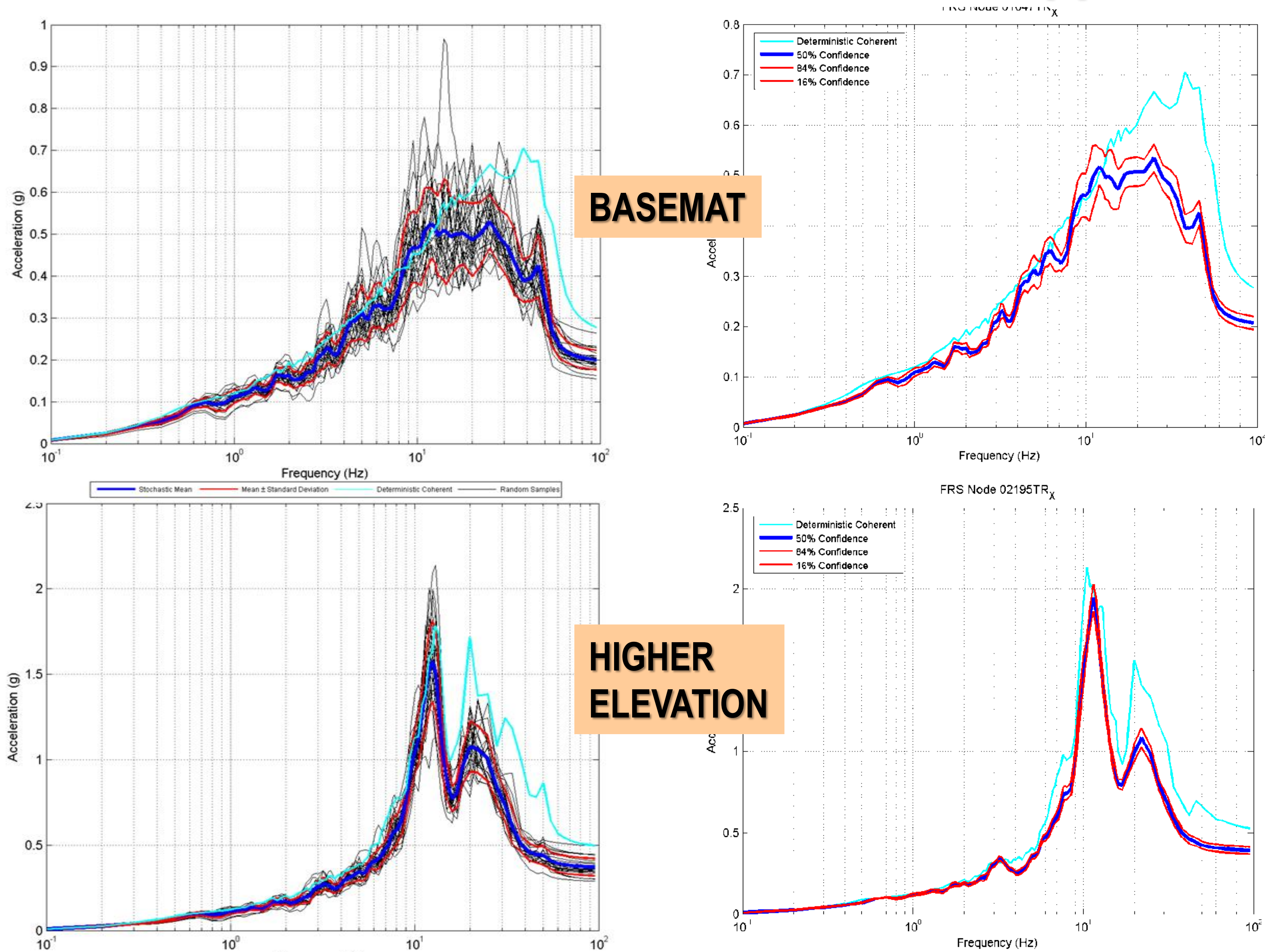

ACS SASSI Motion Coherency Models

There are several plane-wave incoherency models (with wave passage effects):

1) 1986 Luco-Wong model (theoretical, unvalidated, geom anisotropic)
2) 1993 Abrahamson model for all sites and surface foundations
3) 2005 Abrahamson model for all sites and surface foundations
4) 2006 Abrahamson model for all sites and embedded foundations
5) 2007 Abrahamson model for hard-rock sites and all foundations (NRC)
6) 2007 Abrahamson model for soil sites and surface foundations
7) User-Defined Plane-Wave Coherency Functions for X, Y and Z

Radial and Directional Incoherency Using Isotropic and Geometric Anisotropic Models

RADIAL

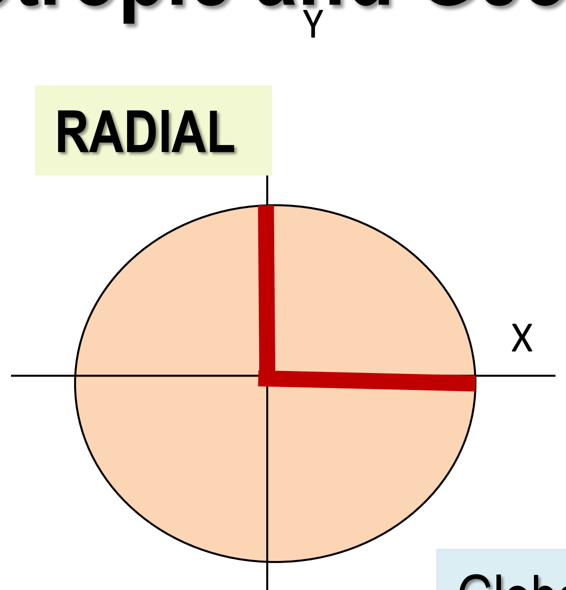

DIRECTIONAL

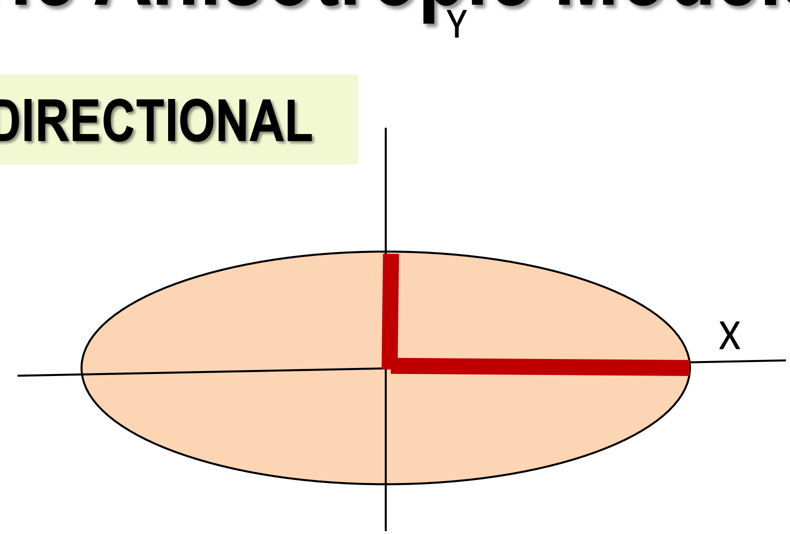

Global Coordinate Axes

$$D\text{^}2 = 2[(1-\alpha)Dx\text{^}2 + \alpha Dy\text{^}2$$

Local Coordinate Rotated Axes

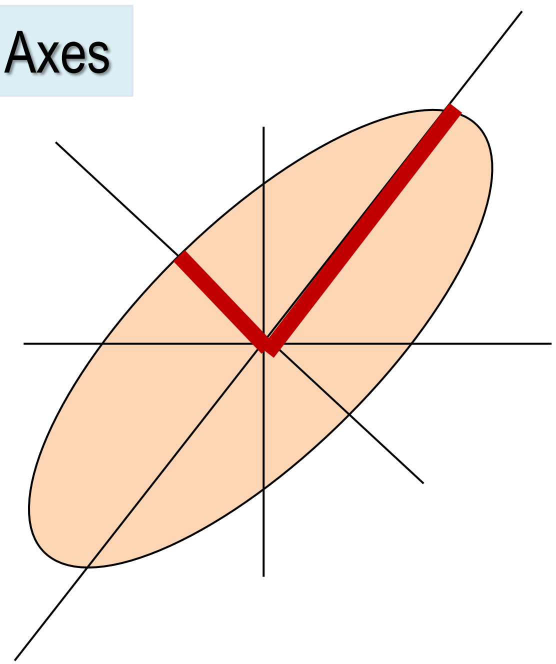

"Site-Specific" Plane-Wave Incoherency Models

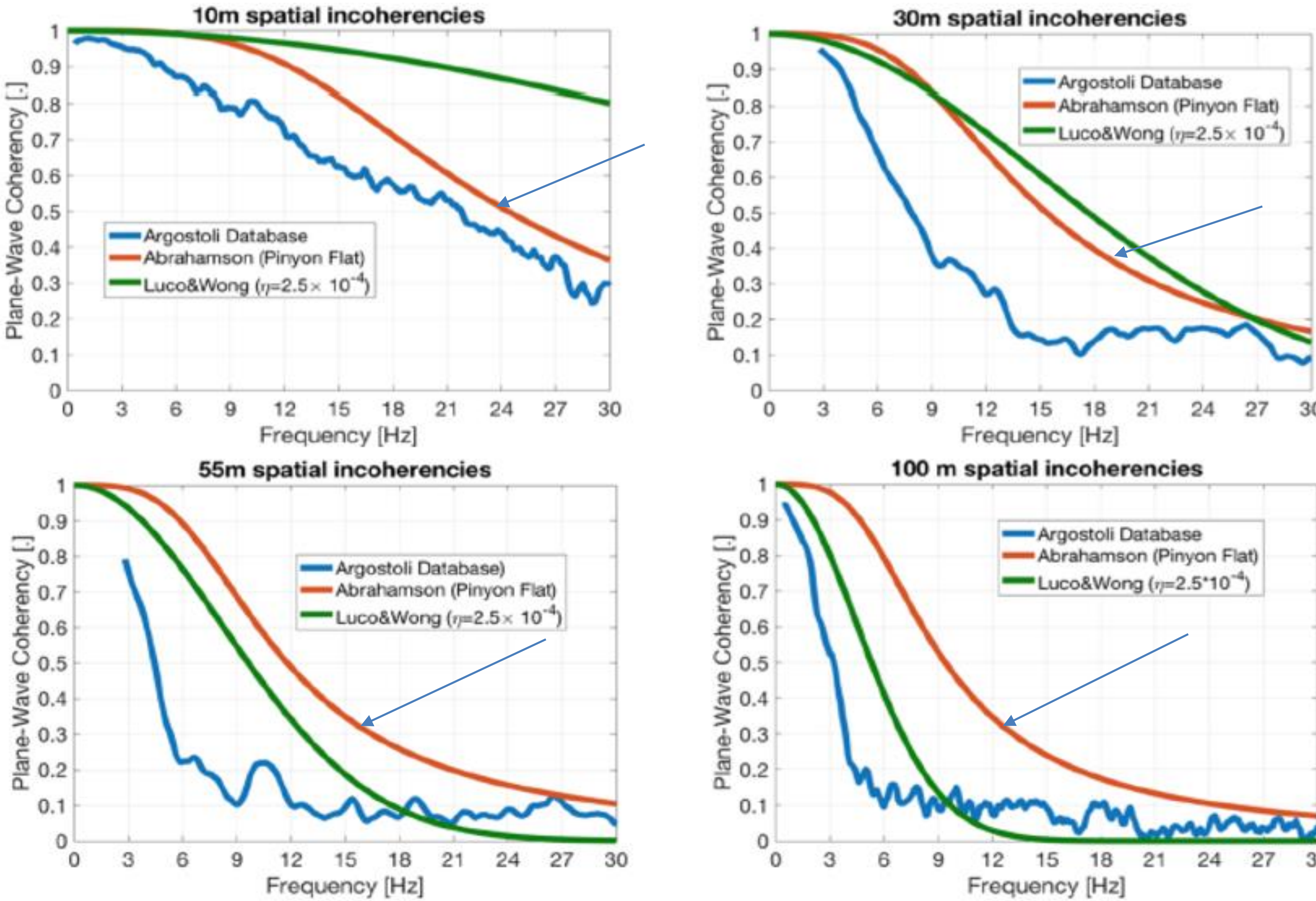

Site-Specific Coherence Function for Argostoli Site (after Svay et al., 2016, EDF)

Armenian NPP Project Used 2D Probabilistic Soil Models

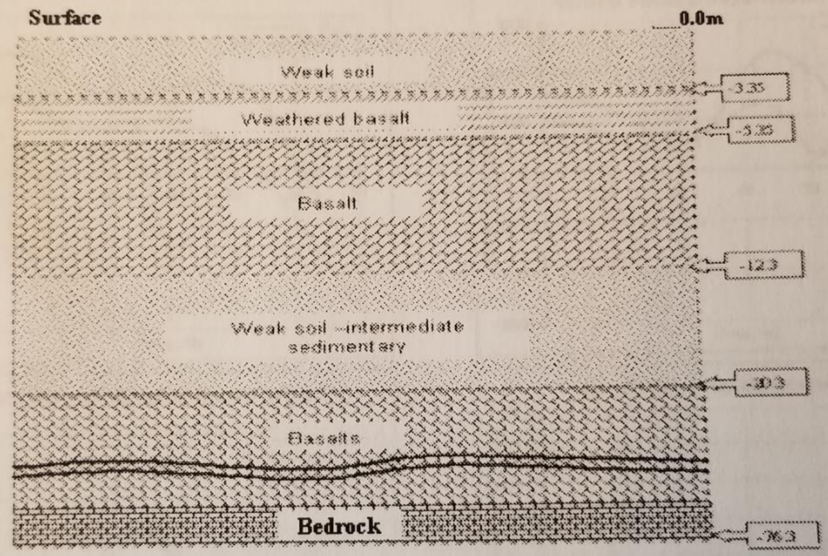

Figure 6. Layered soil profile under the Armenian Nuclear Power Plant (ANPP)

Spatially Correlated Vs Profiles. BNL Report 2006 (Simos and Costantino, 2007).

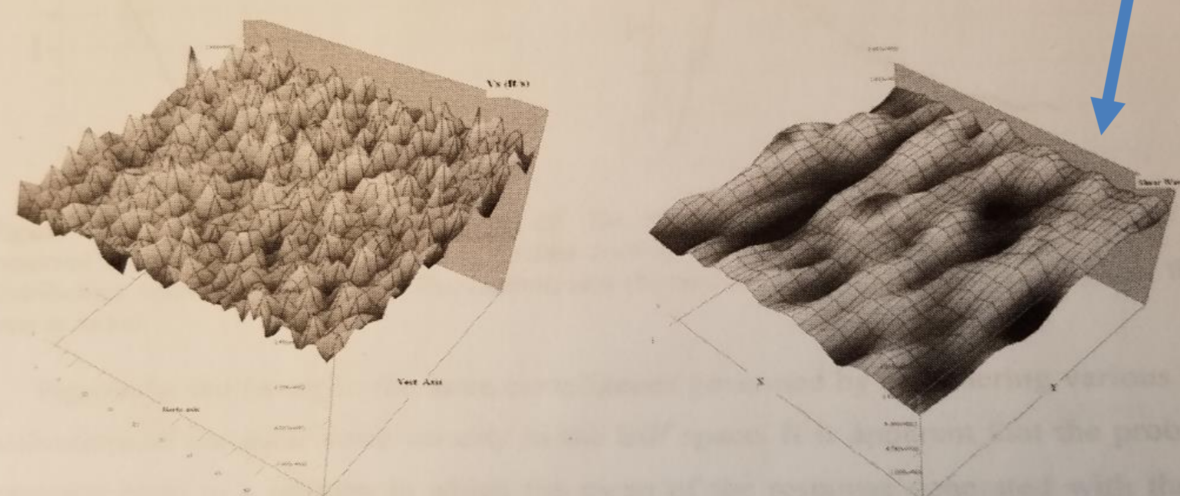

Figure 3. (a) Randomized shear wave velocity in half space domain of Figure 2 without special correlation and (b) resulting shear wave spatial distribution after cross-correlation procedures have been introduced in the randomized field shown in (a).

Option PRO Simulated Vs & D Soil Profiles

Vs and D Simulated Profiles for Correlation Lengths of 60m x 10m (EDF site)

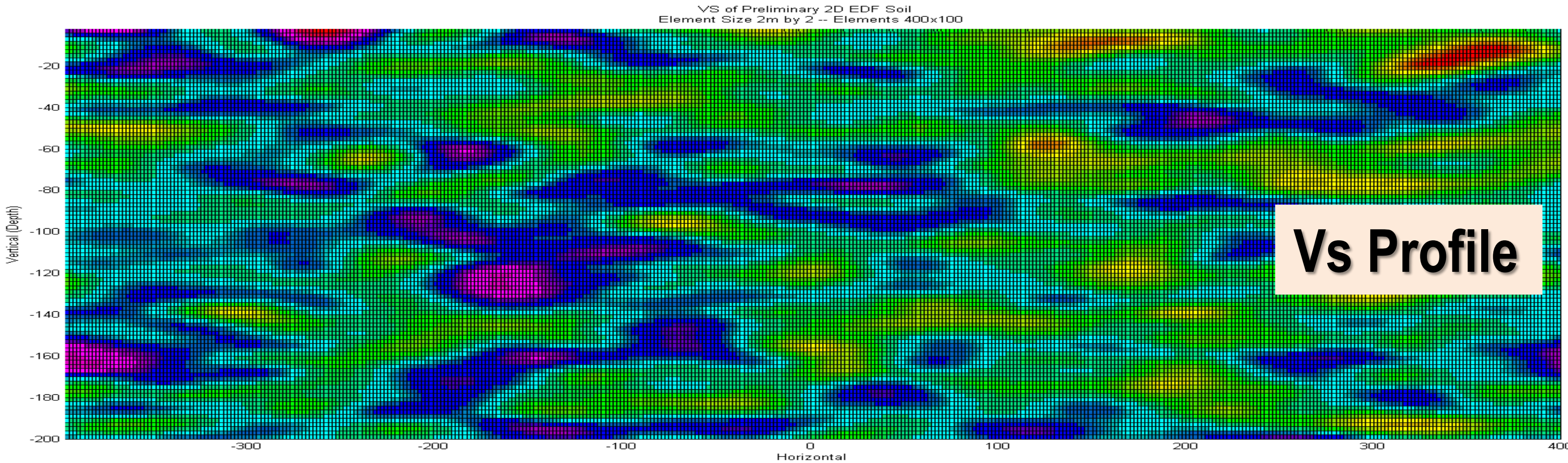

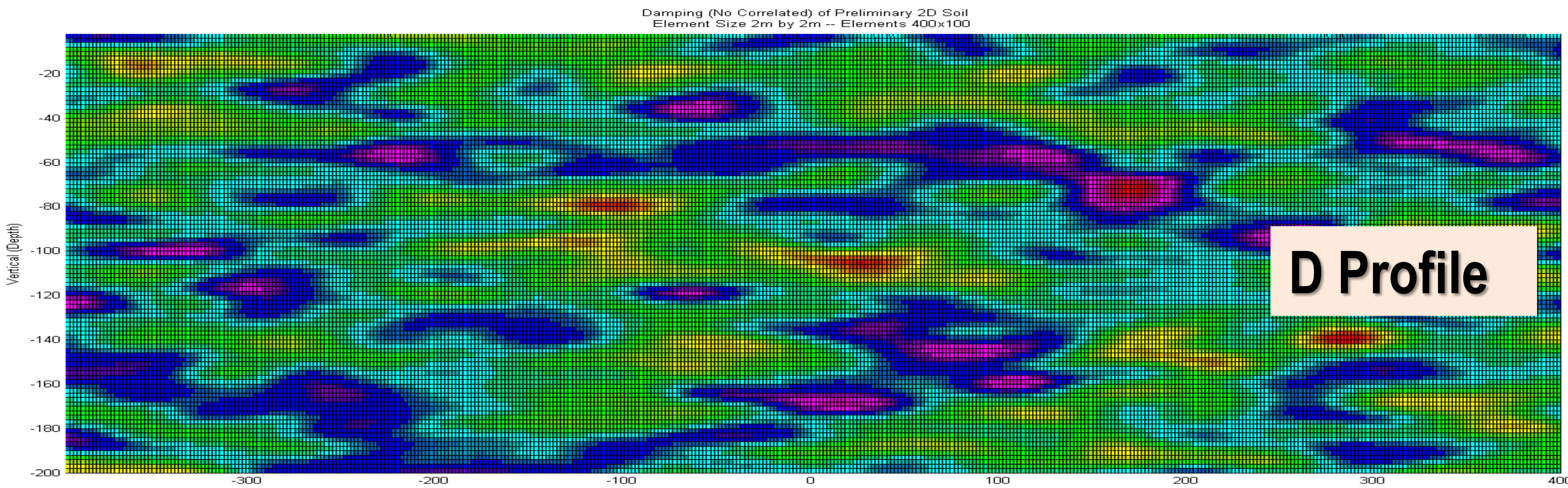

Application of 2D Probabilistic Soil Model Simulations for 1D Pinyon Flat Rock Site Layering Model

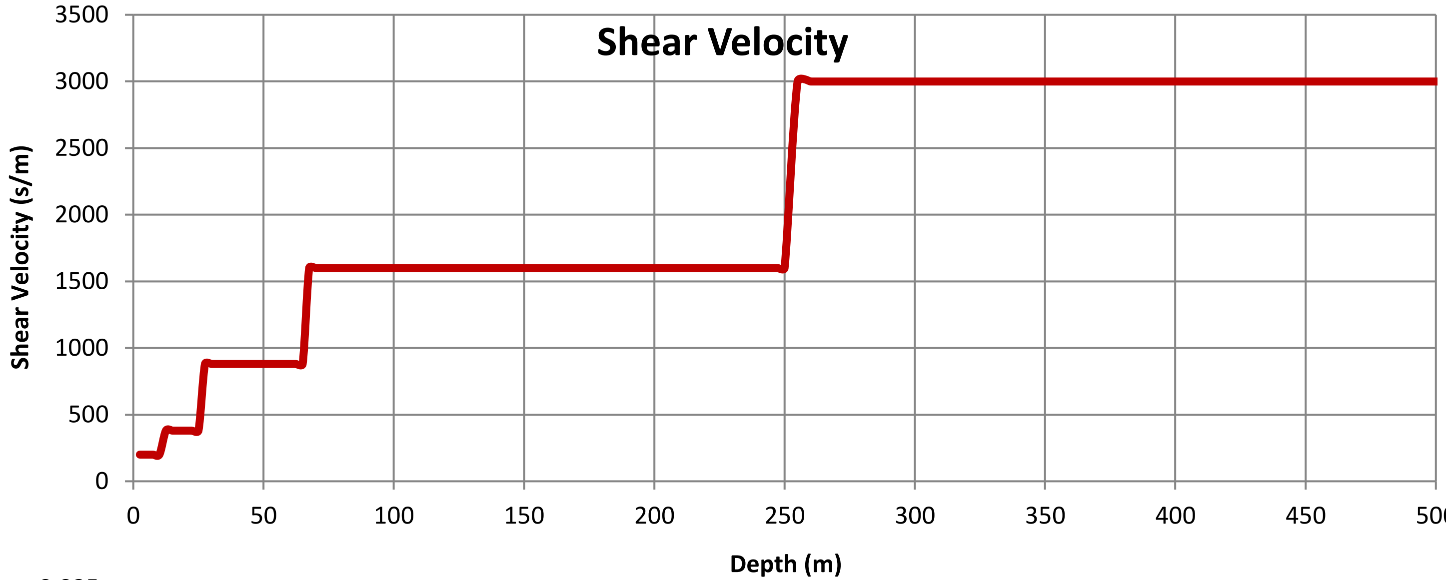

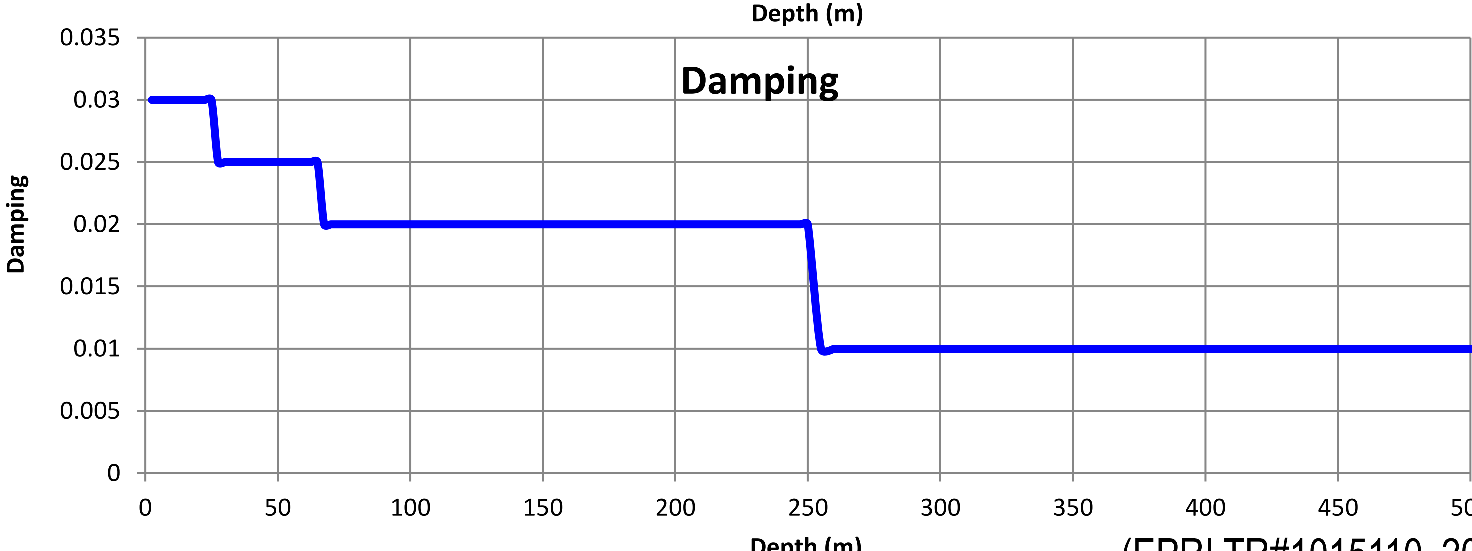

(EPRI TR#1015110, 2007)

Simulated Vs and D Soil Profiles for Pinyon Flat Site (Stochastic Field for 1000m H x 500m V Area)

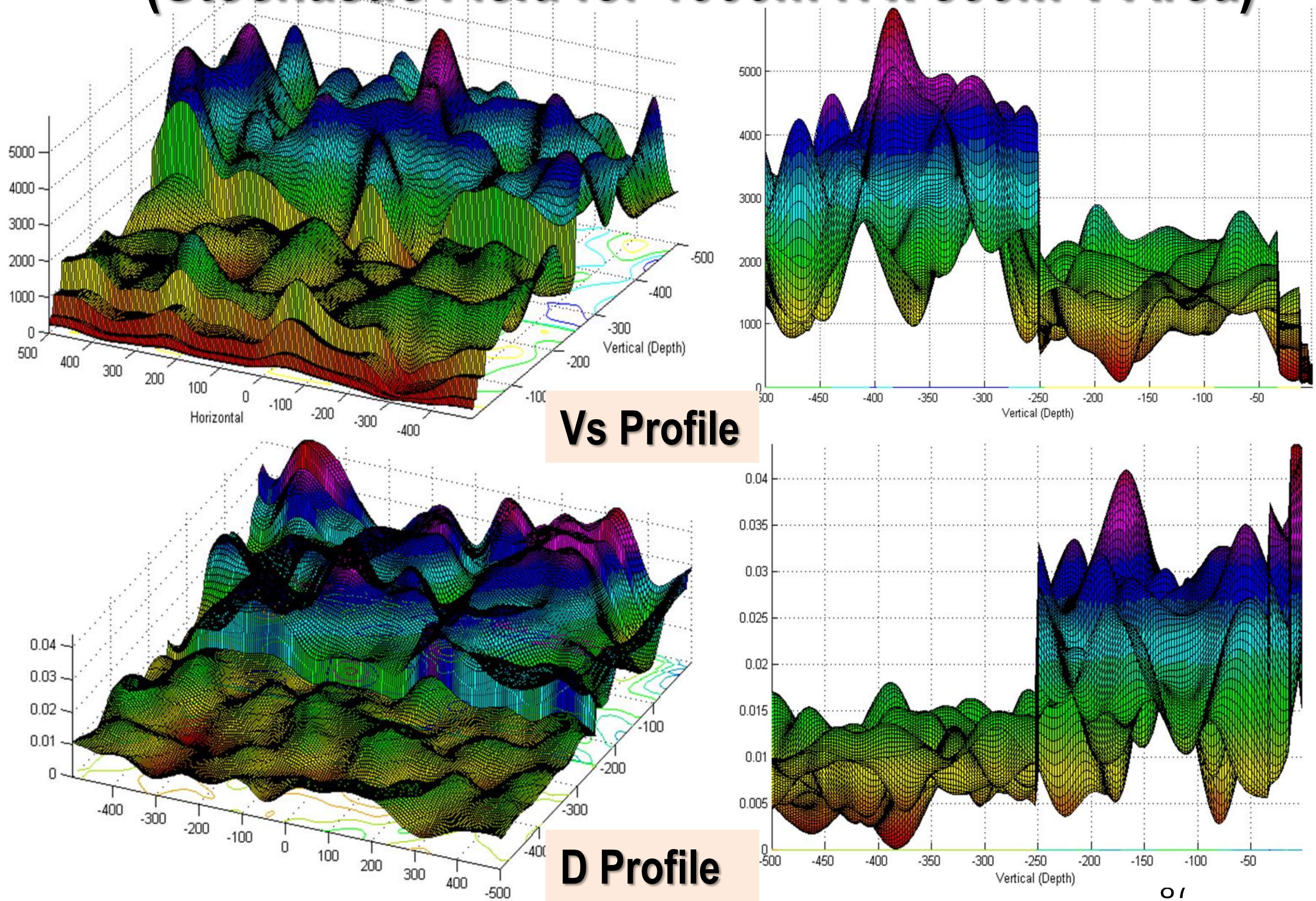

Vs Profile

D Profile

Estimation of Site-Specific Coherence Functions for Pinyon Flat Site

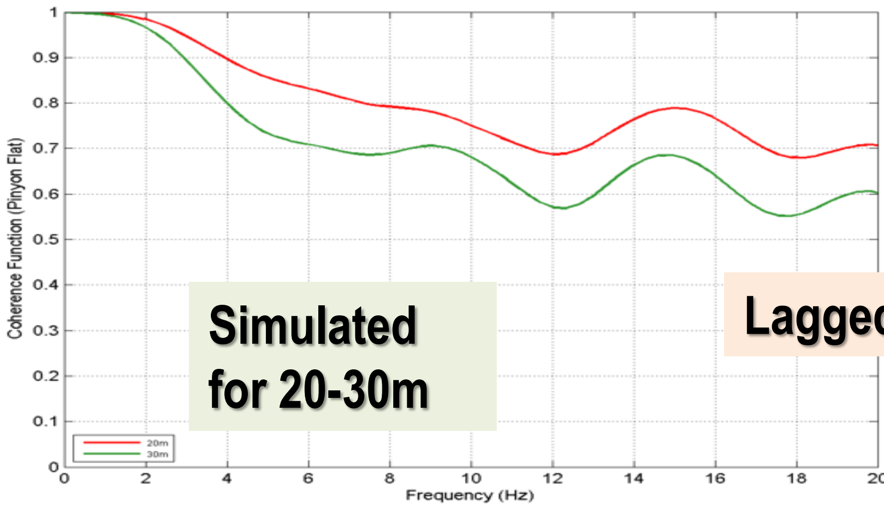

Simulated for 20-30m

Lagged Coherence

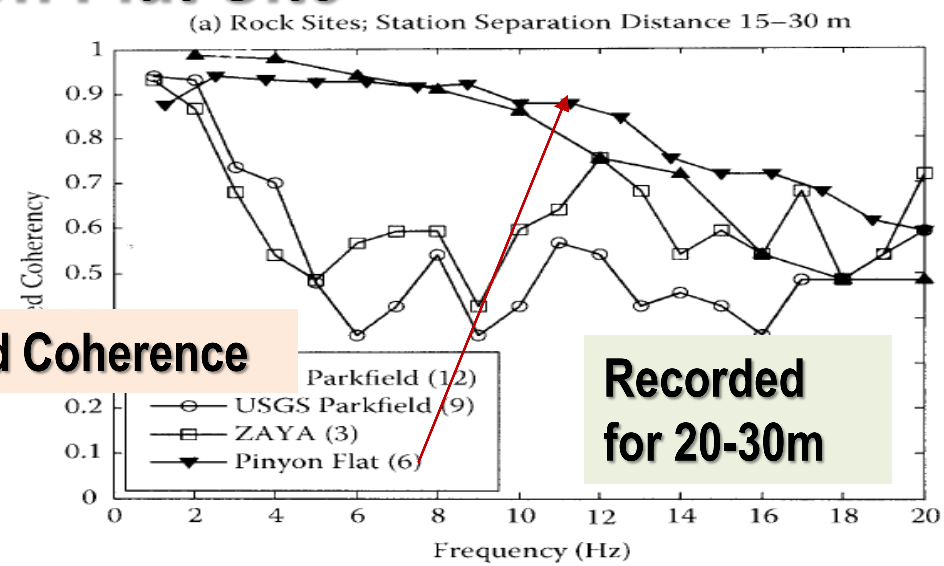

Recorded for 20-30m

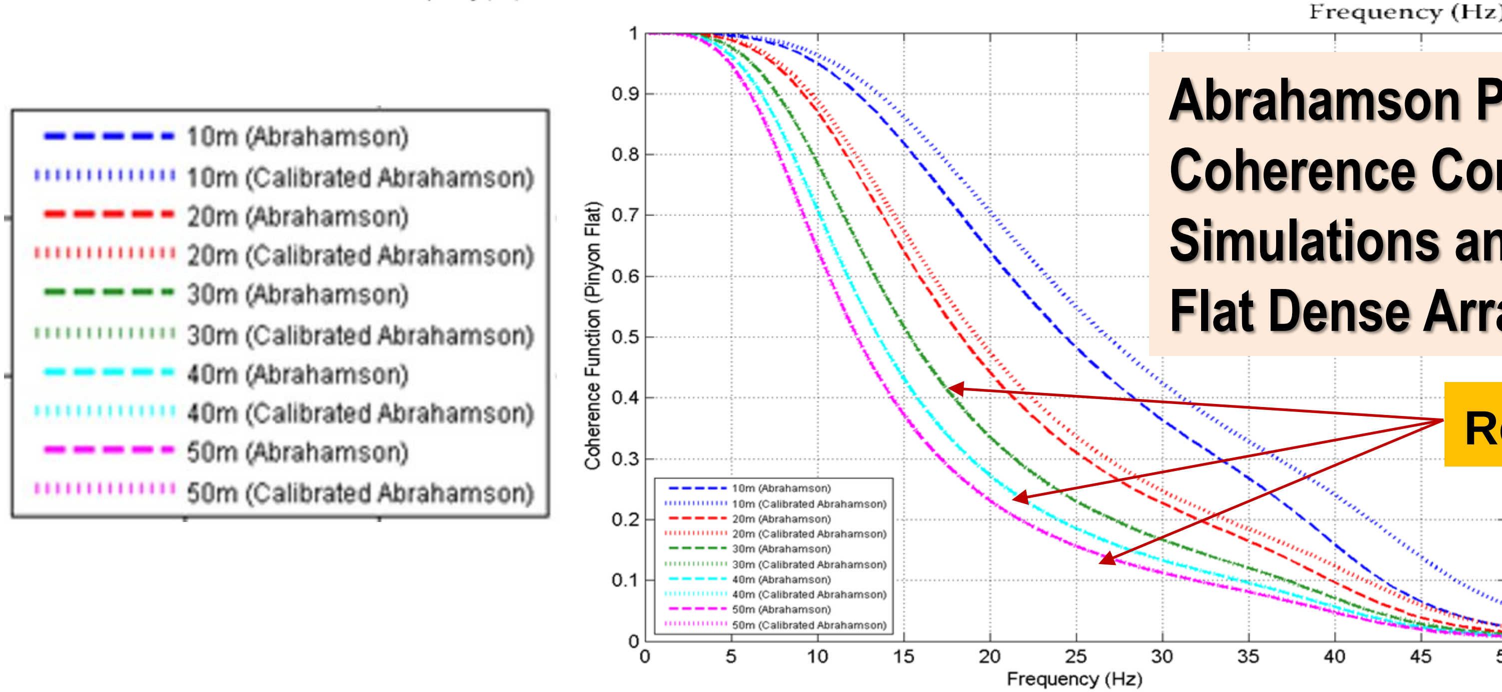

Abrahamson Plane Wave Coherence Computed from Simulations and Pinyon Flat Dense Arrays Records

Results overlap

Typical Application for Incoherent SSI Analysis

ACS SASSI Incoherent SSI Analysis Methodology

Incoherent Approach:

Stochastic Simulation with 20 Incoherent Samples with/without complex response phase adjustment

Coherence Function Model Options (TBD):

Generic Model: 2007 Abrahamson coherence function radial model (Model 5 for rock site, Model 6 for soil sites)

Site-Specific Model: Based on 2D probabilistic nonlinear site response analysis (using Option PRO to define this)

Wave Passage Effects (negligible for rock sites):

Rock Sites: Va = infinite (1.E+8)

Soil Site: Va = 2-4 Km/sec (produces more incoherency effects)

Typical R/B Complex Incoherent SSI Analysis (Summary Information Content)

- Describe Seismic Incoherent Input, Soil Layering & Embedded R/B SSI Model
- Describe Incoherent SSI Methodology Based on SS
- Show Incoherent vs. Coherent SSI Analysis Design Results:
  - ISRS
  - Maximum structural accelerations
  - Maximum structural displacements
  - Seismic soil pressures on foundation walls and basemat
  - Structural forces and moments, and out-of-plane bending moments in foundation walls and basemat
  - Vertical structural displacements at key equipment or primary cooling loop supports wrt to basemat center
- Conclusions

End of Part 2